Gyrofluid and gyrokinetic approaches for multi-scale turbulence simulation in tokamak plasmas

Jiquan Li

Kyoto University, Japan

lijq@energy.kyoto-u.ac.jp

Acknowledgement to collaborators
K. Imadera
Y. Kishimoto
Z. X. Wang

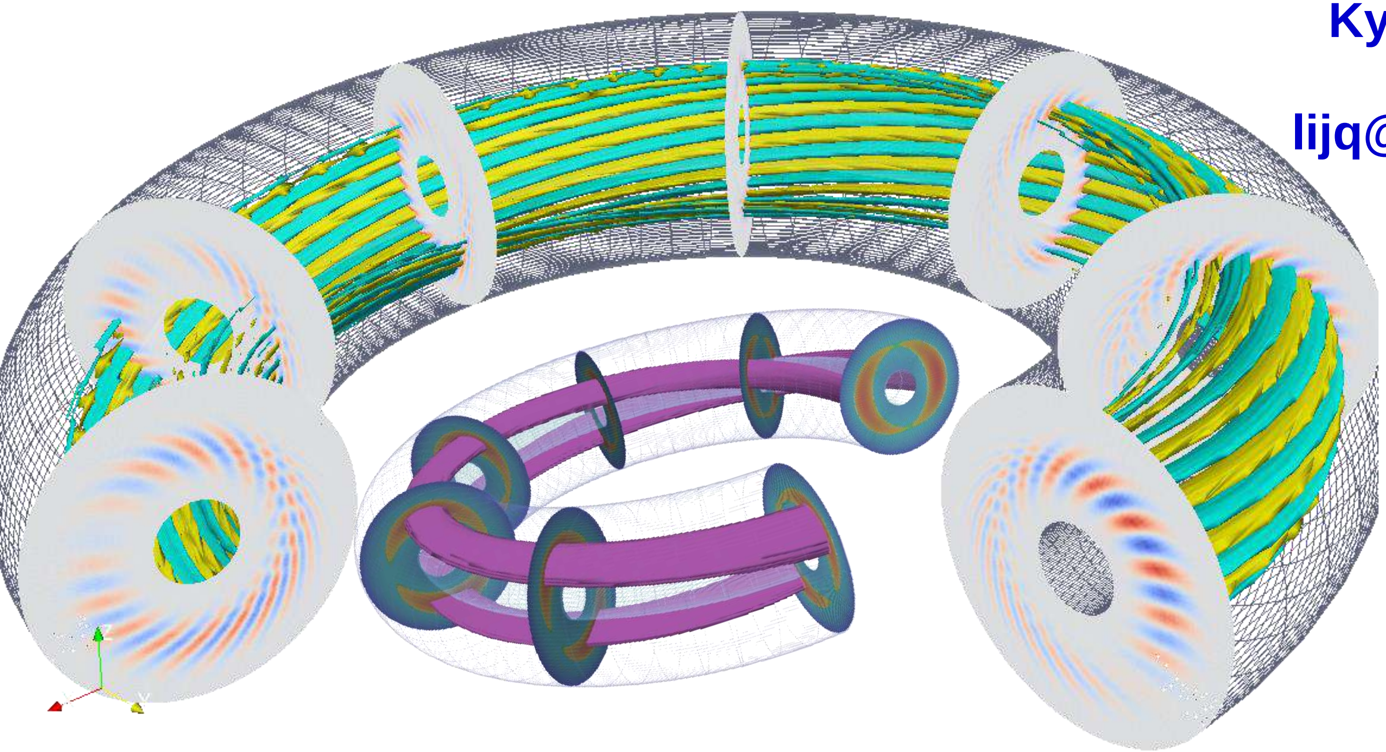

2015 ITER SCHOOL
USTC, Hefei, China
Dec. 14 - 18, 2015

Outline

- ➢ **Overview of multi-scale phenomena in MCF plasmas**
  - ✔ **Origin of multi-scale turbulence**
  - ✔ **Status of multi-scale turbulence simulation**

- ➢ **Gyrofluid approach simulation for multi-scale turbulence**
  - ✔ **Gyrofluid model**
  - ✔ **Multi-scale interaction between MHD and micro-turbulence**
    - — **Magnetic island response to micro-turbulence**
    - — **Micro-turbulence response to MHD island dynamics**

- ➢ **Gyrokinetic approach simulation for multi-scale turbulence**
  - ✔ **Gyrokinetic model**
  - ✔ **Full-*f* gyrokinetic Vlasov code—GKNET**
  - ✔ **GK ITG instability with an island**
  - ✔ **Flux-driven GK turbulence simulation on profile stiffness and ITB**

- ➢ **Summary**

ITER— on the road to fusion energy

EDITORIAL
nature physics Vol.2 No.6 June 2006 www.nature.com/naturephysics

To dream the possible dream

ITER

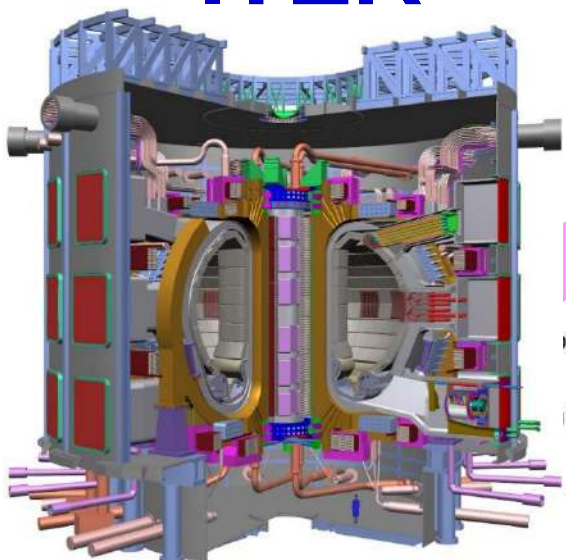

Fusion triple product = $nT\tau_E$

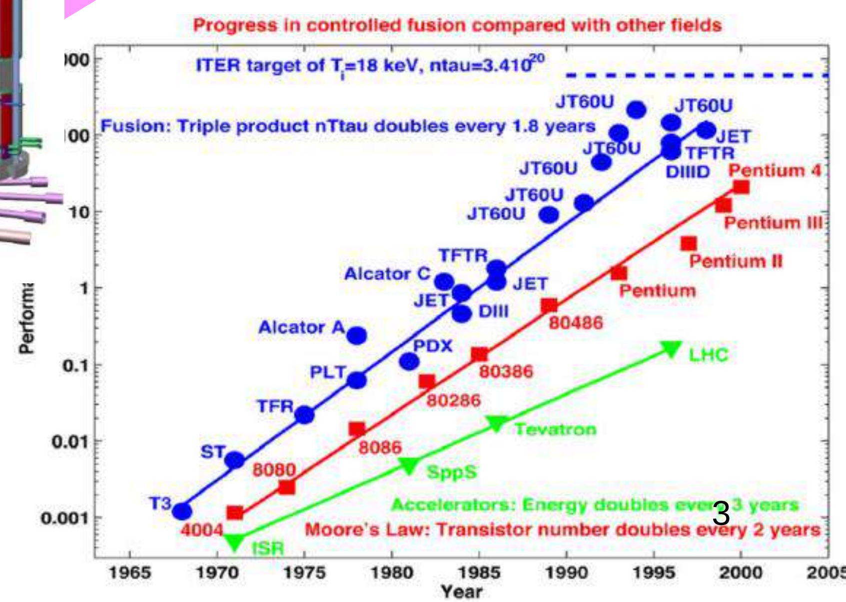

First Tokamak T-1 (1958, USSR)

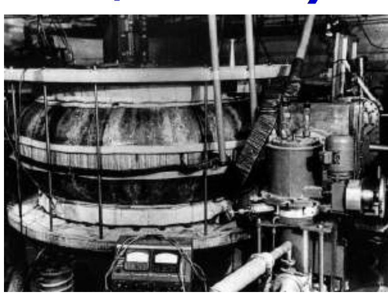

Fusion triple product $= nT\tau_E$

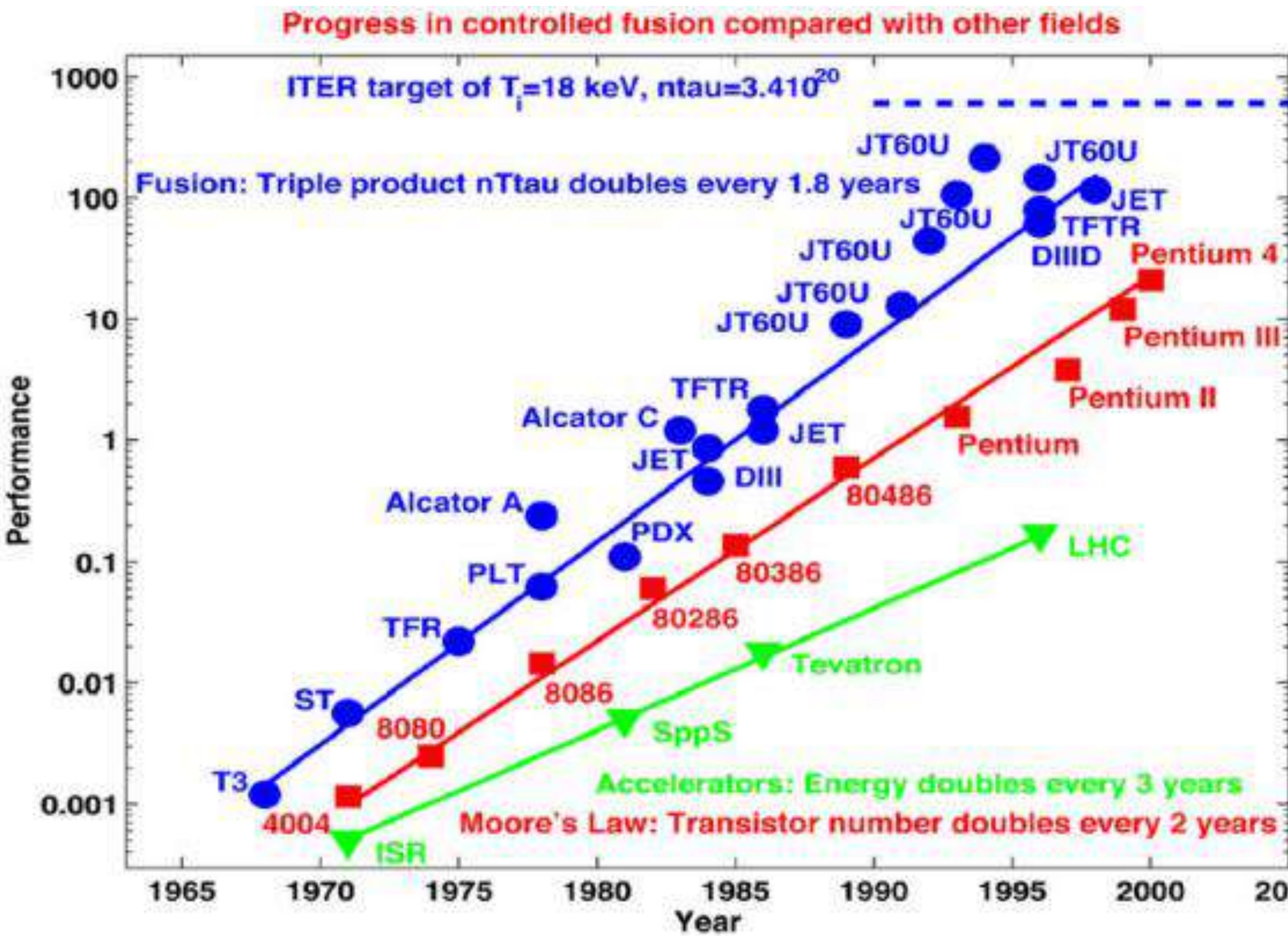

Energy confinement performance

- Plasma confinement is limited by the loss of particle/energy.

Energy confinement time:

$$\tau_E = \frac{W}{P_{Loss}} = \frac{\int \frac{3}{2} n(T_i + T_e) dV}{P_{Loss}}$$

Energy density

Power loss

In a stationary state, heating power is balanced by the losses

$$P_{Input} = Sn\chi\nabla T$$

$$\boxed{\frac{\partial}{\partial t} W = P_{Input} - P_{Loss} = P_{Input} - \frac{W}{\tau_E}}$$

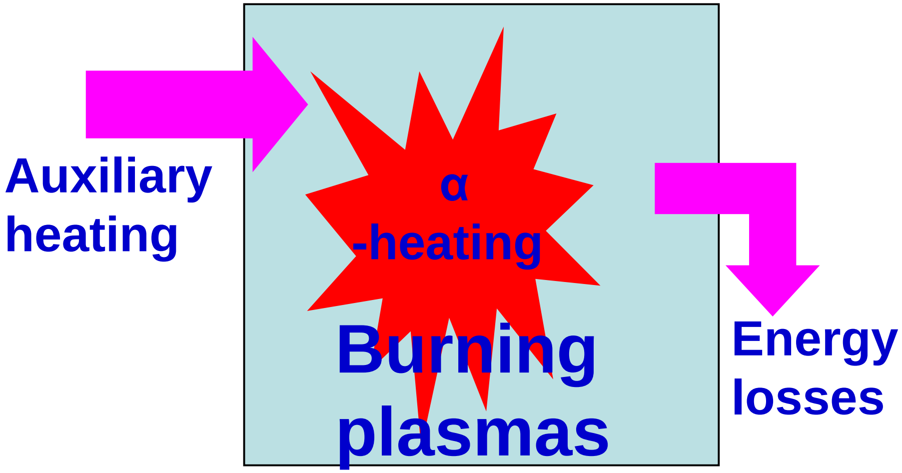

$$\tau_E = \frac{W}{P} = \frac{VnT}{Sn\chi\nabla T} \sim \frac{a^2}{\chi}$$

χ —Transport coefficients

Heat transport coefficients

- Classical ion transport: ~ $0.01 m^2s^{-1}$; Neoclassical ~ $0.5 m^2s^{-1}$, comparable with experimental one;
- Electron transport is much lower than experimental observation.
- Large transport is due to turbulence—anomalous transport.

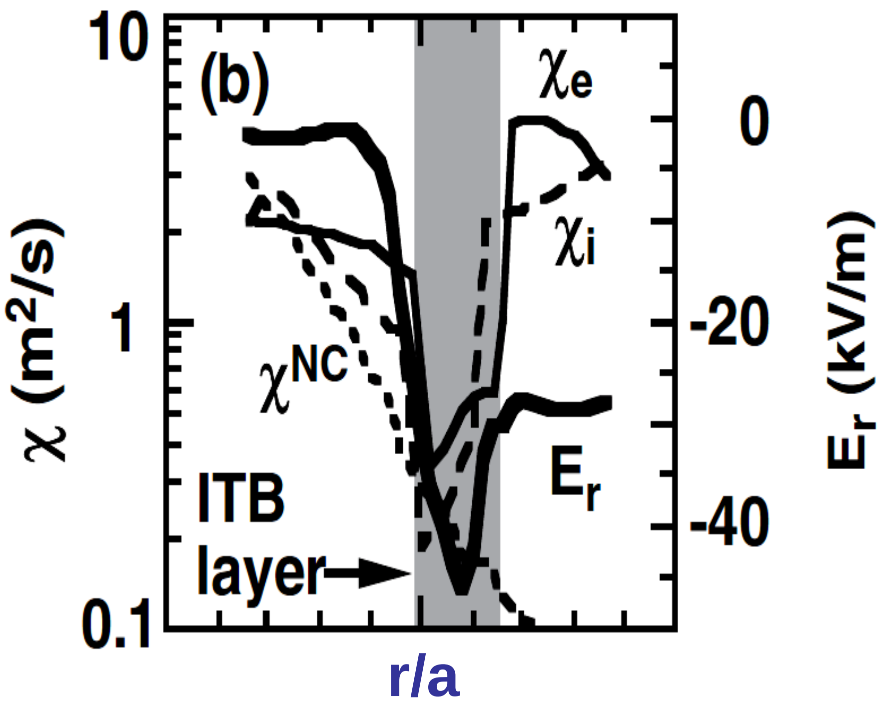

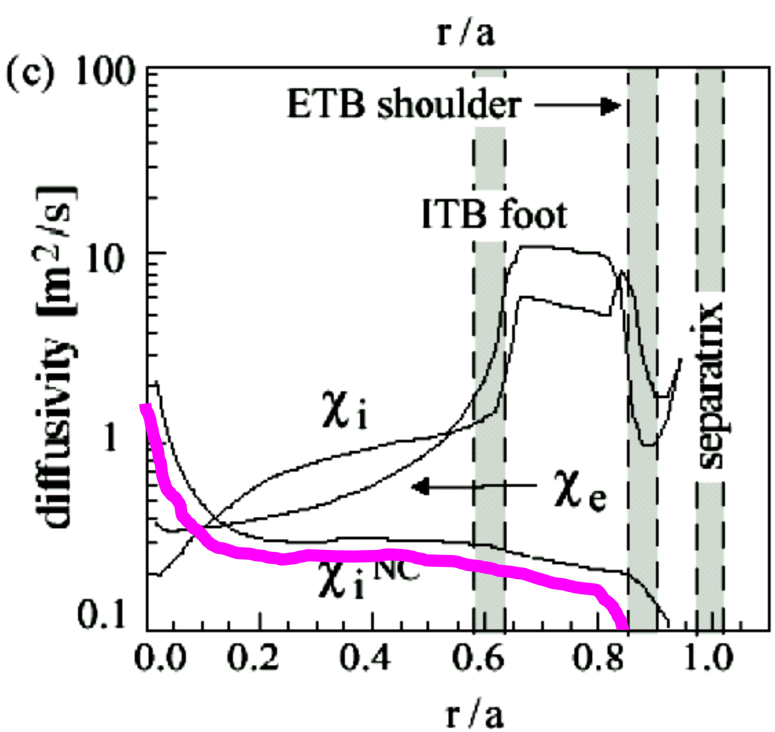

From JT-60U

Obstacles on the road to Fusion-ITER

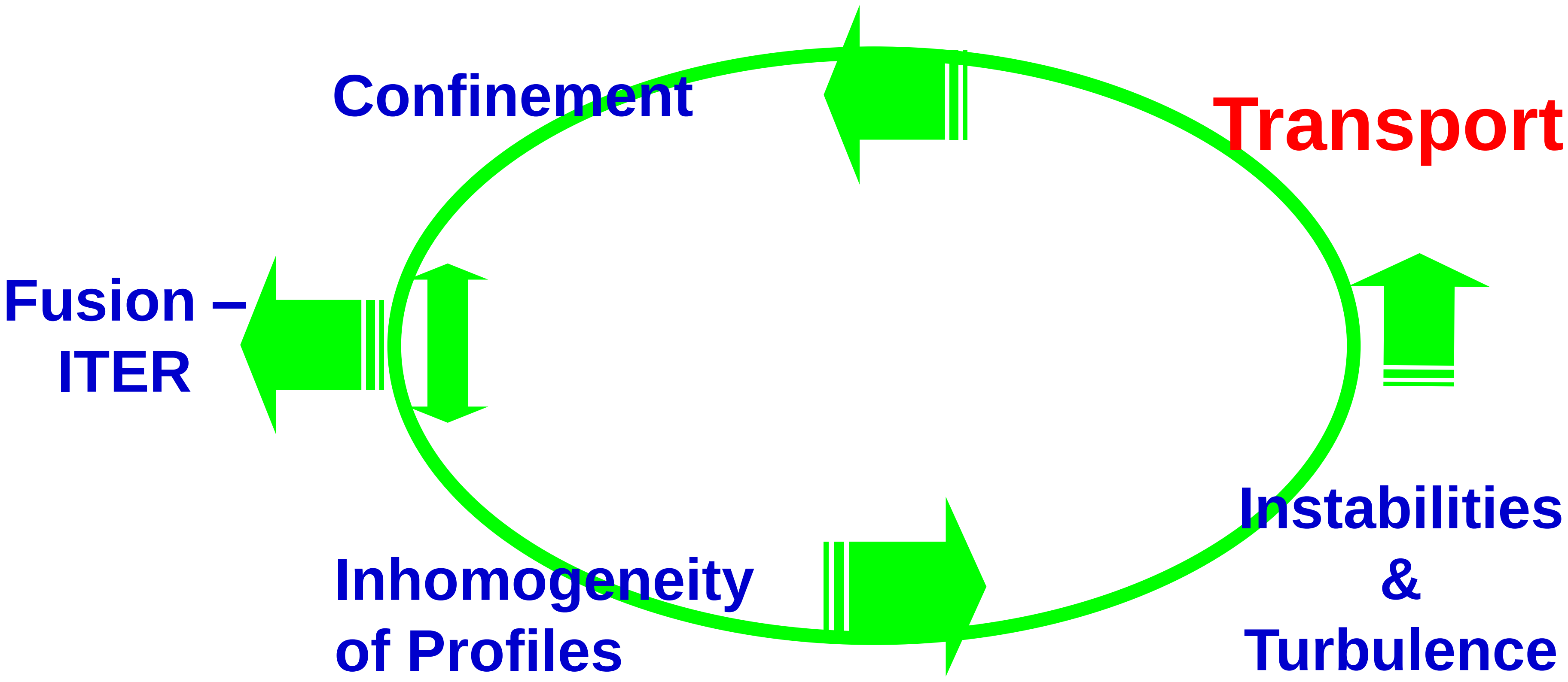

Characteristics of MCF plasma fluctuation

➢ **Plasma fluctuation in MCF is characterized by multi-scale multi-mode electromagnetic fluctuations, which are driven by various linear and nonlinear instabilities.**

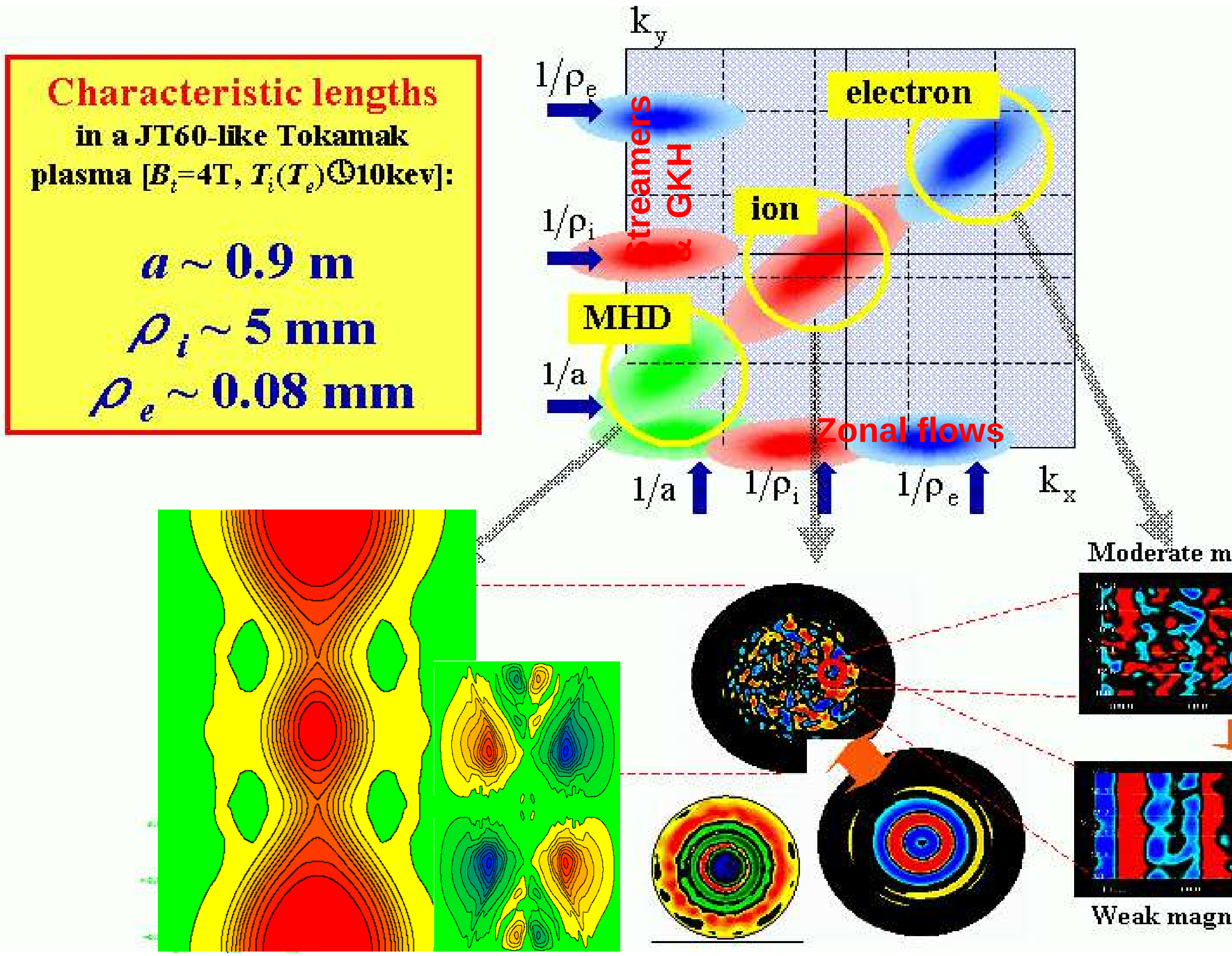

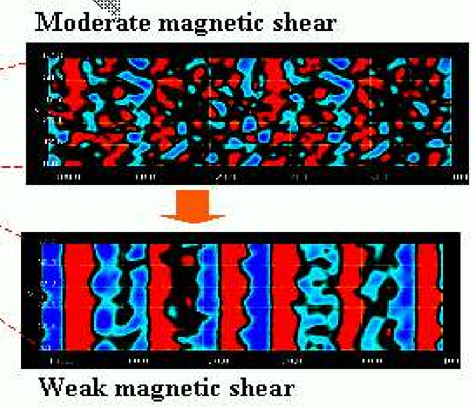

Characteristics of plasma turbulence

- ➢ many eigen modes,
- ➢ wide scale
- ➢ coexistence of multi-scale fluctuations
- ➢ overlap on scales

Eigenmodes in MCF plasma

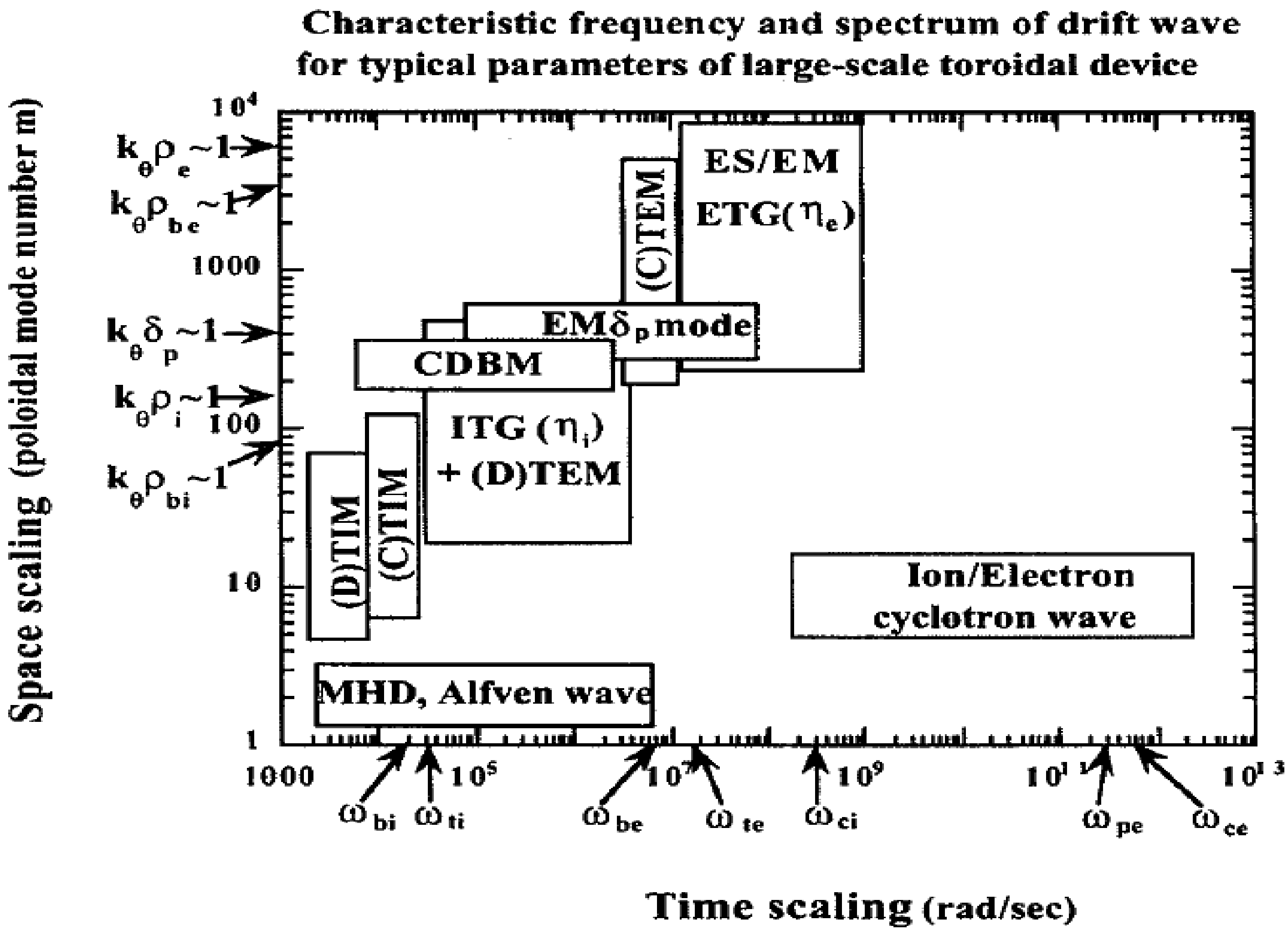

➢ **Coexistence and mutual interaction between various MHD activities and micro-turbulence**

Theory on multi-scale problem in plasmas

➢ **Mathematical description**

$$\frac{\partial f}{\partial t} + L^{(0)} f = N(f, f) + \tilde{S}_{th}$$

S_{th} – thermodynamical excitation

$$N_k(f, f) = -\Gamma_k f_k + D_k f_k + \tilde{S}_k$$

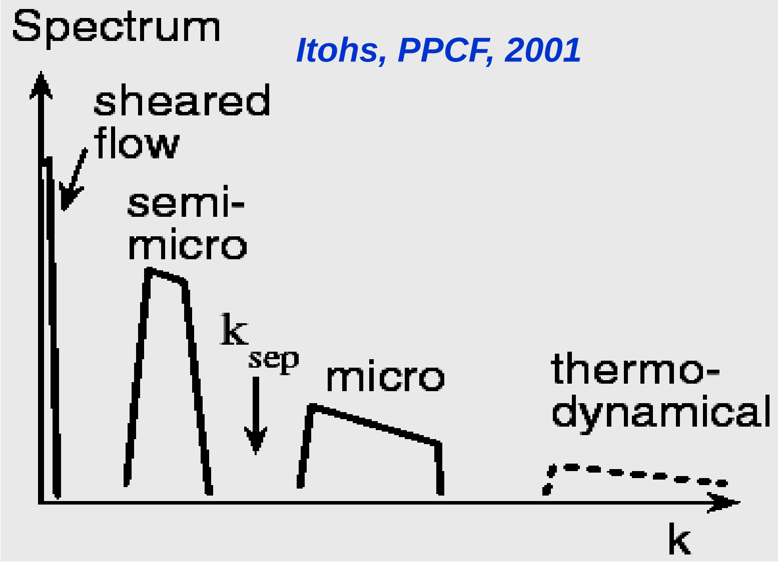

Coherent part:
Drag;
Eddy-
viscosity;
……

Mode interaction
from different
Scale Drive

Incoherent part:
Random noise;
……

Schematics of i-e scale interaction

➢ **Nonlocal mode coupling in multi-scale turbulence**

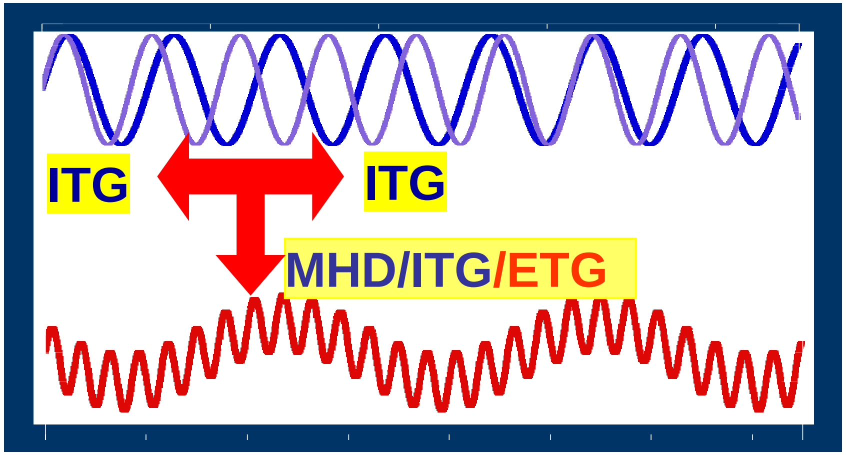

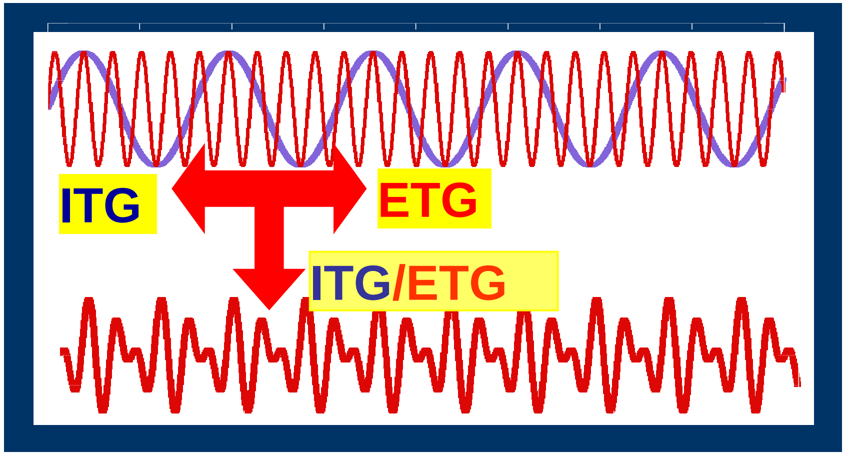

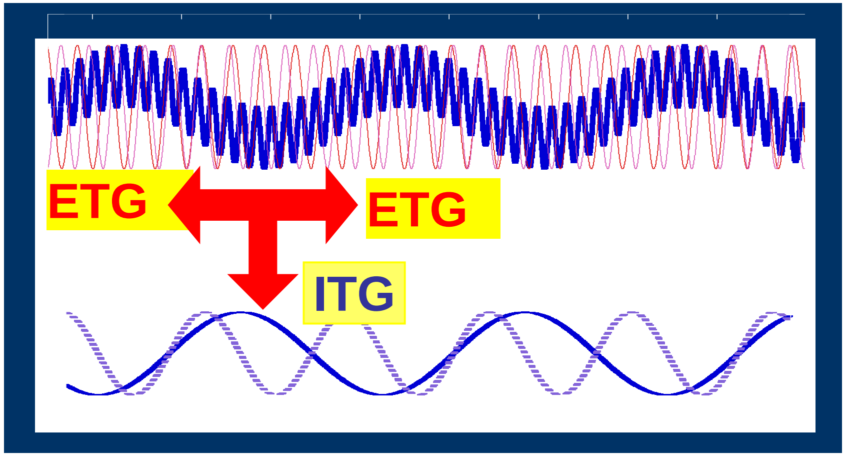

- **Indirect interacting through zonal flows;**
- **Direct mode coupling**
  - ✓ **Beat wave generation;**
  - ✓ **Envelope modulation;**
  - ✓ **Energy cascading (and inverse);**
  - ✓ **……**

Multi-scales in plasma turbulence

➢ **Multi-scale turbulence & flow interaction in fusion plasma**

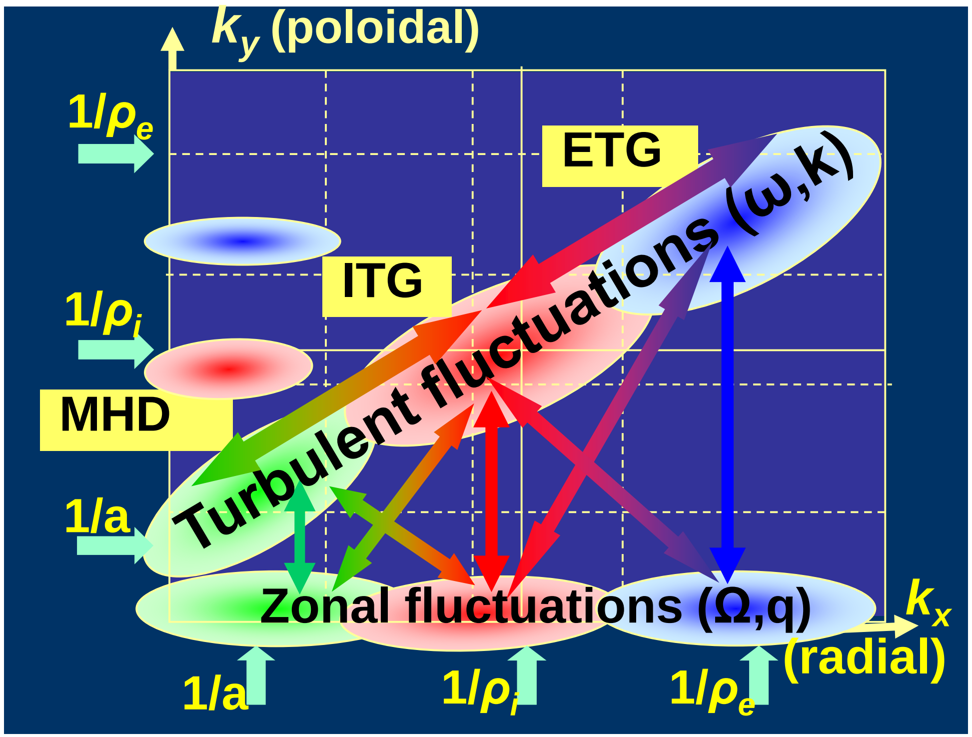

Fluctuations & flows

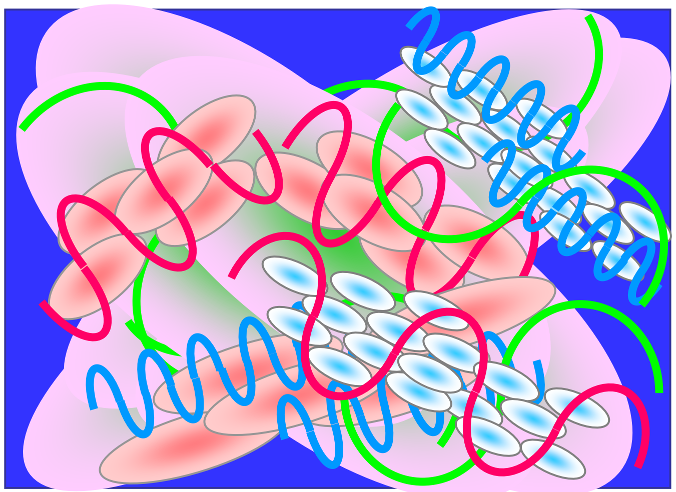

A full scale simulation should involve all interacting processes among scales covering equilibrium scale, ion scale to electron scale.

BUT, this is still an incapable job right now!
Reduced modeling is necessary!
– near-scale model

Fluid Turbulence Modeling

➢ **Direct Numerical Simulation(DNS):**

can include all scales of vortex structures, BUT difficult.

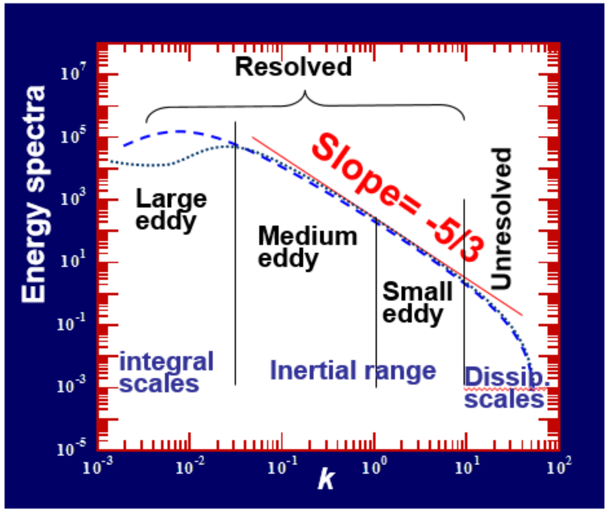

➢ **Turbulence modelling for unresolved scale**

small-scale components are eliminated and their effects are represented by such concepts as turbulent or renormalized viscosity.

➢ **Large Eddy Simulation (LES):**

filter to remove small-scales, viewed as a time- and spatial-averaging.

Reynolds Averaged Navier-Stokes (RANS)

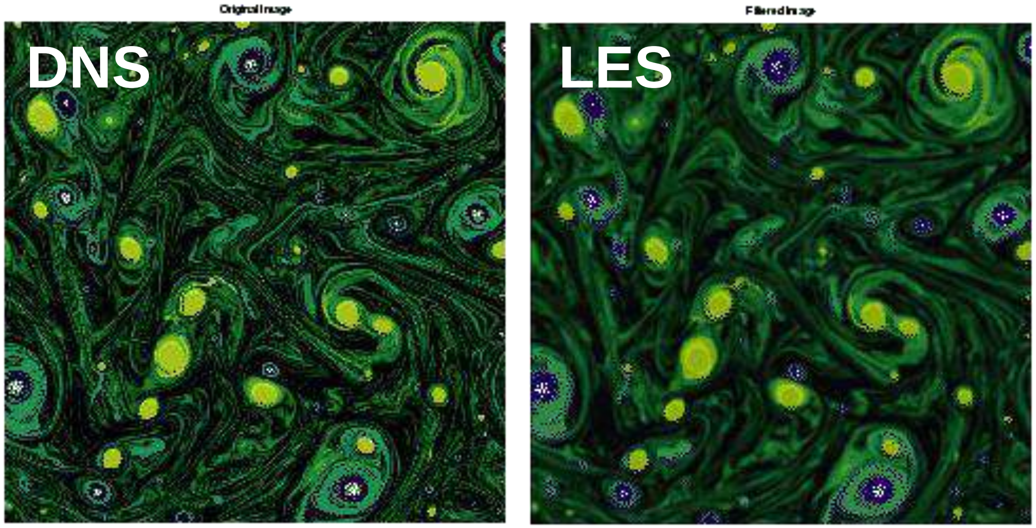

http://www.rsmas.miami.edu/personal/milicak/turbulence/turbulence.html

Simulation modeling on near-scale MHD-ITG

- ➢ **MHD islands exist in tokamak**

Isayama & JT-60 Team, PoP2005; FED 2001

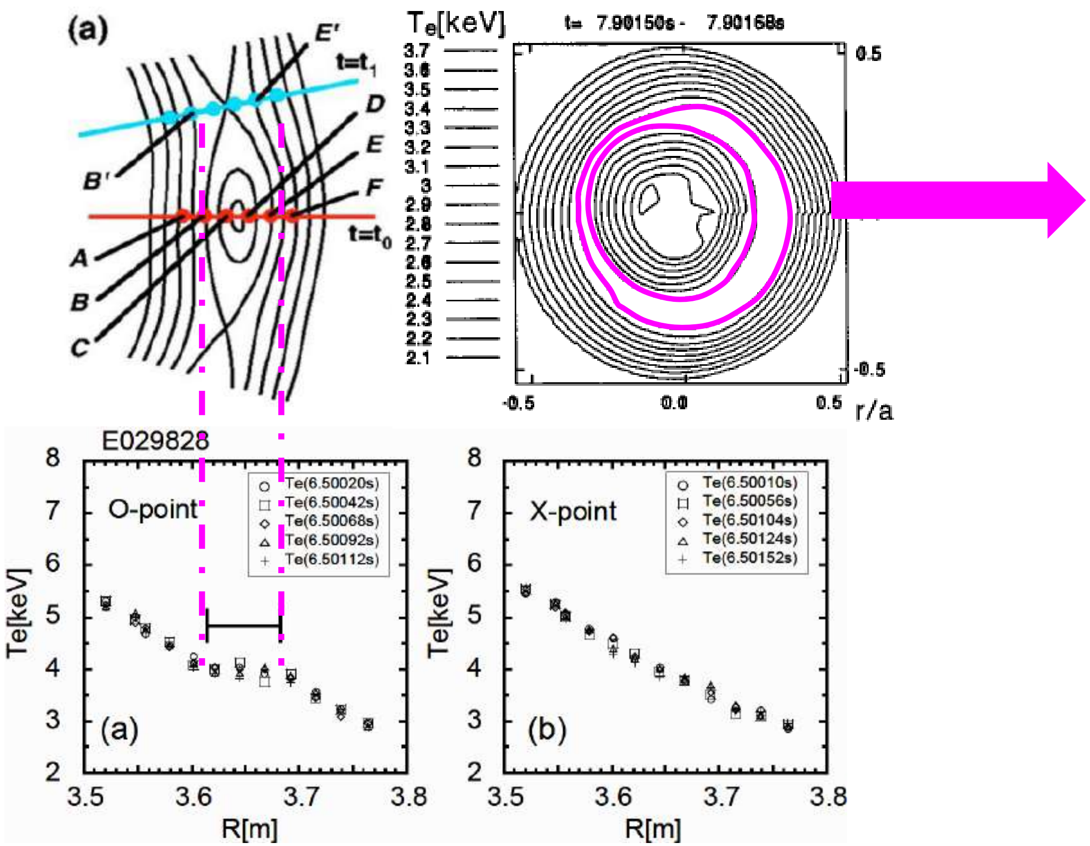

- ➢ **Mixed MHD-ITG EM model**

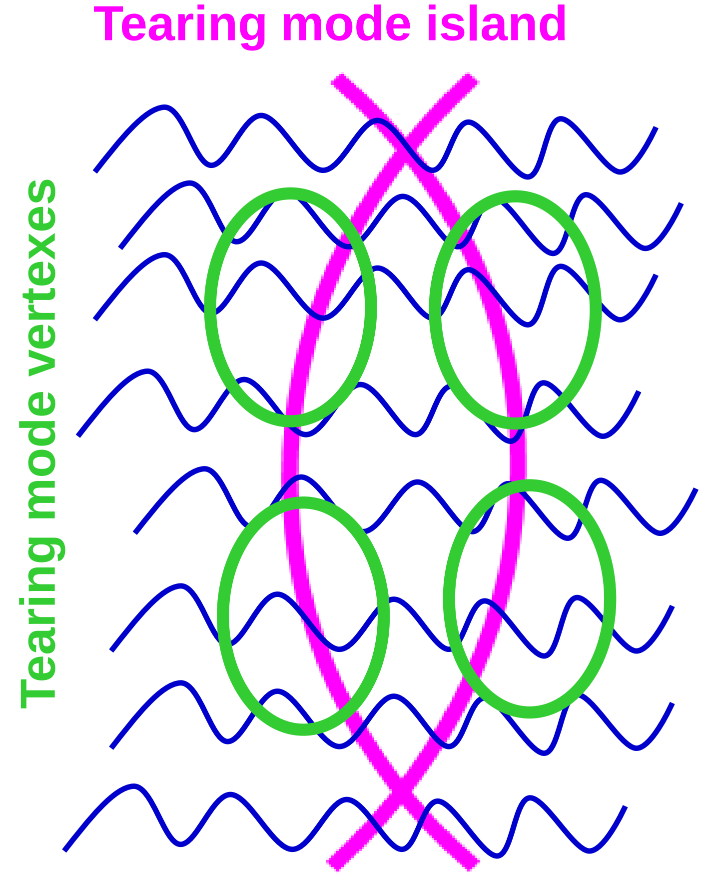

✓ **Islands appear due to a family of tearing mode; RMPs; error fields;……**

Status on MHD-ITG scale problems

- Theoretically, MHD islands (tearing modes) interacting with drift wave (ITG, et al.) is considered through equilibrium modification or flow shearing, ……

Itohs, PPCF, 2001;

McDevitt & Diamond, PoP 2006;

……

Wilson, et al, PPCF 2009;

Waelbroeck, PPCF 2009;

……

- Simulation efforts on indirect or direct MHD-ITG interaction

Yagi, et al, NF, 2005;

Ishizawa et al, PoP 2008, 2013;

Millitelo, et al, PoP 2008;

Muraglia et al, PRL 2009;

….

Li, et al, NF 2009;

Poli ,et al, NF 2009 ;

Wang, et al, PRL 2009; PoP 2009;

Hornsby PoP 2012; 2015;

Jiang, et al PoP, 2015

….

Modeling: configuration with island

➢ **An island is embedded (example in slab)**

Sheared slab w/o island **with island**

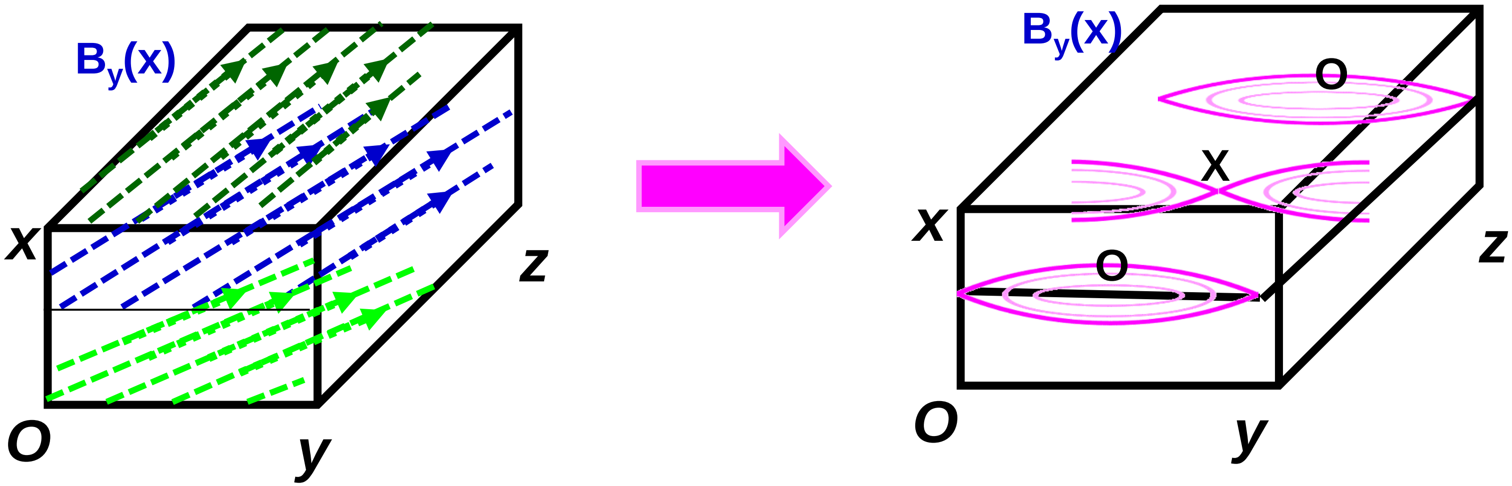

$$\vec{B} = B_0 \nabla z - \nabla\psi \times \nabla z$$

$$\psi = -\frac{B_0 x^2}{2L_s}$$

$$\vec{B} = B_0 \nabla z - \nabla\psi \times \nabla z$$

$$\psi = -\frac{B_0 x^2}{2L_s} + \boxed{\tilde{\psi}\cos(k_y y)}$$

Half width of island $w = 2\sqrt{L_s \tilde{\psi} / B_0}$

Modeling: MHD islands modify configuration

➢ **Stationary island** **is imbedded in DW fluctuations**

ITG growth rate vs island width by Gyro-fluid model

Wang et al, PoP 2009

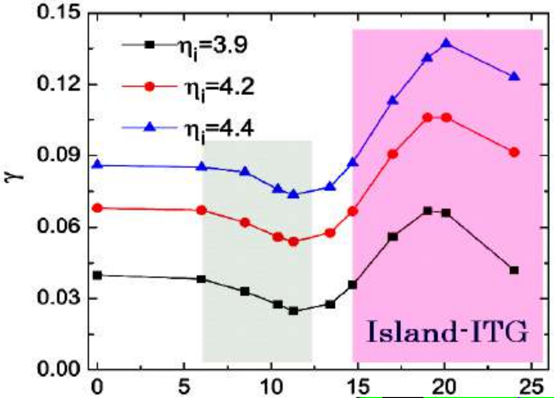

$w \propto \sqrt{\tilde{\psi}}$

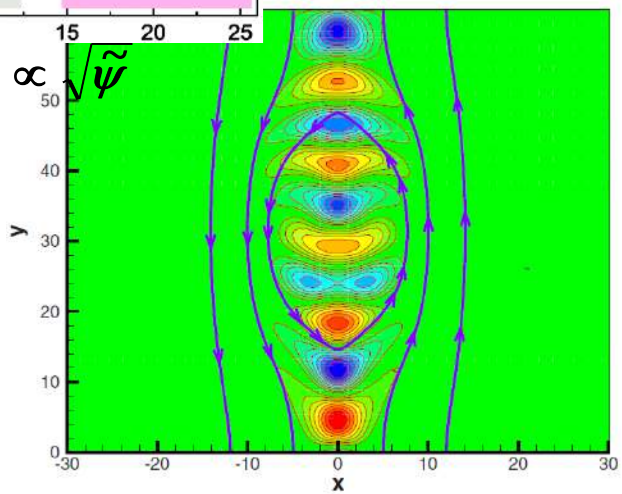

Heat flux around magnetic island by Gyro-kinetic PIC model

Poli et al, NF 2009

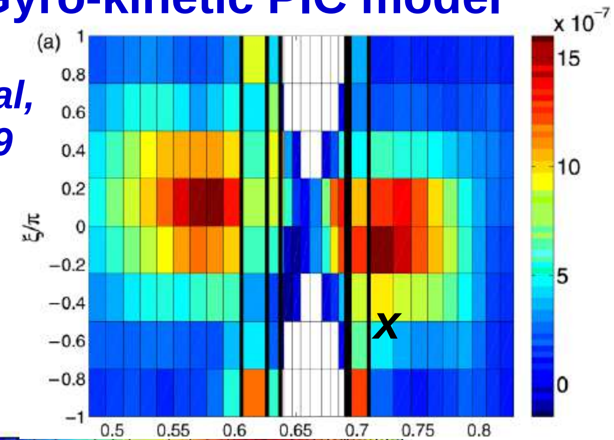

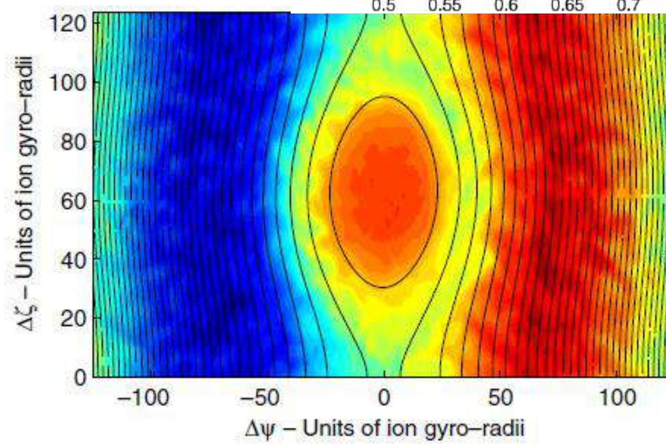

✔ **Small island stabilizes ITG, whereas wider island destabilizes ITG (MITG)**

✔**Larger heat fluxes in the X-point region, reduced around the O-point.**

Theory/modeling: MHD islands modify profile

- Dominant effect of island is from n/T profile modification

$$\eta_i = \eta_0 \frac{1-\varepsilon\cos(k_y y)}{1+\varepsilon}$$

Wilson/Connor, PPCF 2009

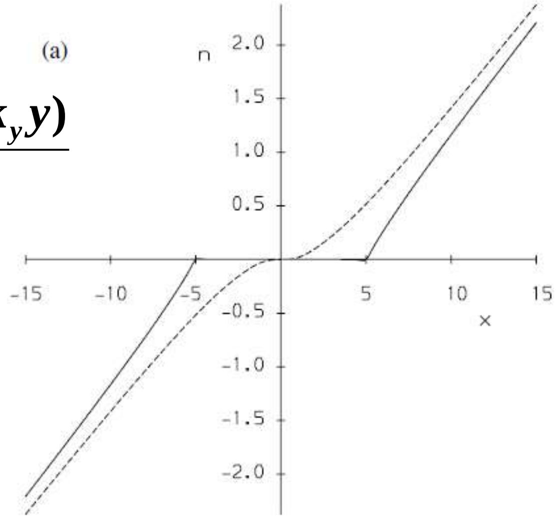

Hu, Li, et al. PoP 2014

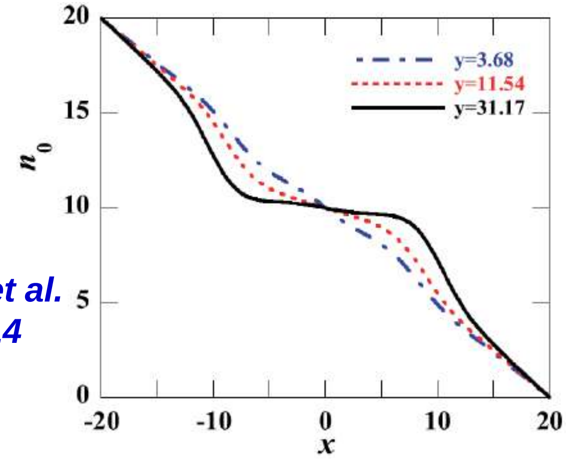

$$L_n(y) = L_{n0}[1+\varepsilon\cos(k_y y)]$$

With island

W/o island BUT n/T varying in y

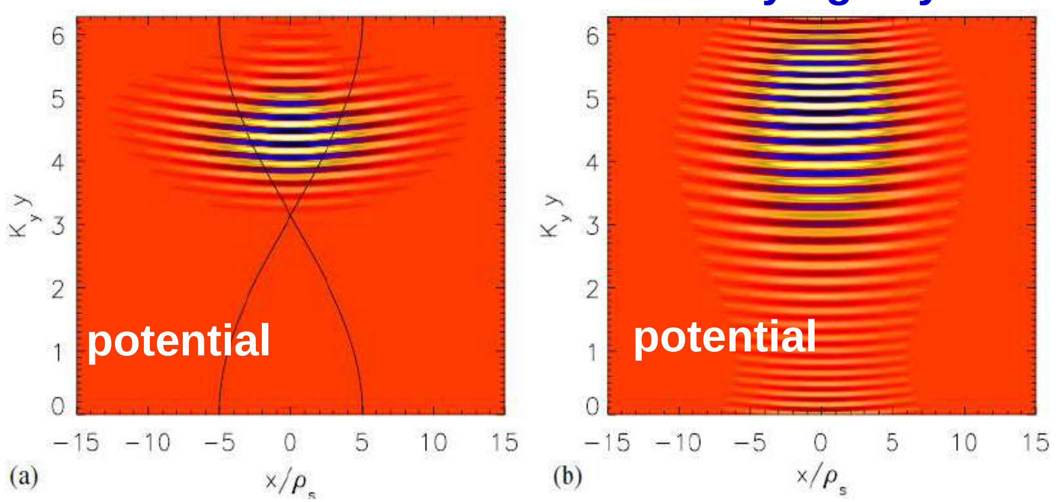

With island

W/o island BUT n/T varying in y

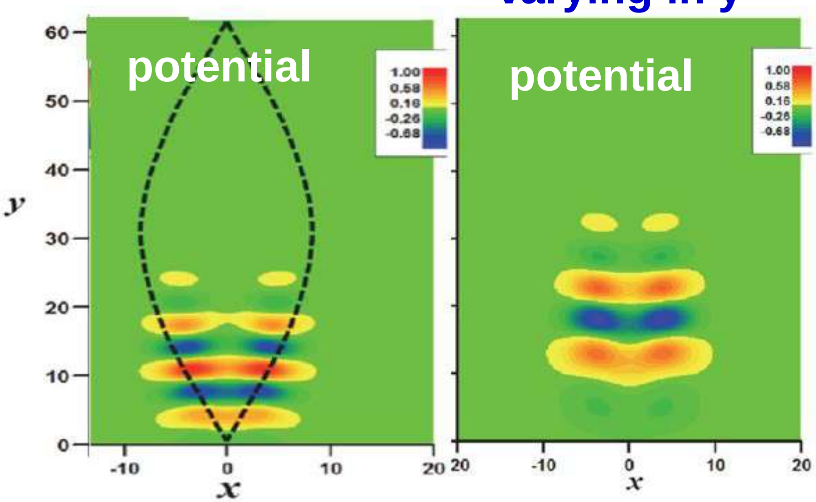

Simulation: MHD & micro-scale turbulence

➢ Fluid: MHD & interchange

Pressure island builds up

Muraglia, et al. PRL 2009

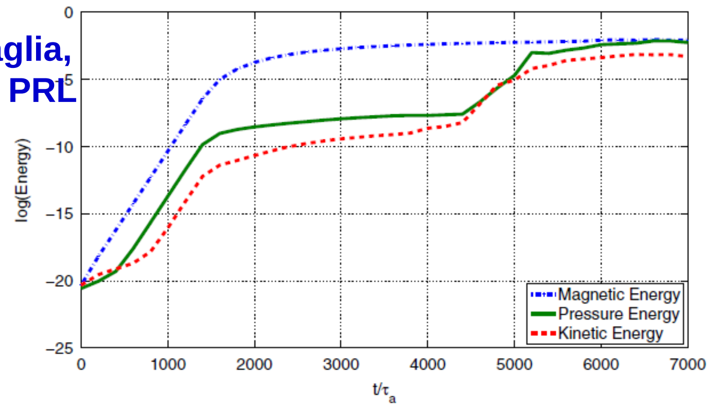

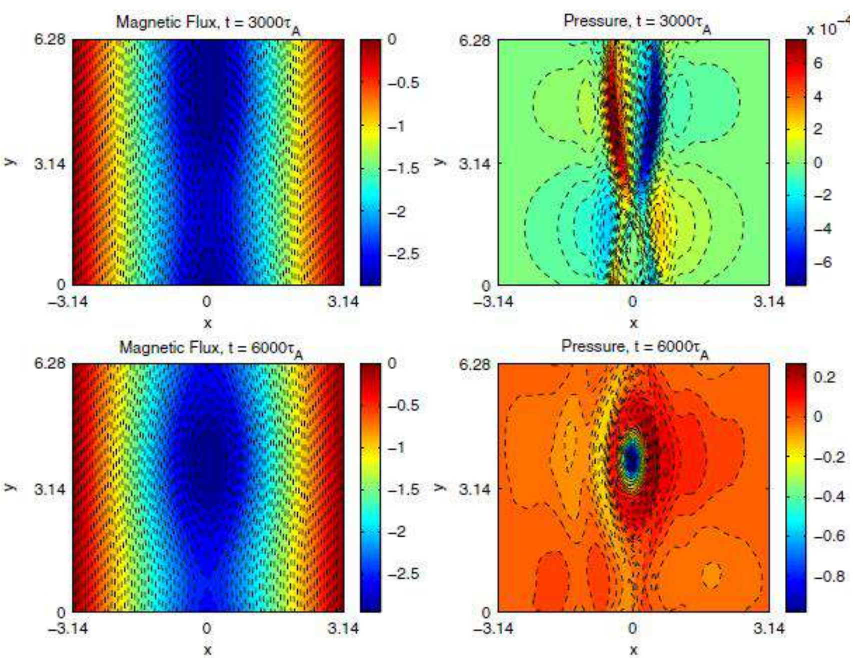

➢ Gyrokinetic: Tearing & ITG

Linear MHD structure is kept in EM ITG

Hornsby, et al. PoP 2015

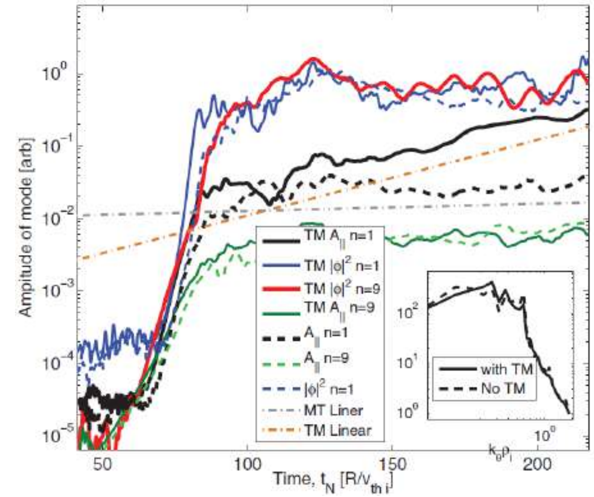

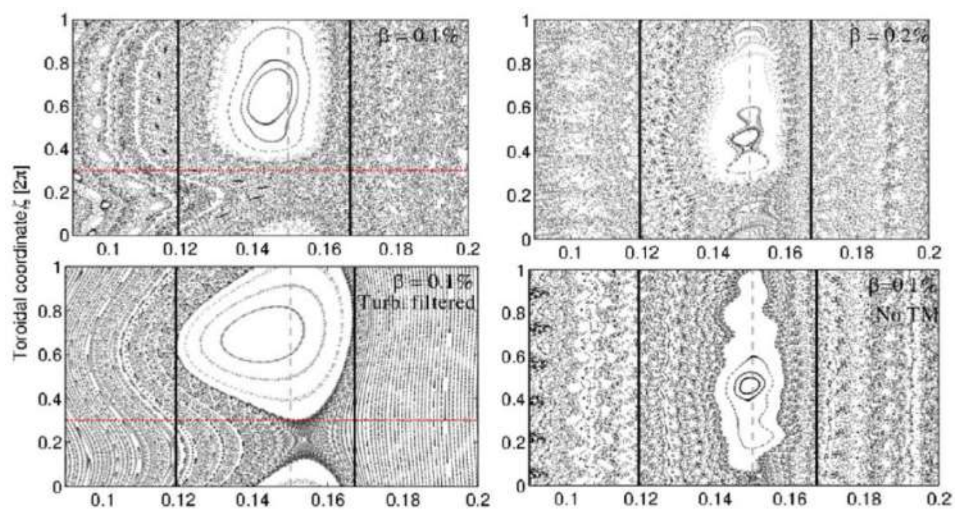

Poincare plot of magnetic field lines

Status on near-scale ITG-ETG problems

➢ **Gyro-fluid and gyrokinetic simulations on ITG & ETG**

Li, et al, PRL 2002
Candy, et al. PPCF 2007
Waltz, et al. PoP 2007
Gorler/Jenko, et al. PRL 2008
Howard, et al. PoP 2014
Maeyama, et al. PRL 2015
……

Local EM ITG + ETG

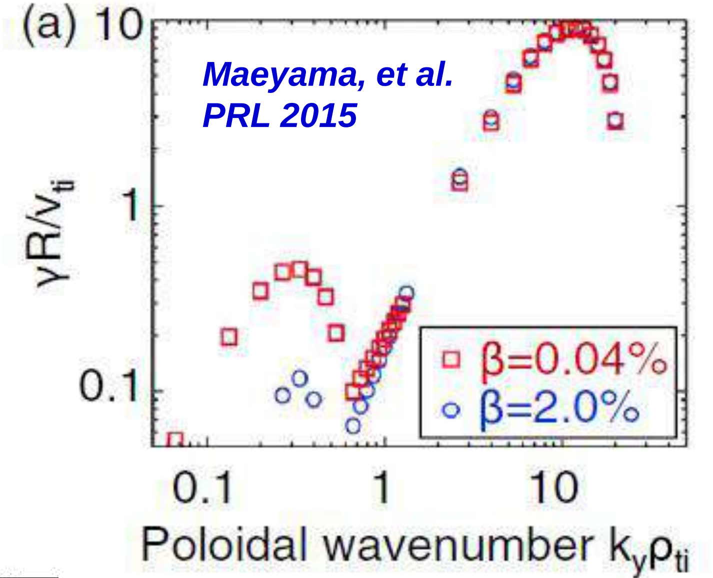

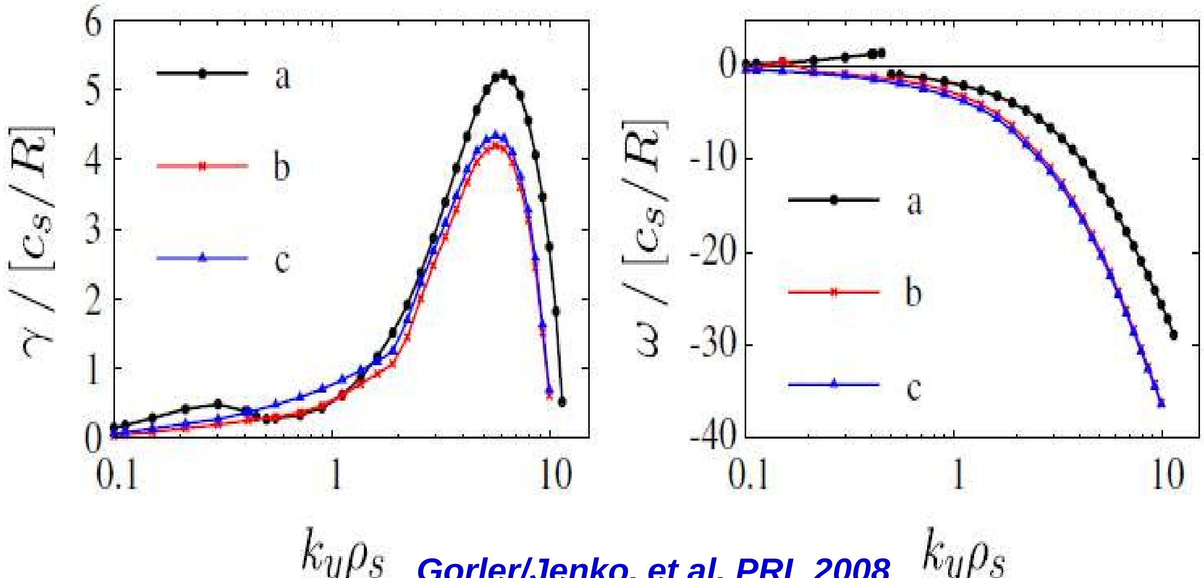

Gorler/Jenko, et al. PRL 2008

Local ES ITG + ETG

Status on ITG-ETG scale simulation

➢ Gyrokinetic simulations on ITG & ETG (local)

Gorler/Jenko, et al. PRL 2008

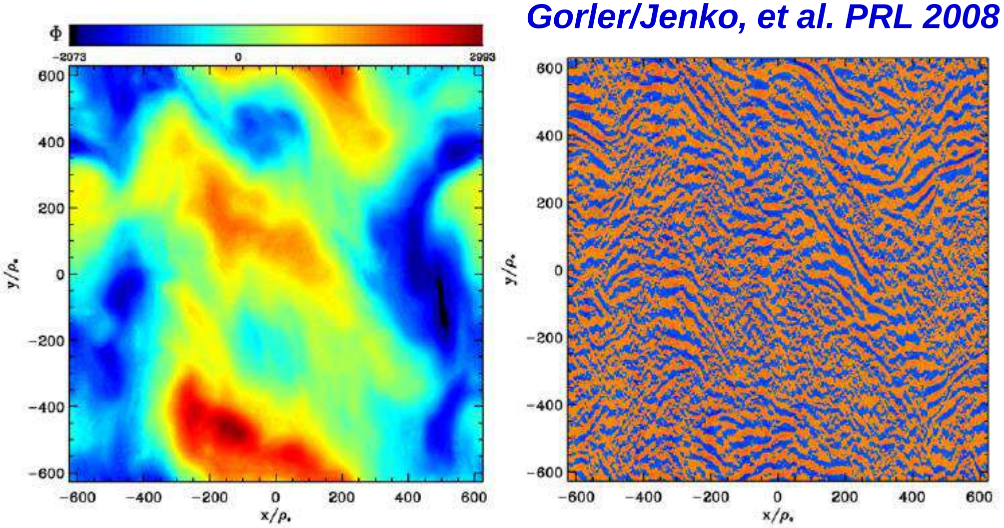

- ✓ **EM potential is dominated by large-scale, isotropic ITG vortices;**
- ✓ **and the same data with all k_y's < 2 modes filtered out, exhibiting the existence of small-scale ETG streamers.**

- ✓ **Suppression of e-scale turbulence by i-scale eddies, rather than by long-wavelength zonal flows.**

Maeyama, et al. PRL 2015

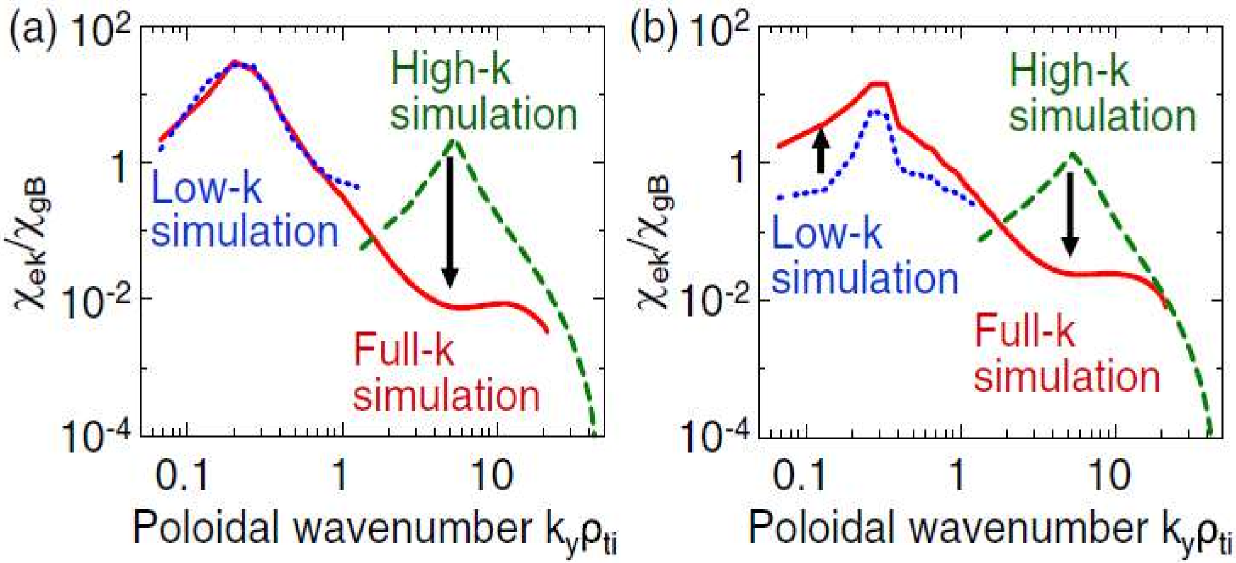

On multi-scale turbulence simulation

- ➢ **Full MHD-ion-electron scale gyrokinetic simulation on nonlinear interaction among MHD(island), ITG and ETG fluctuations is a goal in the future, BUT not realistic right now.**

  For example for local ITG+ETG only,

  Gorler/Jenko, et al. PRL 2008 **Time: m_i/m_e=400, ~100,000CPUh**

  Maeyama, et al. PRL 2015 **Time: m_i/m_e=1860, ~420h with 98,304 cores**

  For global ITG+ETG, Time: ?

  For MHD+ global ITG+ETG, Time: ??

- ➢ **Near-scale (MHD-ion; ion-electron) simulations are in progress; an intense, sustained effort is being made;**

  MHD-ion: Gyro-fluid & gyrokinetic

  Ion-electron: Gyrokinetic & gyro-fluid (TGLF ?)

- ➢ **Physics oriented reduced turbulence modeling is being developed;**

- ➢ **Simulation oriented numerical methodology is being advanced;**

- ➢ **Experimental validation & verification of simulation models is being conducted ……**

Outline

- Overview of multi-scale phenomena in MCF plasmas
  - ✔ Origin of multi-scale turbulence
  - ✔ Status of multi-scale turbulence simulation

- **Gyrofluid approach simulation for multi-scale turbulence**
  - ✔ **Gyrofluid model**
  - ✔ **Multi-scale interaction between MHD and micro-turbulence**
    - — **Magnetic island response to micro-turbulence**
    - — **Micro-turbulence response to MHD island dynamics**

- Gyrokinetic approach simulation for multi-scale turbulence
  - ✔ Gyrokinetic model
  - ✔ Full-*f* gyrokinetic Vlasov code—GKNET
  - ✔ GK ITG instability with an island
  - ✔ Flux-driven GK turbulence simulation on profile stiffness and ITB

- Summary

What is a Gyrofluid model?

- ➢ **Gyrofluid model ≈→ gyrokinetic physics**

Landau fluid
Gyro-Landau fluid

Classical fluid
+ Landau effects + Gyroradius effects
+Toroidal resonance + Trapped effects+……

- ➢ **Why Gyrofluid?**

Fluid picture (clear physics; analyzable;……)
+ save much CPU (turbulence Simulation is very huge……)
GF: 3D; GK: 3D+2D

- ➢ **Gyrofluid People:**

G.W.Hammett; W.Dorland; M.Beer; P.Snyder; S. Smith (PPPL); R.E.Waltz; G.M. Staebler (GA);
B. Scott (MP-IPP); N. Matter (LLNL); A. Brizard (Berkeley,CA); H. Sugama (NIFS);
M. Ottaviani; X. Garbet; B. Labit (Cadarache); J. Q. Li (SWIP); N. Miyato (JAERI); ……

How to obtain a Gyrofluid model?

- **Starting from gyrokinetic equation:**

(*Frieman & Chen PF1982; Hahm, PF1988; Lee, JCP1987*)

$$\frac{\partial}{\partial t}FB+\nabla\cdot\left[FB(\upsilon_{//}\hat{b}+J_0\vec{\upsilon}_E+\vec{\upsilon}_d)\right]$$
$$+\frac{\partial}{\partial t}\left[FB\left(-\frac{e}{m}\hat{b}\cdot\nabla J_0\Phi-\mu\hat{b}\cdot\nabla B+\upsilon_{//}(\hat{b}\cdot\nabla\hat{b})\cdot J_0\vec{\upsilon}_E\right)\right]=C(F)$$

- **Usual velocity-averaging procedure** $g_j(t,\vec{X})=\frac{1}{N}\int_{\vec{\upsilon}}d\upsilon\,\upsilon^j F(t,\vec{X},\vec{\upsilon})$

- **Difference:** closure relation for higher moments with linear benchmark

  - ✓ Gyroradius effects: model the highest moments by lower moments
  - ✓ Landau effects: add damping proportional to $|k_{//}|$. Typical parallel Hammett & Perkins closure: $q_{//}=-i\sqrt{8/\pi}\,k_{//}T/|k_{//}|$
  - ✓ Toroidal effects: add damping proportional to $|\omega_d|$; …
  - ✓ Trapped particle (TGLF)

References: **Hammett & Perkins, PRL1991; Waltz, *et al*., PoP1997; Dorland & Beer & Snyder, PhD theses; Scott, PoP2000; Sugama, *et al*., PoP2003; Staebler, *et al*., PPCF2004; Mattor, PoP1998; Brizard, PF1995;**

Landau-Fluid model with ZF-GAM damping

➢ Landau-fluid ITG model with GAM closure

$$\frac{d}{dt}\nabla_\perp^2\phi-\frac{1}{n_{eq}}\frac{dn}{dt}=-T_{eq}\frac{a}{n_{eq}}\frac{dn_{eq}}{dr}(1+\eta_i)\nabla_\theta\nabla_\perp^2\phi-\frac{a}{n_{eq}}\frac{dn_{eq}}{dr}\nabla_\theta\phi+\nabla_{//}\upsilon_{//}-\omega_d\cdot\left(\phi+T_i+\frac{T_{eq}}{n_{eq}}n\right)+D\nabla_\perp^4\phi$$

$$\frac{d}{dt}\upsilon_{//}=-\nabla_{//}T_i-\frac{T_{eq}}{n_{eq}}\nabla_{//}n-\nabla_{//}\phi+\mu\nabla_\perp^2\upsilon_{//}$$

$$\frac{d}{dt}T_i=T_{eq}\frac{a}{n_{eq}}\frac{dn_{eq}}{dr}\eta_i\nabla_\theta\phi-(\Gamma-1)T_{eq}\nabla_{//}\upsilon_{//}-\boxed{\gamma_{LD}\sqrt{\frac{8T_{eq}}{\pi}}\left|k_{//}\right|T_i}$$
$$+T_{eq}\omega_d\cdot\left((\Gamma-1)\phi+(2\Gamma-1)T_i+(\Gamma-1)\frac{T_{eq}}{n_{eq}}n\right)+\chi\nabla_\perp^2T_i$$

➢ New Landau closure relation (*empirical*):

$$\gamma_{LD}=\begin{cases}\Gamma-1 & \text{for ITG}\\ 3\Gamma & \text{for GAM}\end{cases}\qquad \nabla_{//}=ik_{//}=\begin{cases}\varepsilon\left(\dfrac{\partial}{q\partial\theta}-\dfrac{\partial}{\partial\varphi}\right) & \text{for ITG}\\ \Gamma\left(\dfrac{q}{1.6}\right)^{1/4}\varepsilon^{1/2}\dfrac{\varepsilon\partial}{q\partial\theta} & \text{for GAM}\end{cases}$$

ZF-GAM damping in Landau-Fluid model

- **Residual level of zonal flows due to the collisionless damping**

  [Rosenbluth & Hinton, PRL1998]

$$\frac{V_{ZF}}{V_{ZF0}} = \left(1 + \frac{1.6q^2}{\varepsilon^{1/2}}\right)^{-1}$$

- **Initial flow:** $V_{ZF0}(t=0) = \sin(0.19x)$

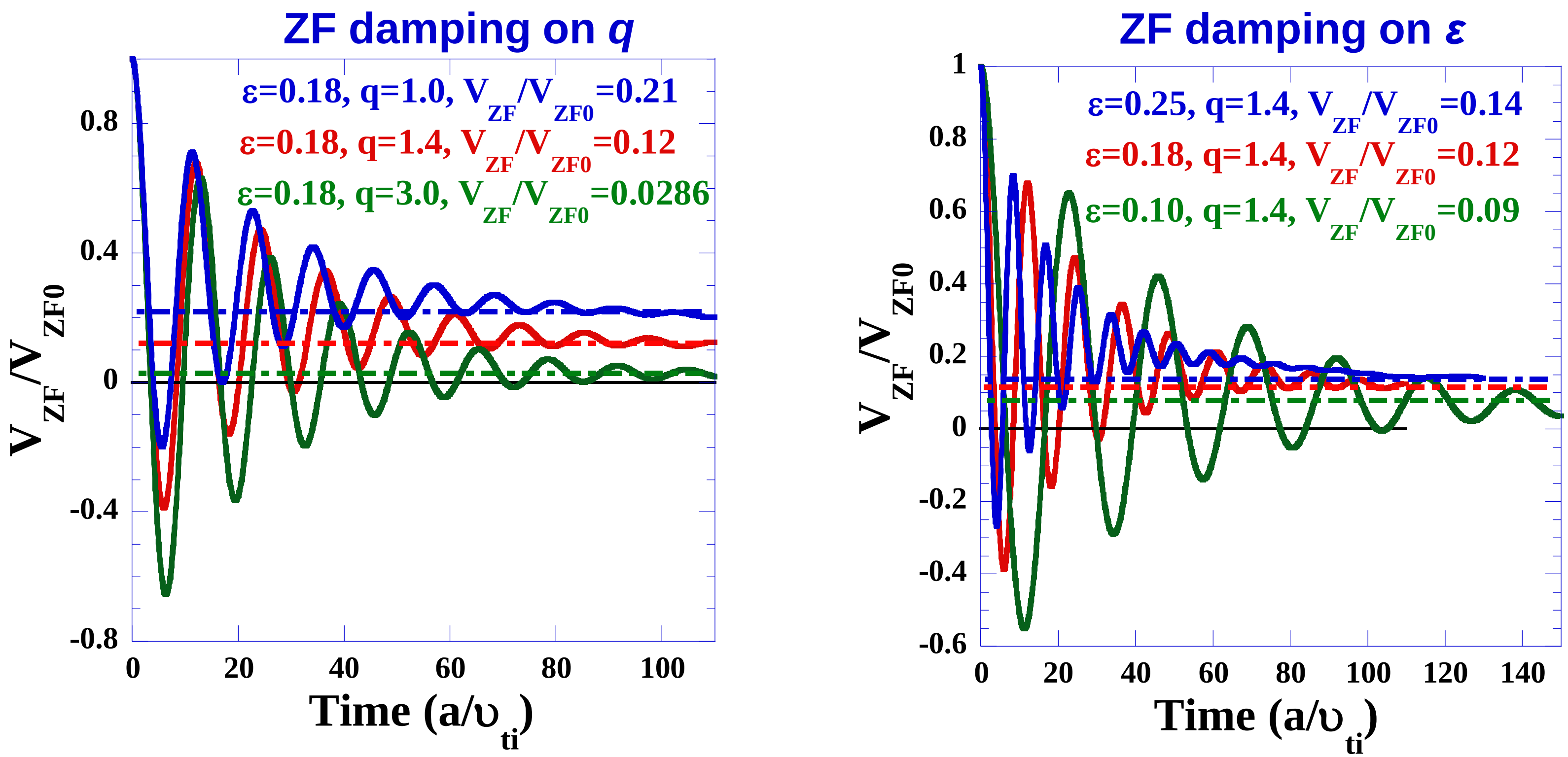

✓ **ZF damping and the residual levels are well reproduced as the gyrokinetics.**

Li et al. CiCP2008

Nonlinear excitation of GAM by ITG

➢ **Wavelet energy analysis for nonlinear excitation of GAM**

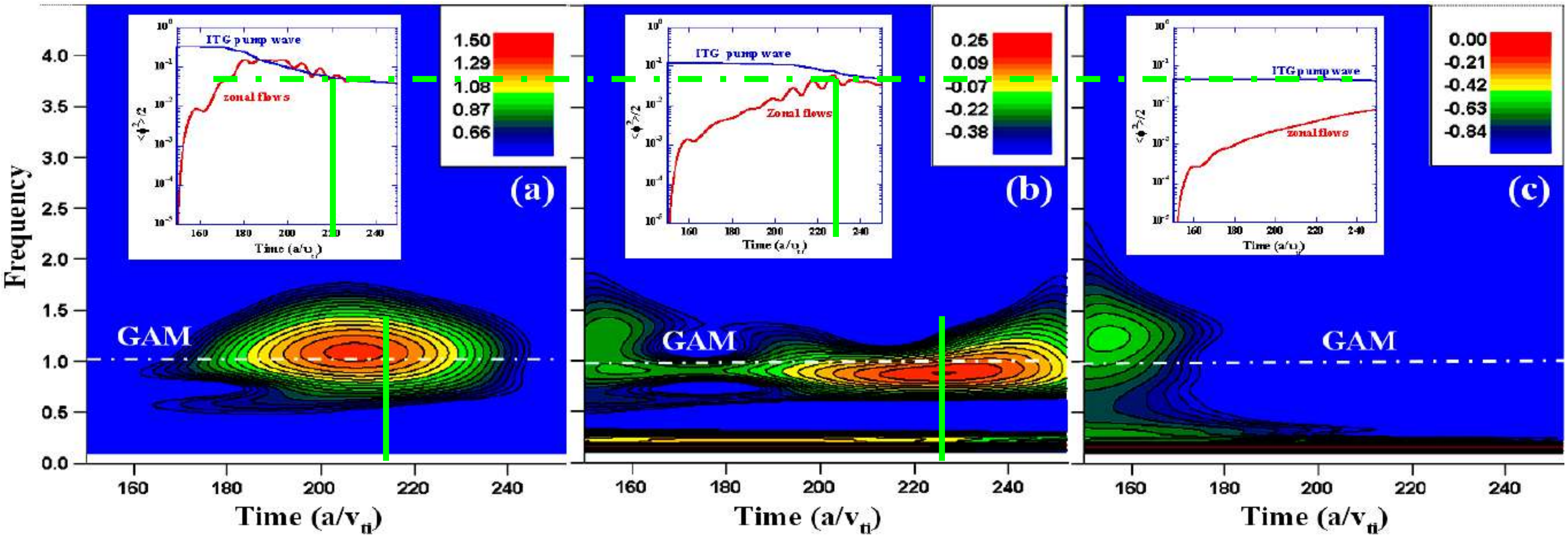

GAM instability | weak GAM instability | no GAM instability

✓ **GAM instability: occur in ITG fluctuations with larger amplitude; is determined by the competition between nonlinear driving force and the Landau damping;**

✓ ***Amplitude threshold:*** **pump amplitude threshold of GAM instability is higher than that of ZF instability;**

Radial structure of GAMs

➢ **GAMs are characterized by finite frequency and radial structure**

Two simulations with & w/o GAMs

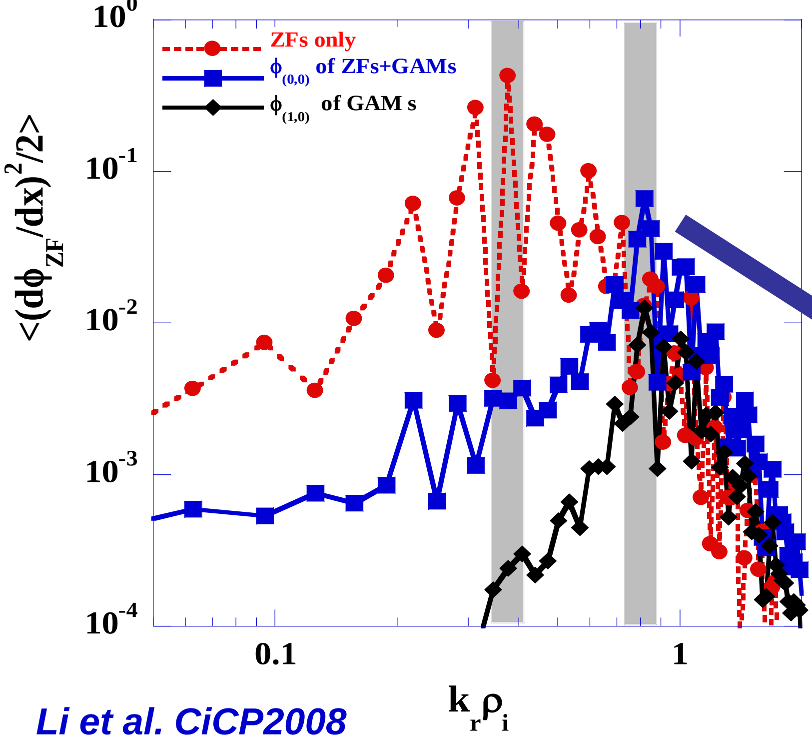

Li et al. CiCP2008

Radial distribution of zonal flow frequency spectra

$k_r \rho_i \approx 1.0$

ρ_* = 0.0125 **ρ_* =0.005** **ρ_* = 0.003**

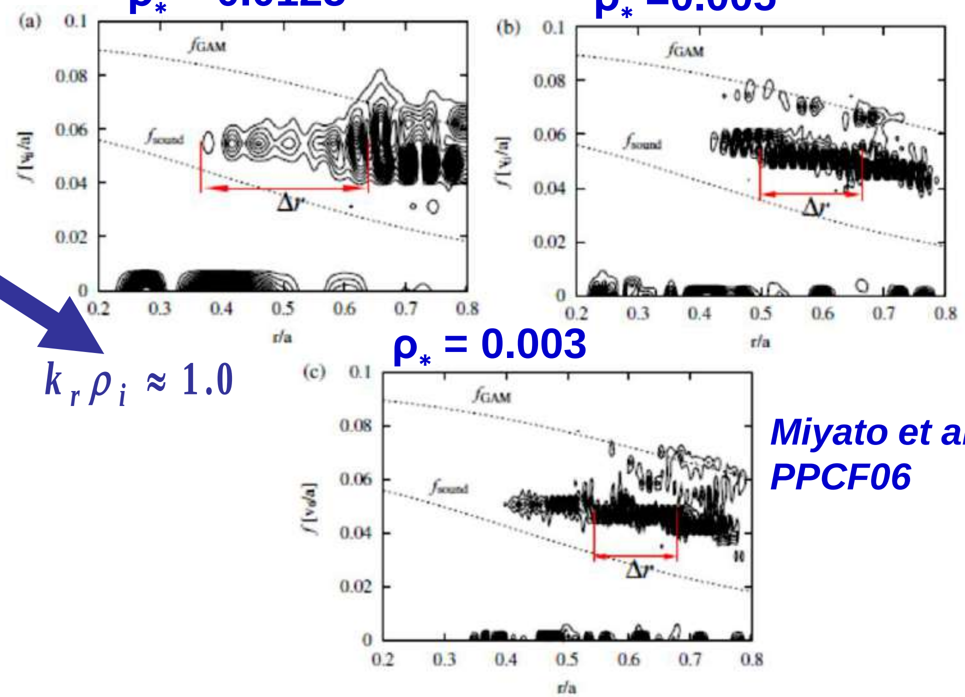

Miyato et al. PPCF06

✓ **Radial structure of GAMs is shorter than that of the pure zonal flow fluctuation, about** $k_r\rho_i \leq 1.0$

Multi-scale MHD & ITG nonlinear interaction

➢ possible direct & indirect cross nonlinear processes

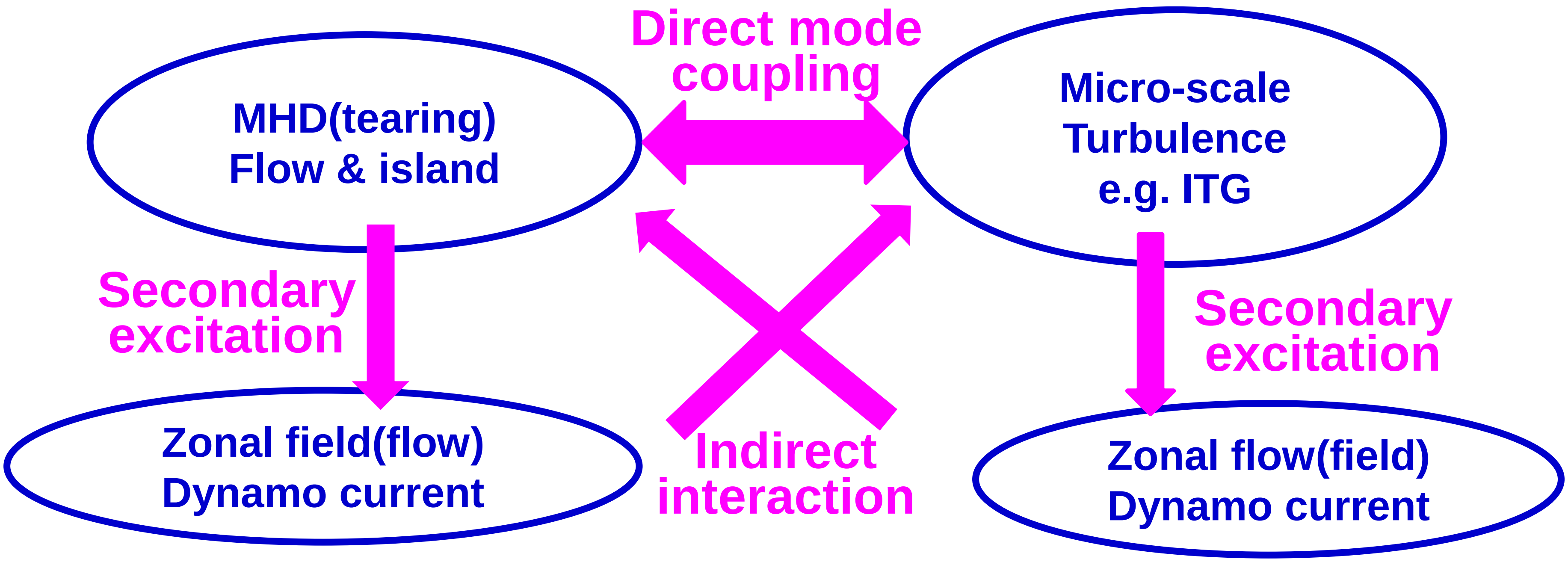

✓ MHD response to micro-turbulence(ITG);

✓ ITG response to MHD island dynamics

Gyrofluid model for mixed MHD & ITG

- **Modeling equ. – 5-field EM Landau-fluid ITG with MHD in slab**

$$
\begin{cases}
\partial_t \nabla_\perp^2 \phi = -[\phi, \nabla_\perp^2 \phi] + (1+\eta_i)\partial_y \nabla_\perp^2 \phi + \nabla_{//} j_{//} + D_U \nabla_\perp^4 \phi \\
\partial_t n = -[n, \phi] + \partial_y \phi - \nabla_{//} \upsilon_{//i} + \nabla_{//} j_{//} + D_n \nabla_\perp^2 n \\
\beta \partial_t A_{//} = -\nabla_{//}\phi + \tau \nabla_{//} n + \beta\tau \partial_y A_{//} - \eta j_{//} + \boxed{\sqrt{\frac{\pi}{2}\tau \frac{m_e}{m_i}} \left|\nabla_{//}\right| (\upsilon_{//i} - j_{//})} \\
\partial_t \upsilon_{//i} = -[\phi, \upsilon_{//i}] - 2\nabla_{//} n - \nabla_{//} T_i + \beta(2+\eta_i)\partial_y A_{//} - \eta j_{//} + D_\upsilon \nabla_\perp^2 \upsilon_{//i} \\
\partial_t T_i = -[\phi, T_i] - \eta_i \partial_y \phi - (\gamma - 1)\nabla_{//} \upsilon_{//i} - \boxed{(\gamma - 1)\sqrt{\frac{8}{\pi}} \left|\nabla_{//}\right| T_i} + D_\upsilon \nabla_\perp^2 T_i
\end{cases}
$$

$$
j_{//} = -\nabla_\perp^2 A_{//} \qquad A_{//} = -\psi
$$

Landau damping terms

- **Mean parameters**

$$
\begin{cases}
\eta_i & \text{for ITG fluctuations} \\
\eta & \text{for MHD (kink-tearing) modes}
\end{cases}
$$

Configuration models

➢ Equilibrium magnetic field models

Model I

$$B_{y2} = B_0 \hat{s} \lambda_2 \frac{\tanh(x/\lambda_2)}{\cosh^2(x/\lambda_2)}$$

$$k_{//} = \frac{\vec{k}\cdot\vec{B}}{B} = k_z - k_y \hat{s} \lambda_1 \frac{\sinh(x/\lambda_1)}{\cosh^3(x/\lambda_1)}$$

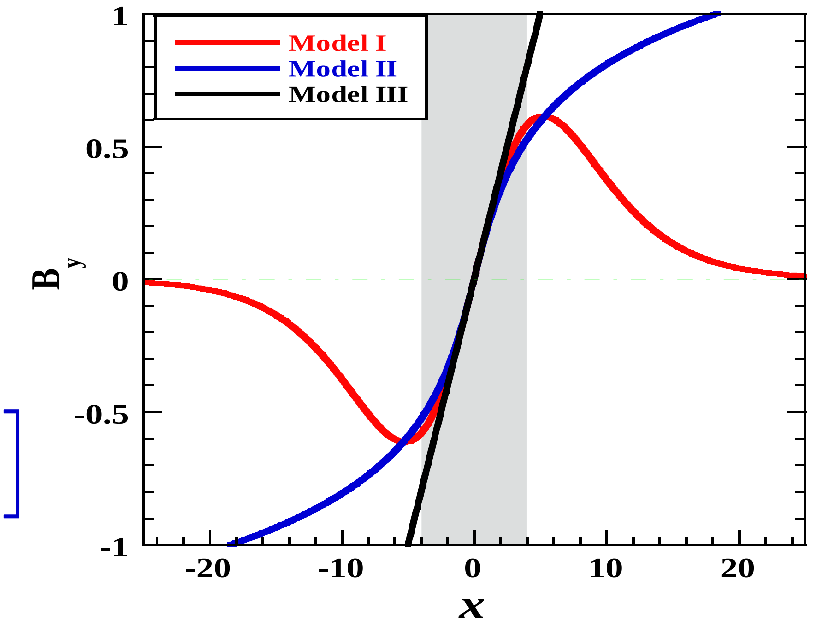

Model II

$$B_{y1} = B_0 \hat{s} \lambda_1 \log\left[\left(x/\lambda_1\right) + \sqrt{1+\left(x/\lambda_1\right)^2}\right]$$

Model III (for reference) $B_{y3} = B_0 \hat{s} x$

Cross-scale MHD and ITG instability

➢ Co-existence of MHD and ITG

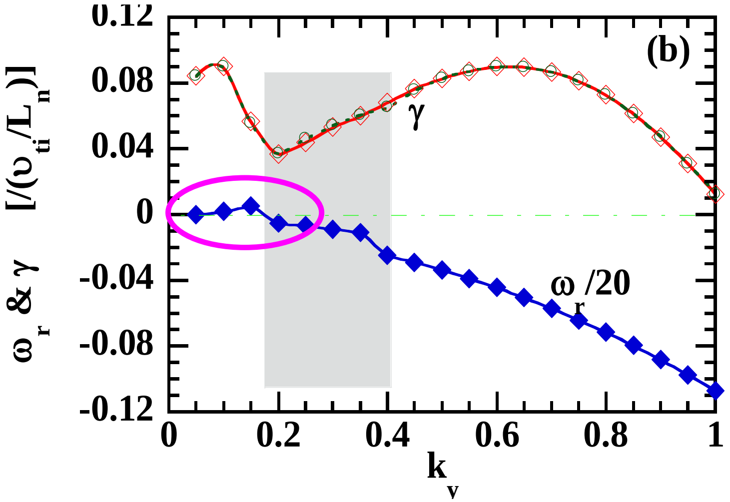

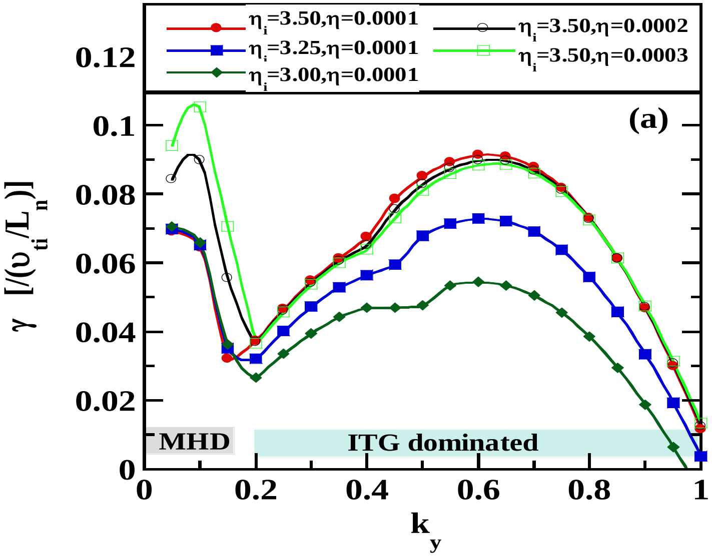

➢ Eigen functions

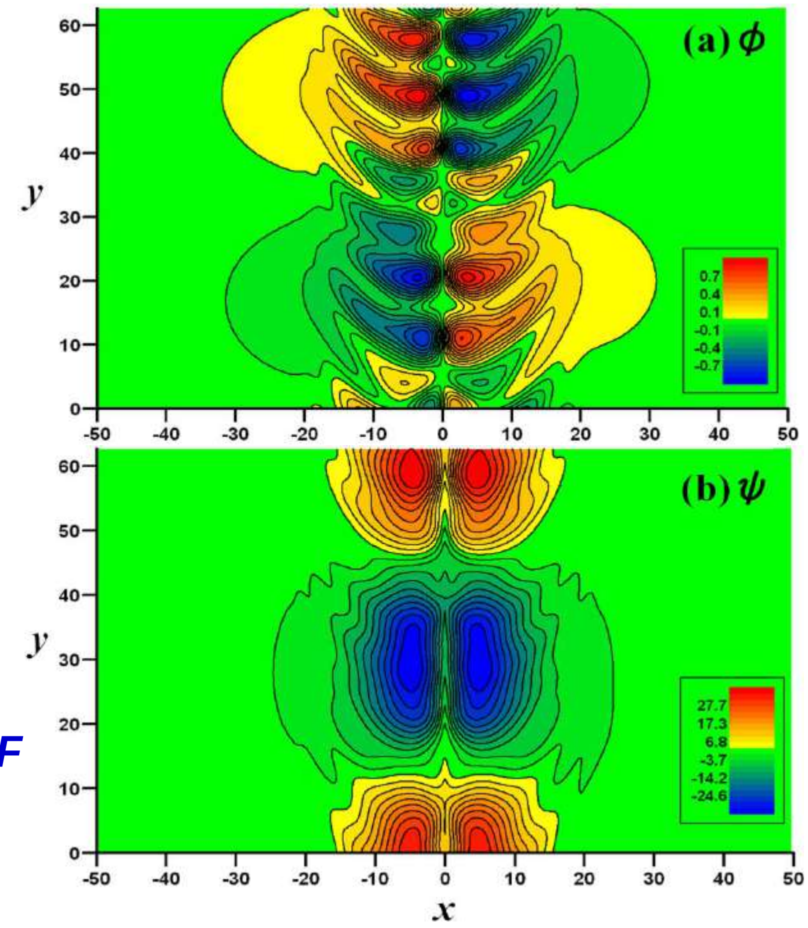

Li, et al, NF 2009

✔ **MHD/ITG coexist and propagate in electron/ and ion diamagnetic direction, respectively.**

Multi-scale interaction: ITG affects MHD

$\gamma_{MHD} < \gamma_{ITG}$ $\eta = 1 \times 10^{-4}$ $\eta_i = 2; \beta = 0.01; \hat{s} = 0.2; L_x = 100; L_y = 20\pi$

Kinetic energy

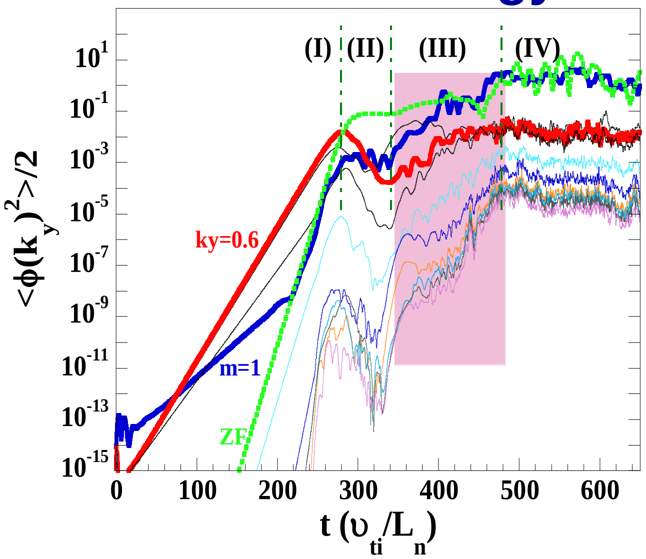

Magnetic energy

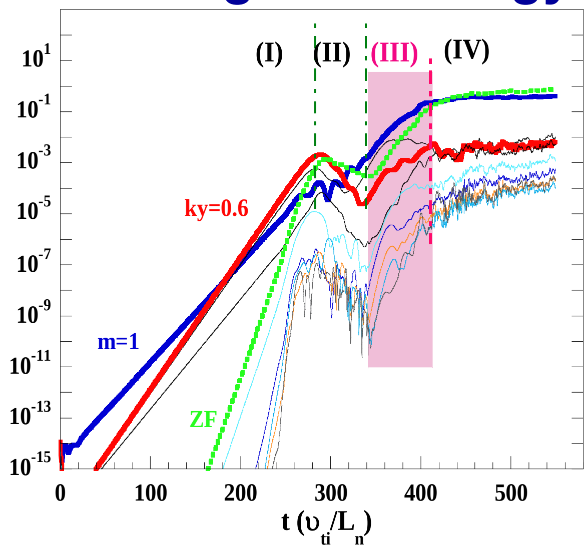

Spectra in (II) (IV)

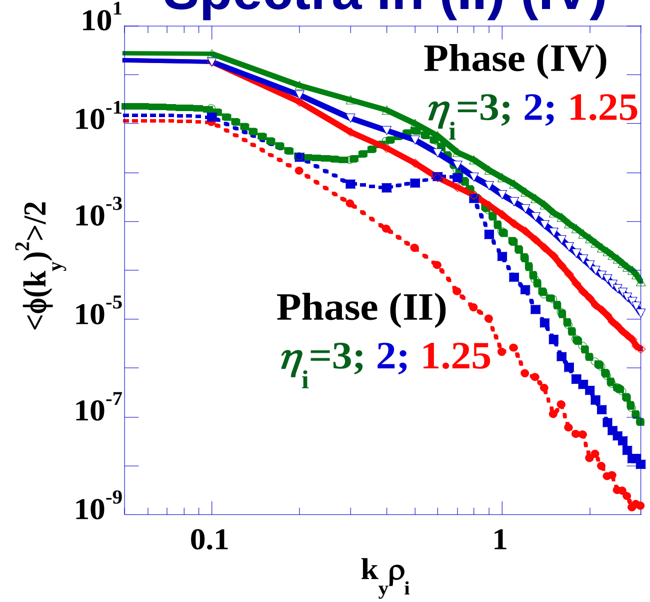

✔ **Four phases for mixed turbulence evolution:**

- **(I) linear;**
- **(II) first saturation;**
- **(III) second growing;**
- **(IV) quasi-steady state;**

✔ **As ITG increases, turbulent spectrum is enhanced for all components, and is characterized by MHD fluctuation.**

Zonal flow dynamics in cross-scale MHD-ITG

➢ **Multi-scale MHD and ITG simulation: oscillatory zonal flows**

Time evolution of zonal flow structures

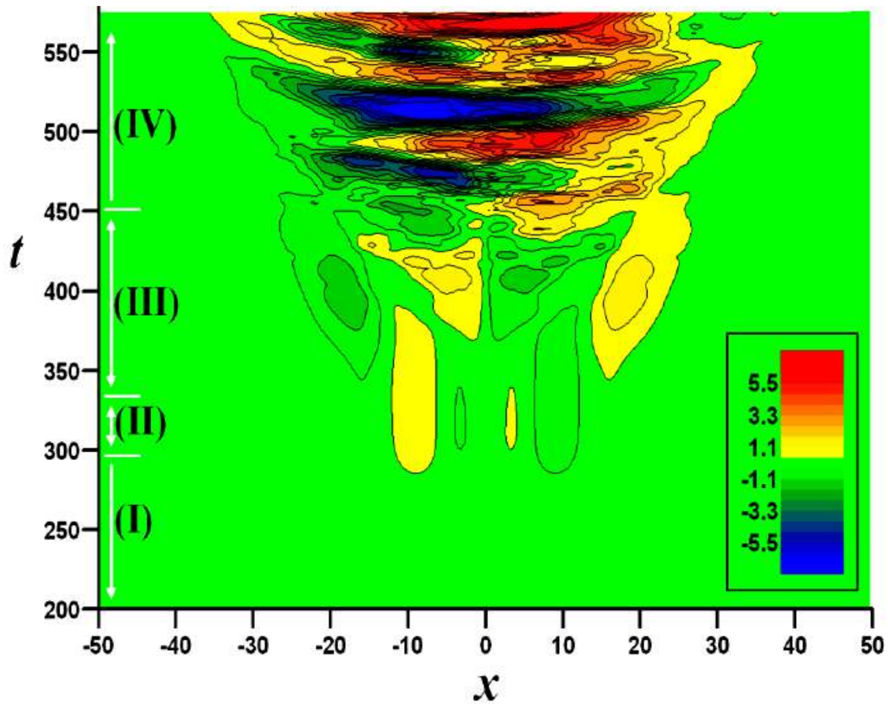

Parametric dependence of ZF frequency

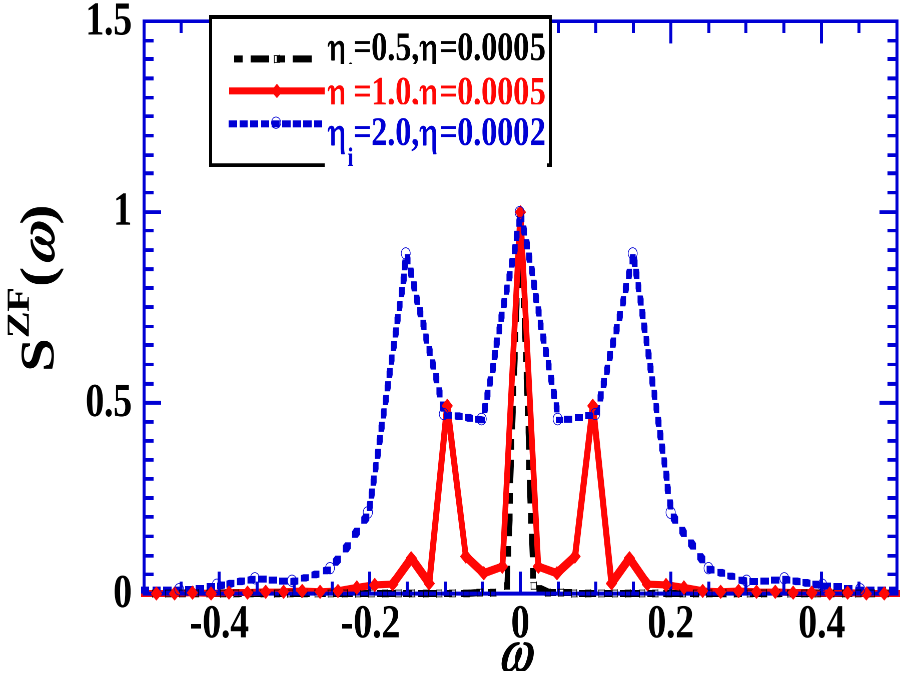

✔ **oscillatory ZF with frequency about (0.1~0.2)ω_* , weakly depending on η_i & η**

Magnetic island seesaw

➢ Magnetic island seesaw in multi-scale MHD and ITG

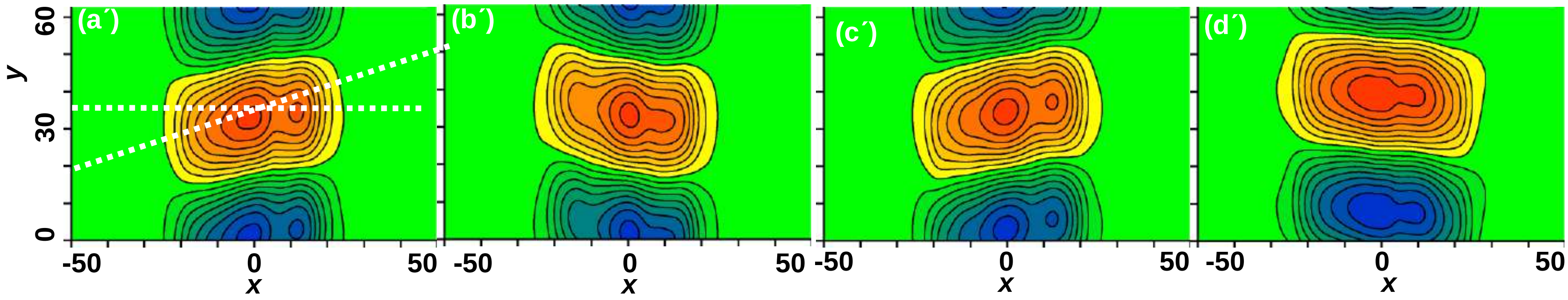

➢ Electromagnetic torque

$$T_{EMy}\hat{e}_z = \iint_{xy} x\hat{e}_x \times (\vec{j}\times\vec{B})_y \, dx\, dy / L_x L_y$$

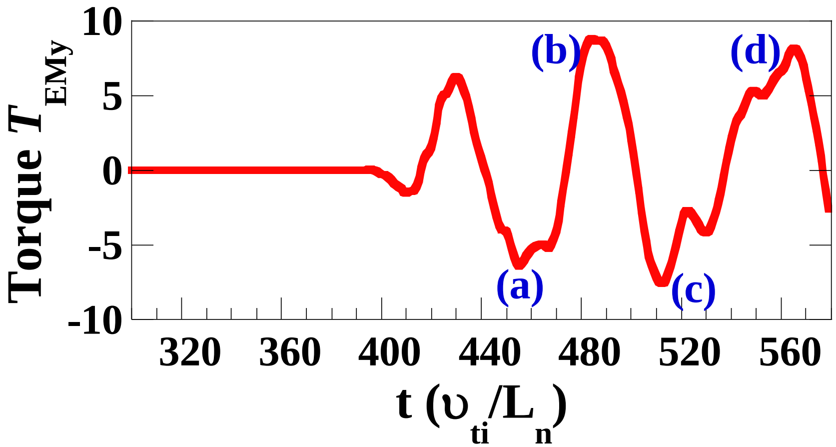

✔ Stronger ITG drives larger EM torque; leads to island seesaw;

✔ EM torque has same oscillation as the seesaw

Minimal model

- **Minimal model with essential ingredients:**

  reduced MHD +ITG mode

$$\begin{cases} \partial_t \nabla_\perp^2 \phi = -[\phi, \nabla_\perp^2 \phi] + \nabla_{//} j_{//} \\ \beta \partial_t A_{//} = -\nabla_{//} \phi - \eta j_{//} \end{cases}$$

➡ **For MHD such as tearing, kink …**

$$\boxed{\phi = \tilde{\phi}^{MHD}(t,x,y) + \phi^{ITG}(t,x,k_y^{ITG})}$$

➡ **ITG eigen mode**

(Li *et al*, PoP 1998, 2004)

$$\phi^{ITG}(t,x,k_y^{ITG}) \sim \hat{\phi}^{(n)}(x) e^{-i\Omega t + ik_y^{ITG} y}$$

$$\hat{\phi}^{(n)} = H_n\left(\sqrt{i\frac{L_n|\hat{s}|}{\Omega R q_0}}\,\hat{x}\right)\exp\left(-i\frac{L_n|\hat{s}|}{2\Omega R q_0}\hat{x}^2\right)$$ **with** $$-k_y^2 + \frac{1-\Omega}{\Omega+K} = i\frac{L_n|\hat{s}|}{\Omega R q_0}(2n+1)$$

Evidence of cross-scale dynamo current

➢ **Current snapshots in modeling simulations**

Li/Kishimoto POP 2013

With radial even-parity ITG **With radial odd-parity ITG**

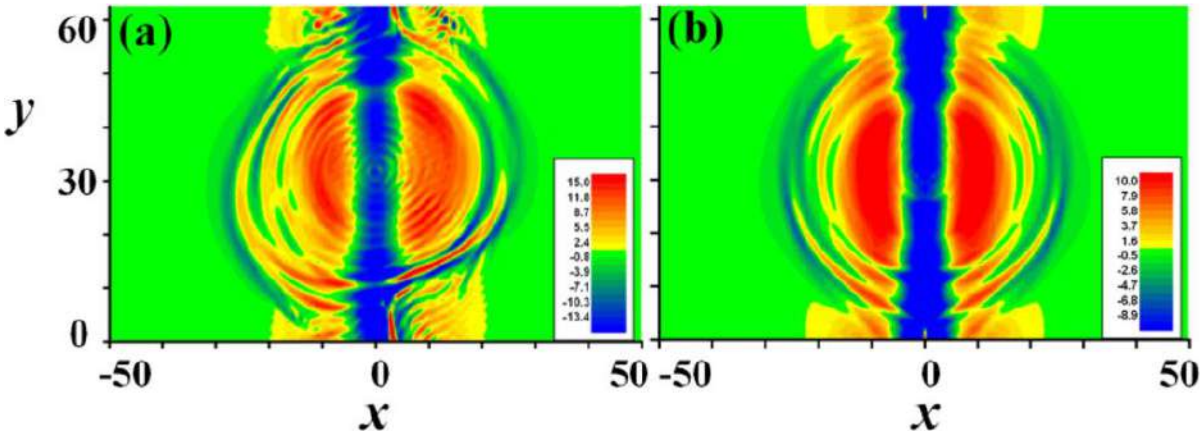

✔ **Radially even-parity ITG potential induces asymmetric dynamo current, which can drive oscillatory EM torque.**

➢ **EM torque oscillation in direct and modeling simulations**

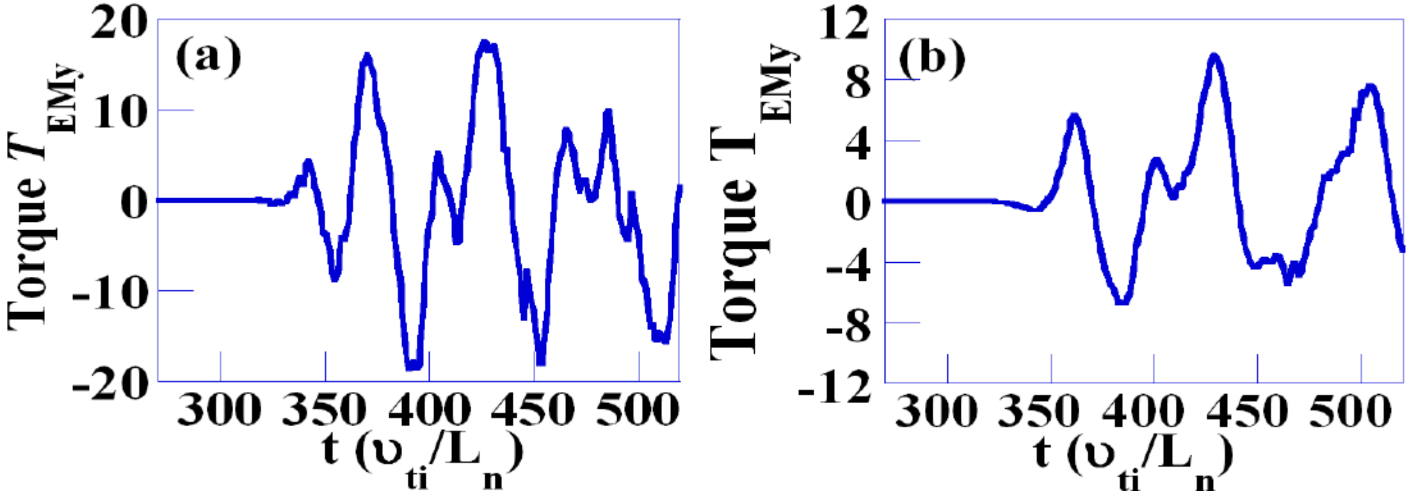

Multi-scale MHD & ITG nonlinear interaction

- possible direct & indirect cross nonlinear processes

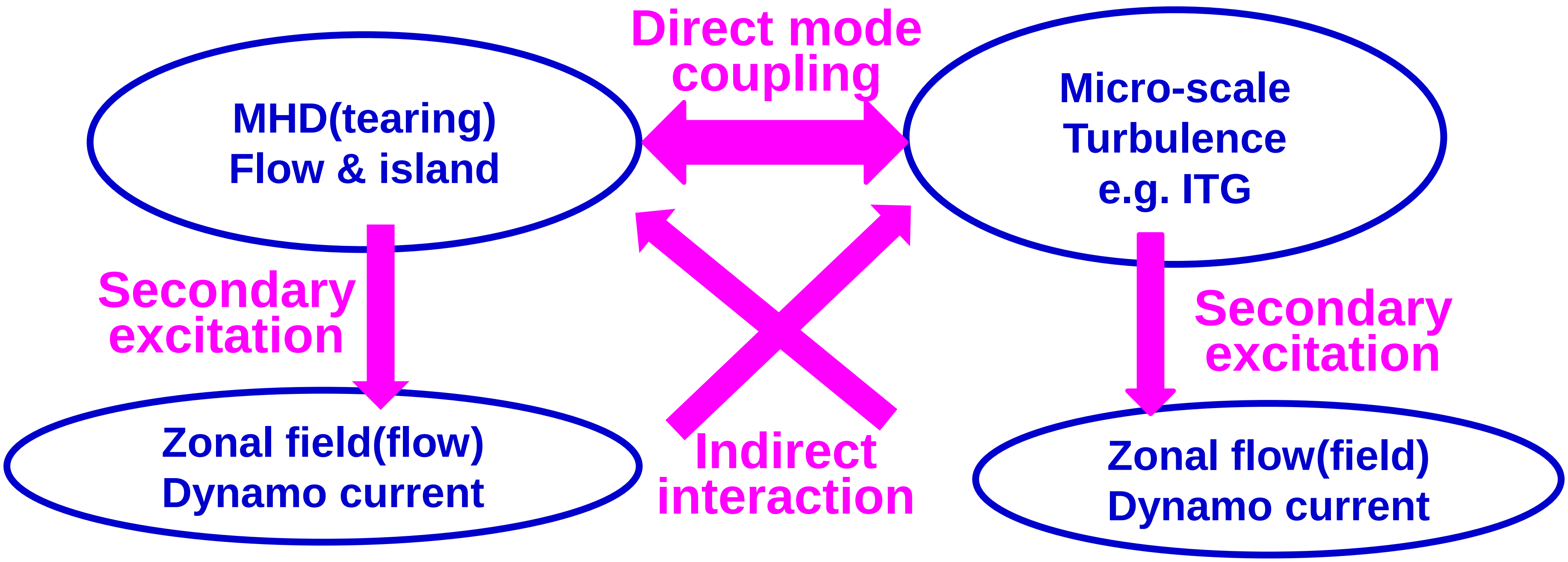

✓ MHD response to micro-turbulence(ITG);

✓ ITG response to MHD island dynamics

Multi-scale MHD & ITG turbulence

➢ Multi-scale MHD & ITG turbulence with **linearly stable** ITG

$\gamma_{MHD} > 0$

$\gamma_{ITG} < 0$

$\eta_i = 0.75$
$\eta = 1 \times 10^{-3}$
$\beta = 0.01$
$\hat{s} = 0.2$

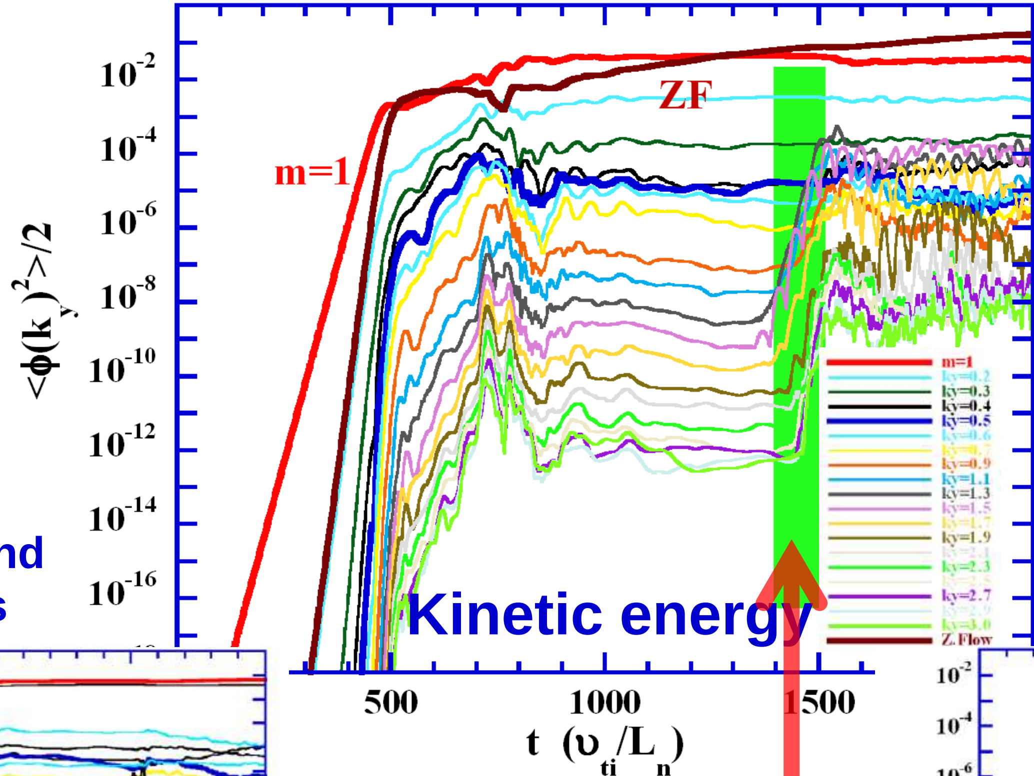

✔ Magnetic island slowly increases

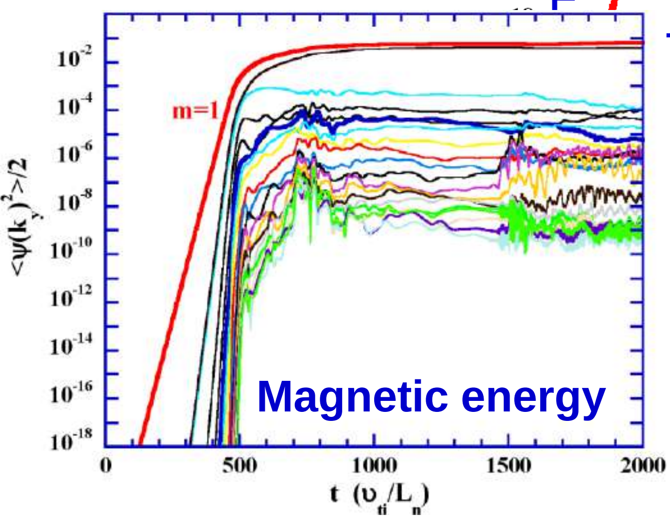

✔ New secondary instability (Short wavelengths with same growth rate; electrostatic)

✔ Temperature island collapses

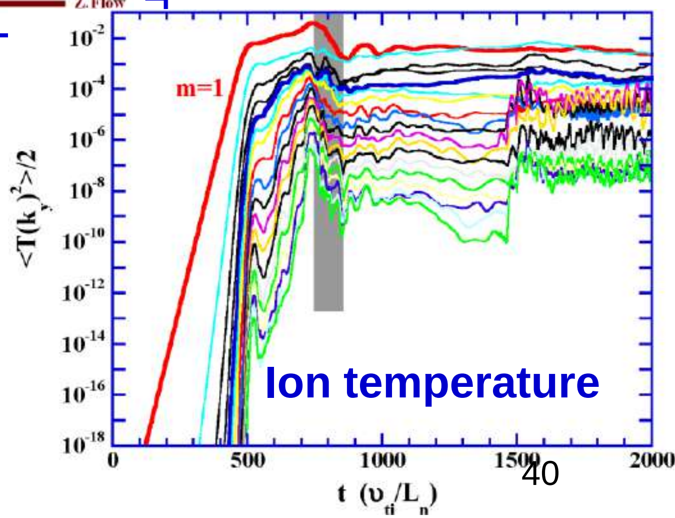

A new instability (Animation)

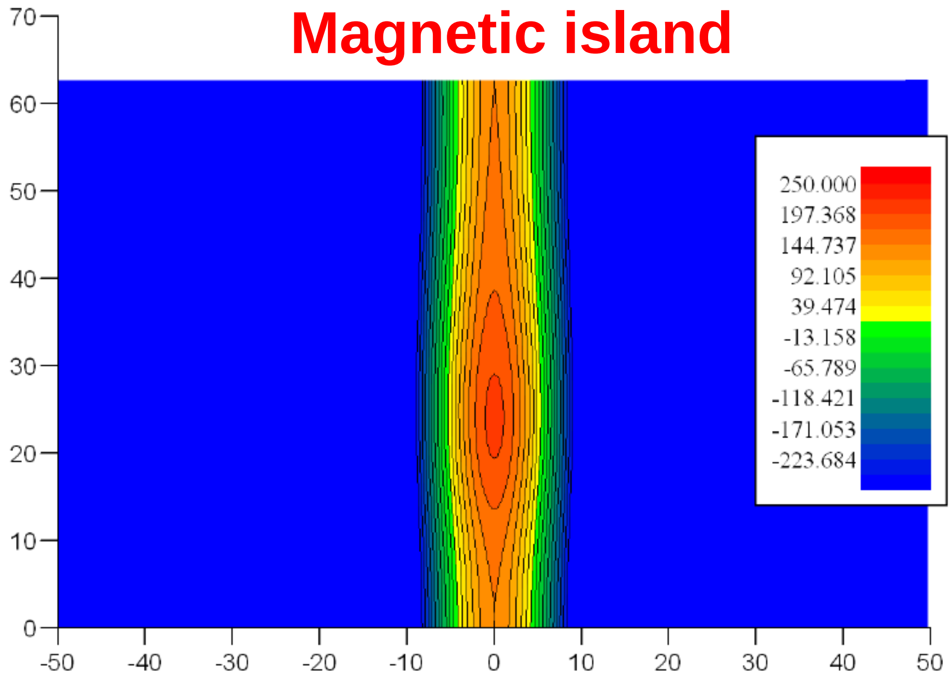

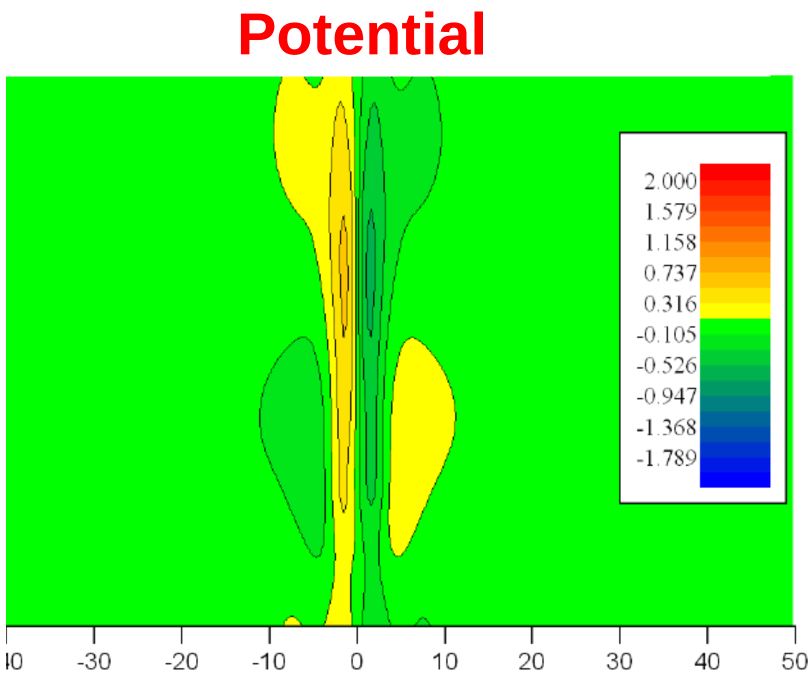

✔ **New instability is excited in the boundary region around the separatrix, global-type structure propagating along ion diamagnetic drift direction;**
✔ **Magnetic island induced ITG – MITG.**

Dispersion characteristics of MITG

➢ Energy spectra of MITG

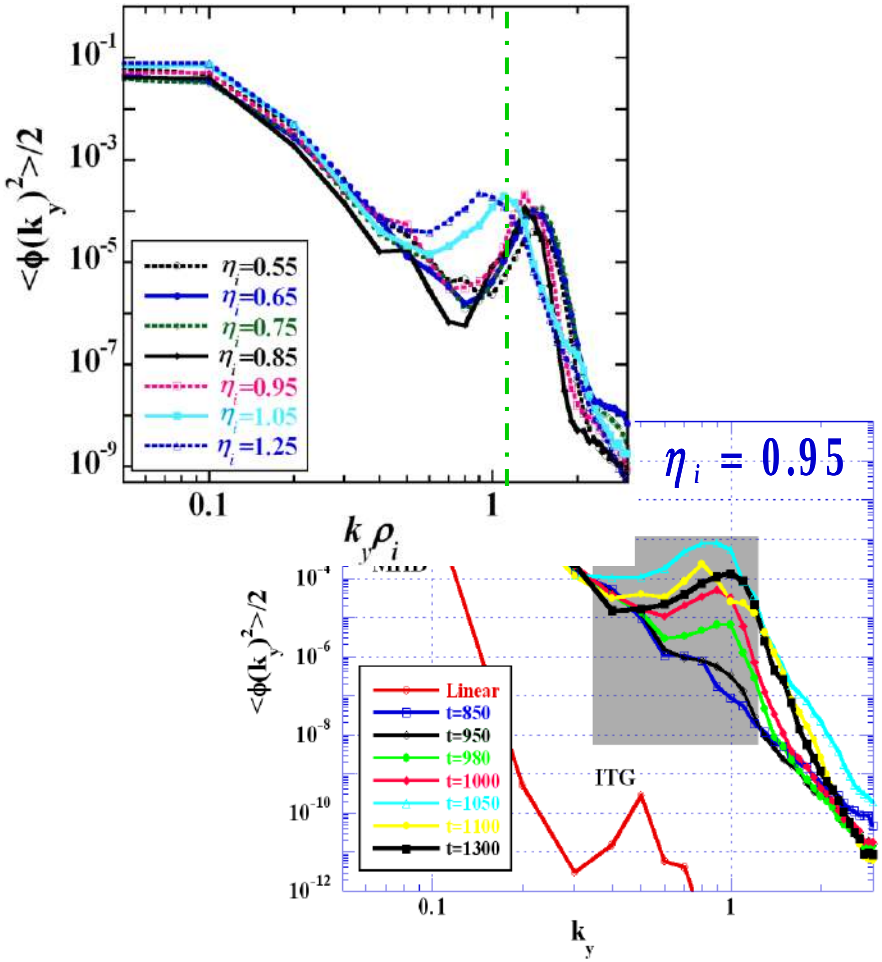

✔ MITG drives a spectral hump around k_y~1, but almost no effect on low-k_y region.

➢ Growth rate vs η_i

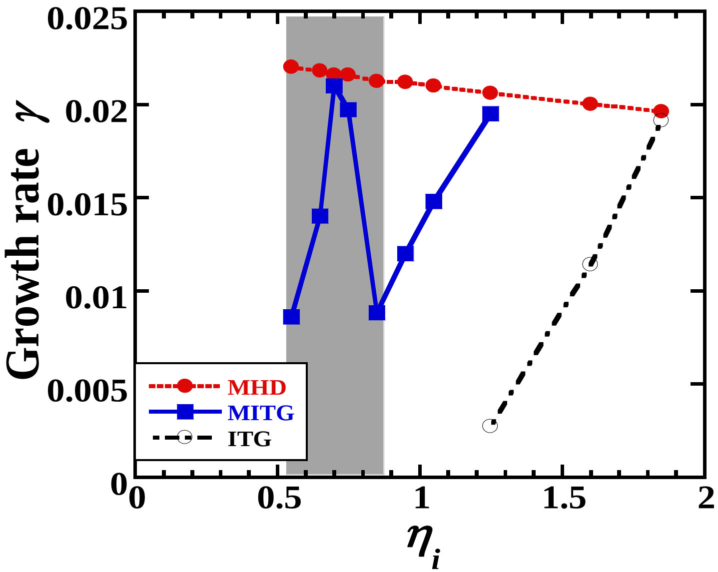

✔ MITG has lower stability threshold of η_i. Why?*(If frozen-in law is satisfied, no T_i gradient inside magnetic island, then no ITG)*

✔ Dependence of MITG growth rate on η_i is non-monotonic. Why?(what determines the instability?)

Excitation condition of MITG mode

➢ MITG is subject to magnetic and temperature island dynamics

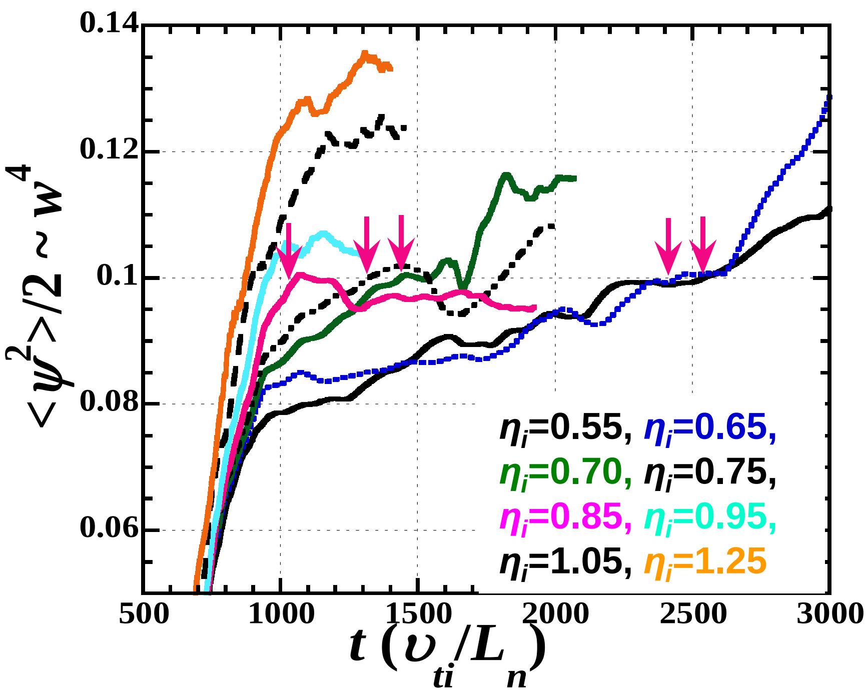

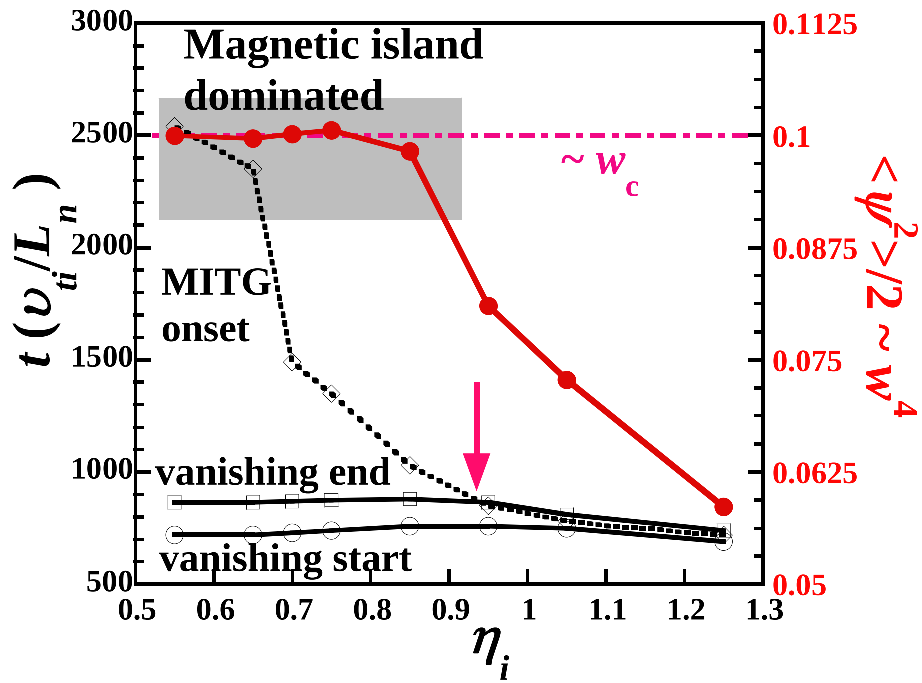

✔ A critical island width w_c for MITG excitation after T_i island collapse.

✔ MITG is excited during T_i island collapse for $\eta_i \gtrsim 0.9$; otherwise, after T_i island collapse as magnetic island approaches w_c.

Li/Kishimoto POP 2014

Probable mechanism of T_i island collapse

➢ Heat flux evolution

Before T_i island collapse

Boundary region tends to thicken

During T_i island collapse

Heat flux crosses magnetic island

After T_i island collapse

MITG enhances heat flux

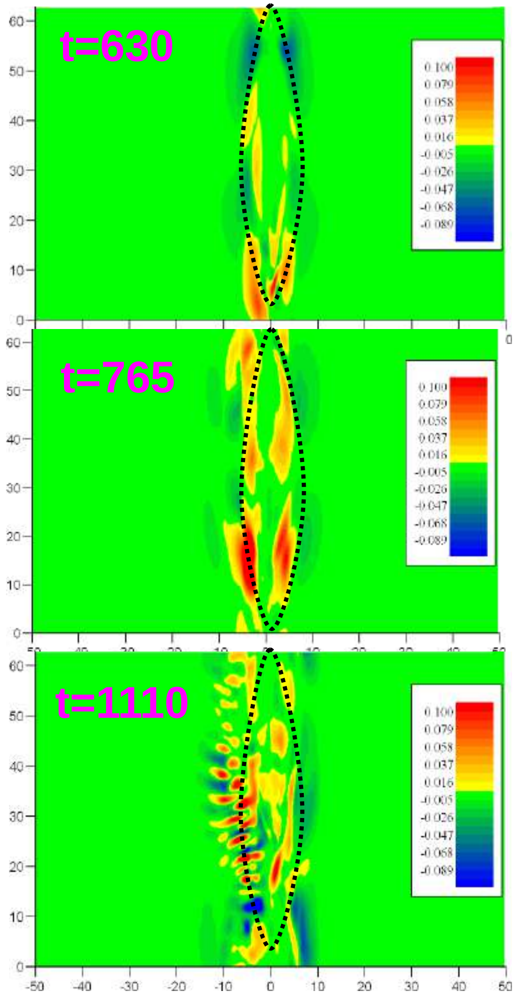

✔ Enhanced radial transport near separatrix leads to T_i island collapse

➢ Transport around magnetic island

$$\nabla \cdot (\chi_{//} \nabla_{//} T) + \nabla \cdot (\chi_{\perp} \nabla_{\perp} T) + P(r)/n = 0$$

➢ Critical island width

$$w_C \propto a\left(\chi_{\perp}/\chi_{//}\right)^{1/4}$$

Fitzpatrick, PoP 1995

➢ For $w < w_C$, T is not a function of island flux surfaces.

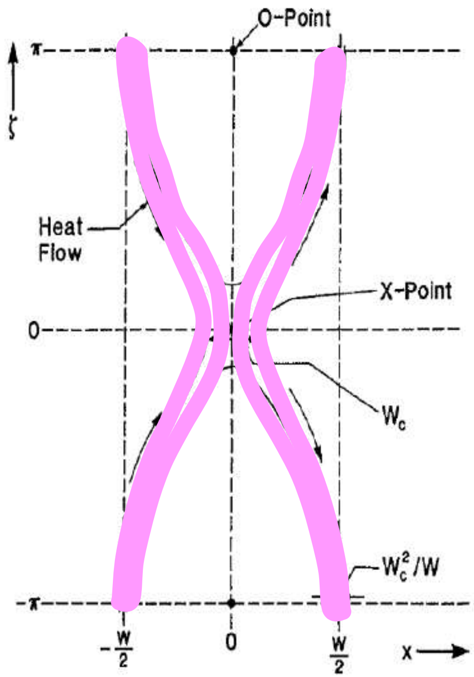

➢ Physical understanding:

ITG ⇒ $\chi_{\perp}$ ⇗ ⇒ w_C ⇗; $w_C{}^2/w$ ⇗ ⇒
$w < w_C$ ⇒ T_i island collapse
+
Magnetic island growth

⇒ MITG

Transport feature of MITG

➢ Case with unstable ITG

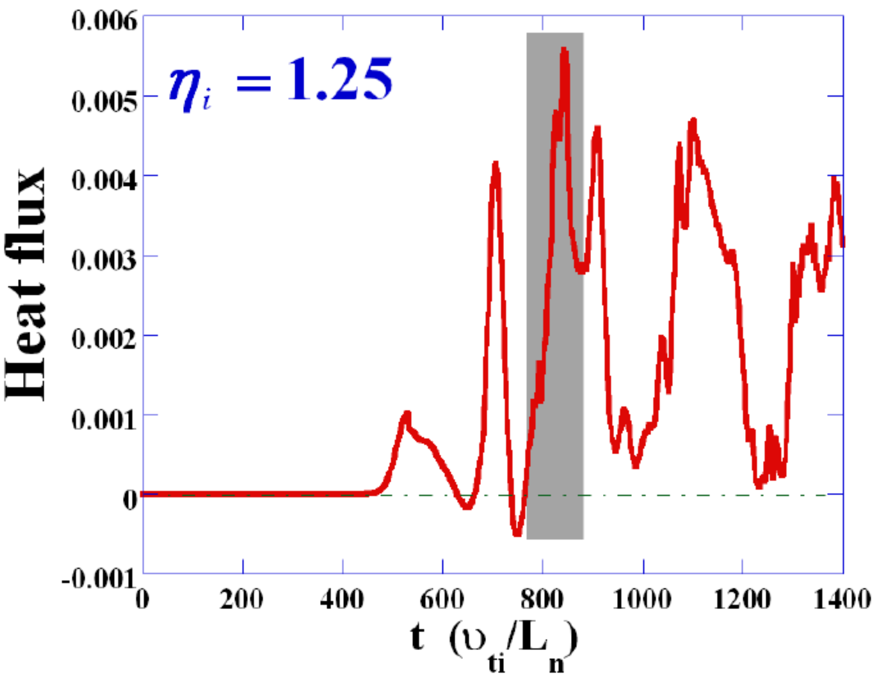

➢ Case with stable ITG

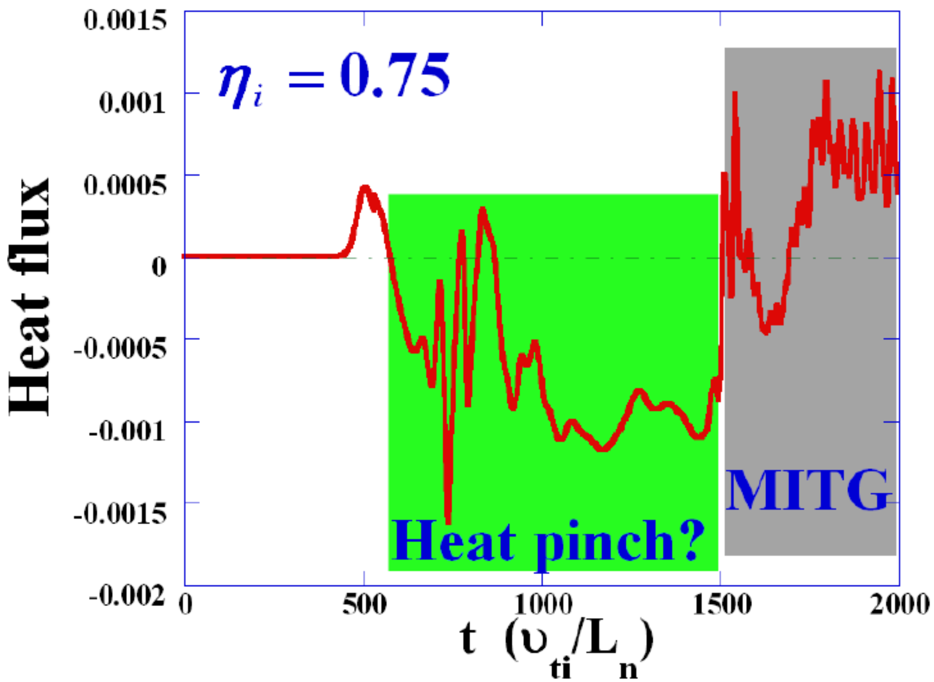

✔ MITG enhances heat transport;
✔ Transport displays intermittency due to strong excitation of MITG;
✔ Mixed MHD and ITG turbulence may cause heat pinch, especially for small η_i.

Outline

- ➢ Overview of multi-scale phenomena in MCF plasmas
  - ✔ Origin of multi-scale turbulence
  - ✔ Status of multi-scale turbulence simulation
- ➢ Gyrofluid approach simulation for multi-scale turbulence
  - ✔ Gyrofluid model
  - ✔ Multi-scale interaction between MHD and micro-turbulence
    - — Magnetic island response to micro-turbulence
    - — Micro-turbulence response to MHD island dynamics
- ➢ **Gyrokinetic approach simulation for multi-scale turbulence**
  - ✔ **Gyrokinetic model**
  - ✔ **Full-*f* gyrokinetic Vlasov code—GKNET**
  - ✔ **GK ITG instability with an island**
  - ✔ **Flux-driven GK turbulence simulation on profile stiffness and ITB**
- ➢ Summary

First-principle model: Gyrokinetics

- **Gyrokinetic theory**

Topical review: Gyrokinetic simulations of turbulent transport,
X. Garbet, et al., Nucl. Fusion 50, 043002 (2010)

$$\frac{\partial}{\partial t}FB+\nabla\cdot\left[FB(\upsilon_{//}\hat{b}+J_0\vec{\upsilon}_E+\vec{\upsilon}_d)\right]$$

$$+\frac{\partial}{\partial t}\left[FB\left(-\frac{e}{m}\hat{b}\cdot\nabla J_0\Phi-\mu\hat{b}\cdot\nabla B+\upsilon_{//}(\hat{b}\cdot\nabla\hat{b})\cdot J_0\vec{\upsilon}_E\right)\right]=C(F)$$

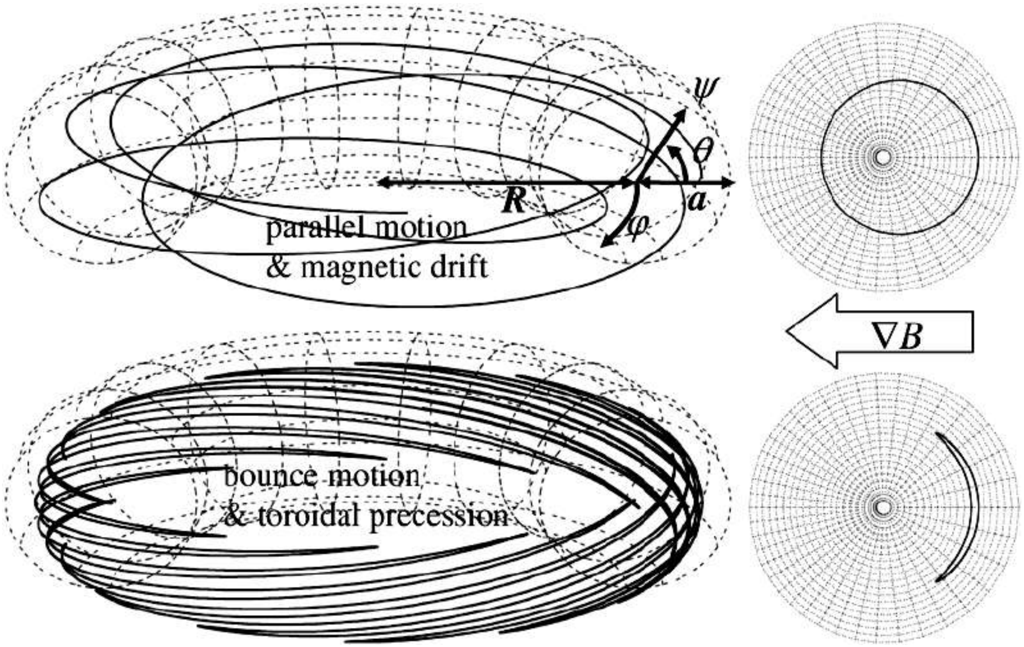

X. Garbet, et al., NF 50(2010)

- **Why Gyrokinetic:**

✔ Precise ion and electron dynamics (FLR effects) and Landau damping along perturbed field lines are crucial in a wide spectrum.

✔ Particle resonances and trapped particle effects are important

✔ Nonlinear dynamics in velocity space is non-negligible

✔ ……

GKNET code

➢ **GKNET: GyroKinetic Numerical Experiment of Tokamak**

➢ **Features of GKNET**

Imadera, et.al. 25th IAEA 2014; Kevin et al. PFR 2015

- ✓ **Full-*f* (Global): neoclassical flow (E_r) satisfying radial force balance;**
- ✓ **Flux-driven: heat source in the core and sink at edge;**
- ✓ **Momentum-driven: momentum injection;**
- ✓ **Collisional: Linearized Fokker–Planck collision operator (test-particle and field-particle parts);**
- ✓ **Gyrokinetic ions + adiabatic (or kinetic) electrons;**
- ✓ **Electrostatic (or electromagnetic);**
- ✓ **Circular (or non-circular with analytical equilibrium) cross-section plasmas;**
- ✓ **……**
- ✓ **Vlasov approach: finite difference (Morinishi scheme) in 5D with FFT solver (or real space solver) for gyro-average;**
- ✓ **Conservation;**
- ✓ **……**

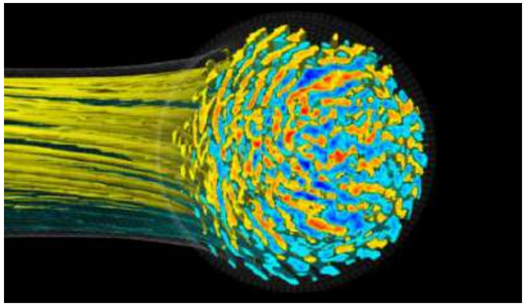
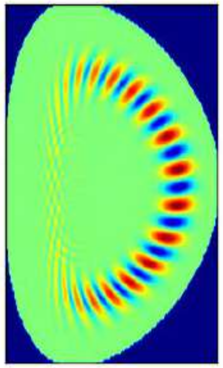
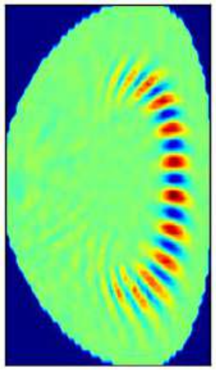

Typical global ITG turbulence and linear ITG mode structures

Animation: flux-driven ITG turbulence

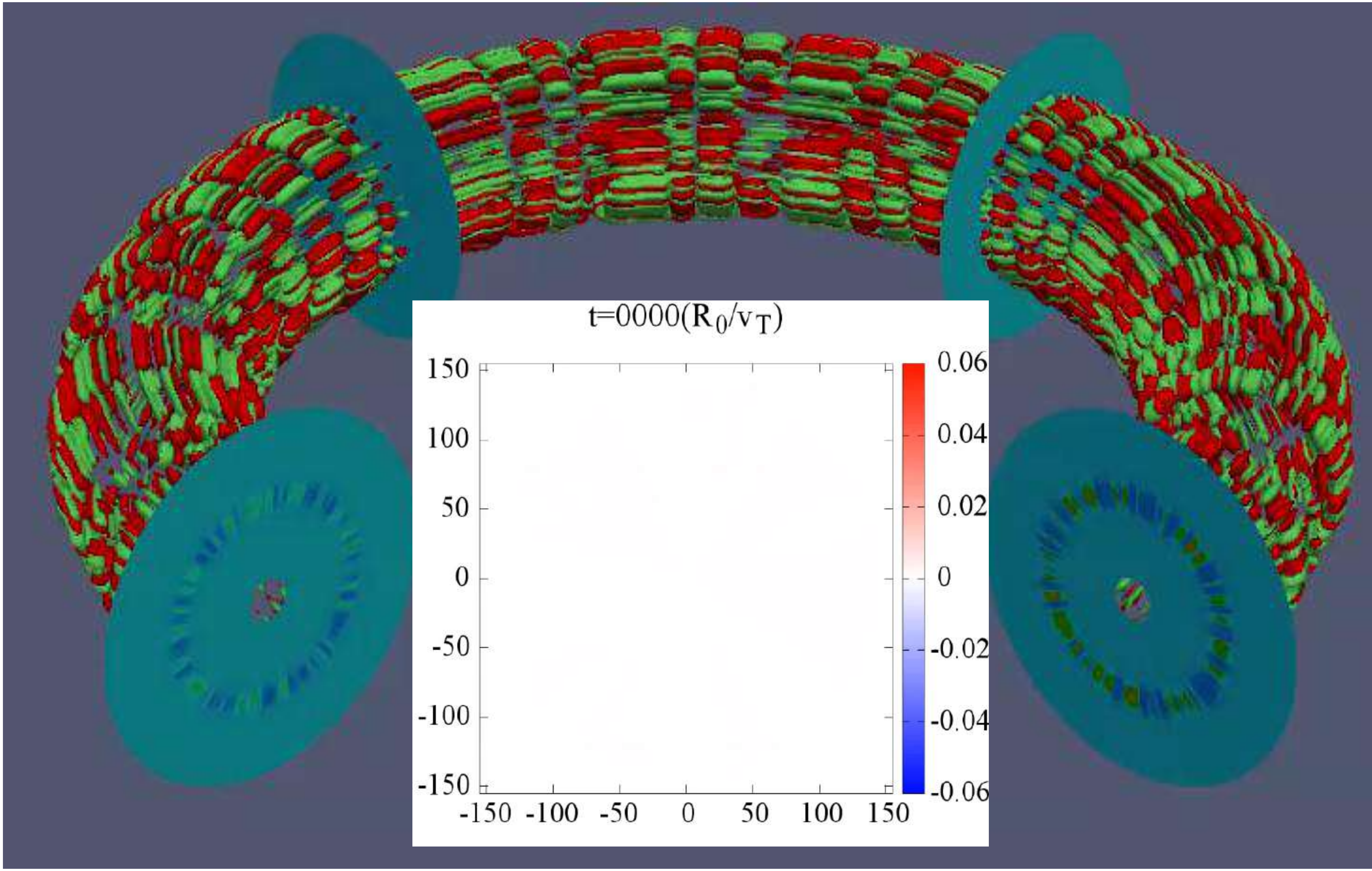

GyroKinetic formulism in GKNET

➢ GK Vlasov equation for ions

Imadera, et.al. 25th IAEA 2014

$$\frac{\partial}{\partial t} f_i + \frac{d\vec{R}}{dt}\cdot\nabla f_i + \frac{d\upsilon_{//}}{dt}\frac{\partial}{\partial \upsilon_{//}} f_i = C_{coll} + S_{src} + S_{snk} \qquad H = \frac{\upsilon_{//}^2}{2} + \mu B + \left\langle \phi \right\rangle_\alpha$$

$$\frac{d\vec{R}}{dt} = \{\vec{R}, H\} = \frac{\vec{B}_{//}^*}{B_{//}^*}\frac{\partial H}{\partial \upsilon_{//}} + \frac{1}{B_{//}^*}\vec{b}\times\nabla H \qquad \frac{d\upsilon_{//}}{dt} = \{\upsilon_{//}, H\} = -\frac{\vec{B}_{//}^*}{B_{//}^*}\nabla H \qquad \hat{\vec{B}}_{//}^* = \hat{\vec{B}} + \upsilon_{//}\nabla\times\hat{\vec{b}}$$

➢ GK quasi-neutrality condition

$$\phi - \left\langle\left\langle \phi \right\rangle\right\rangle_\alpha + \frac{1}{T_{e0}(r)}\left(\phi - \left\langle \phi \right\rangle_\alpha\right) = \frac{1}{n_{i0}(r)}\iint \left\langle \delta f \right\rangle_\alpha B_{//}^* d\upsilon_{//} d\mu$$

➢ DK collision operator

$$C_{coll}(f) = \frac{\partial}{\partial u}\left[\frac{3\sqrt{\pi}}{2}\frac{n}{\upsilon_{th}}\frac{\Phi(\nu)-\Psi(\nu)}{2\nu}\frac{\varepsilon^{3/2}}{qR_0}\nu_*\left(\frac{\partial f}{\partial u}\right) + \frac{u}{\upsilon_{th}^2} f\right] - C_F(f)$$

$$\Phi(\nu) = \frac{2}{\sqrt{\pi}}\int_0^\nu e^{-x^2}dx \qquad \Psi(\nu) = \frac{1}{\sqrt{\pi}\nu^2}\left(\int_0^\nu e^{-x^2}dx - \nu e^{-\nu^2}\right)$$

Dif-Pradalier, et.al. PoP 2011; Satake, et.al. CPC 2010

Applications of GKNET code

➢ **Effect of 3D helical island on GK toroidal ITG instability;**

➢ **Simulation of flux-driven GK turbulence on profile stiffness and ITB formation**

GK ITG mode with 3D helical resonant island

- **Configuration with 3D island**

$$\vec{B} = B_0\hat{b} + \delta\vec{B}_I = B_0\hat{b} + \nabla\times(A_{//I}\vec{b}) = B_0\hat{b} + \boxed{\nabla\times[A_{//I0}(r)\cos(m_I\theta - n_I\varphi)\hat{b}]}$$

- **Model for resonant magnetic island** (e.g., tearing mode island)

$$\psi_{He} = \psi_p - \frac{\psi_t}{q_s} + \psi_I$$

$$\psi_I = \boxed{\kappa(r)\frac{\hat{s}_s w^2}{4r_s}}[1+\cos(m_I\theta - n_I\varphi)]$$

Under constant-ψ approximation with island width: $w(\psi) \propto \sqrt{\tilde{\psi}}$

- **Flux contours**

  w~25

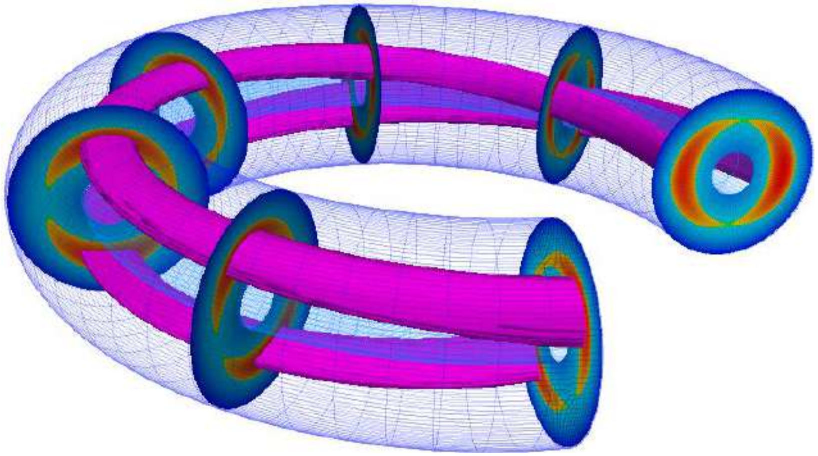

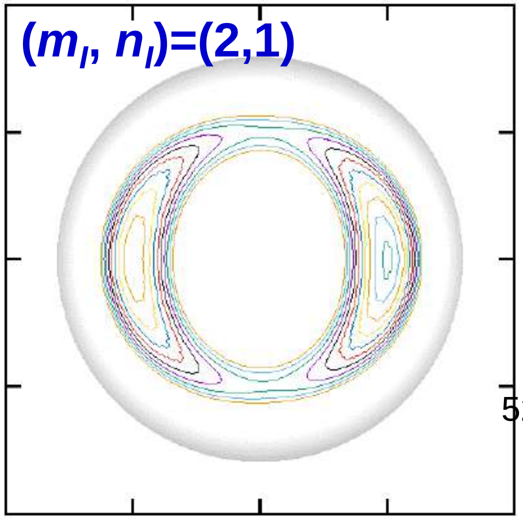

Ballooning mode in a torus

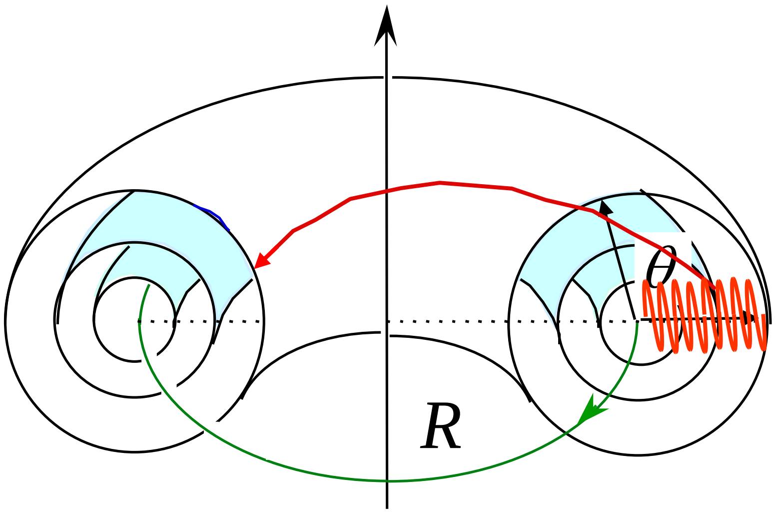

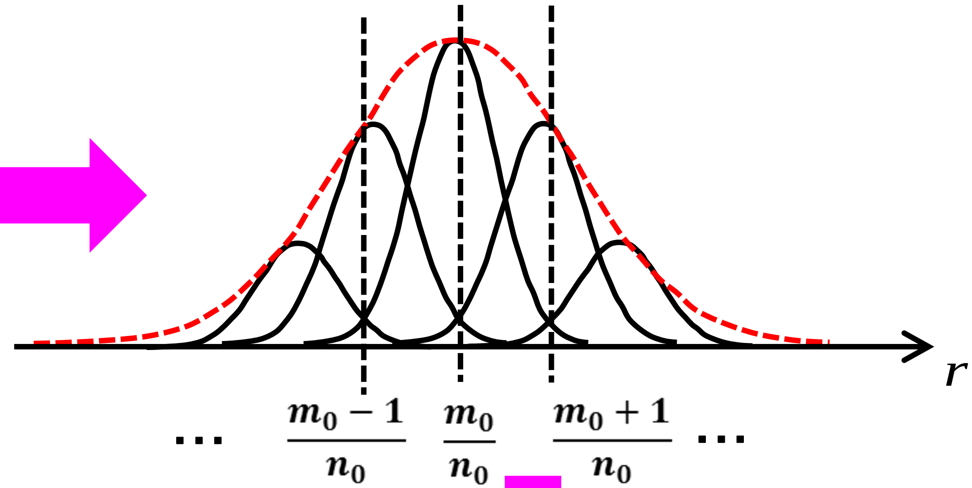

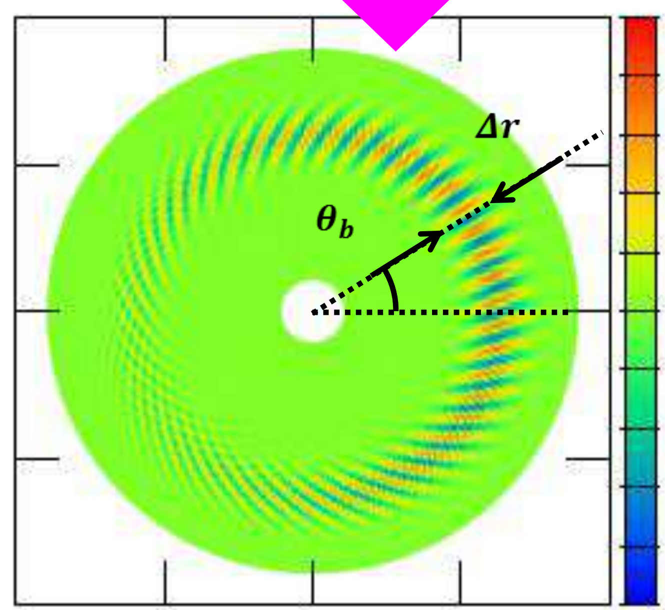

- ✓ **Ballooning mode structure is formed through “toroidal coupling” in “bad” curvature region for a given toroidal mode number *n*;**
- ✓ **Ballooning angle θ_b and mode width Δr are determined by q and pressure profiles.**

Role of 3D helical Island in ITG fluctuation?

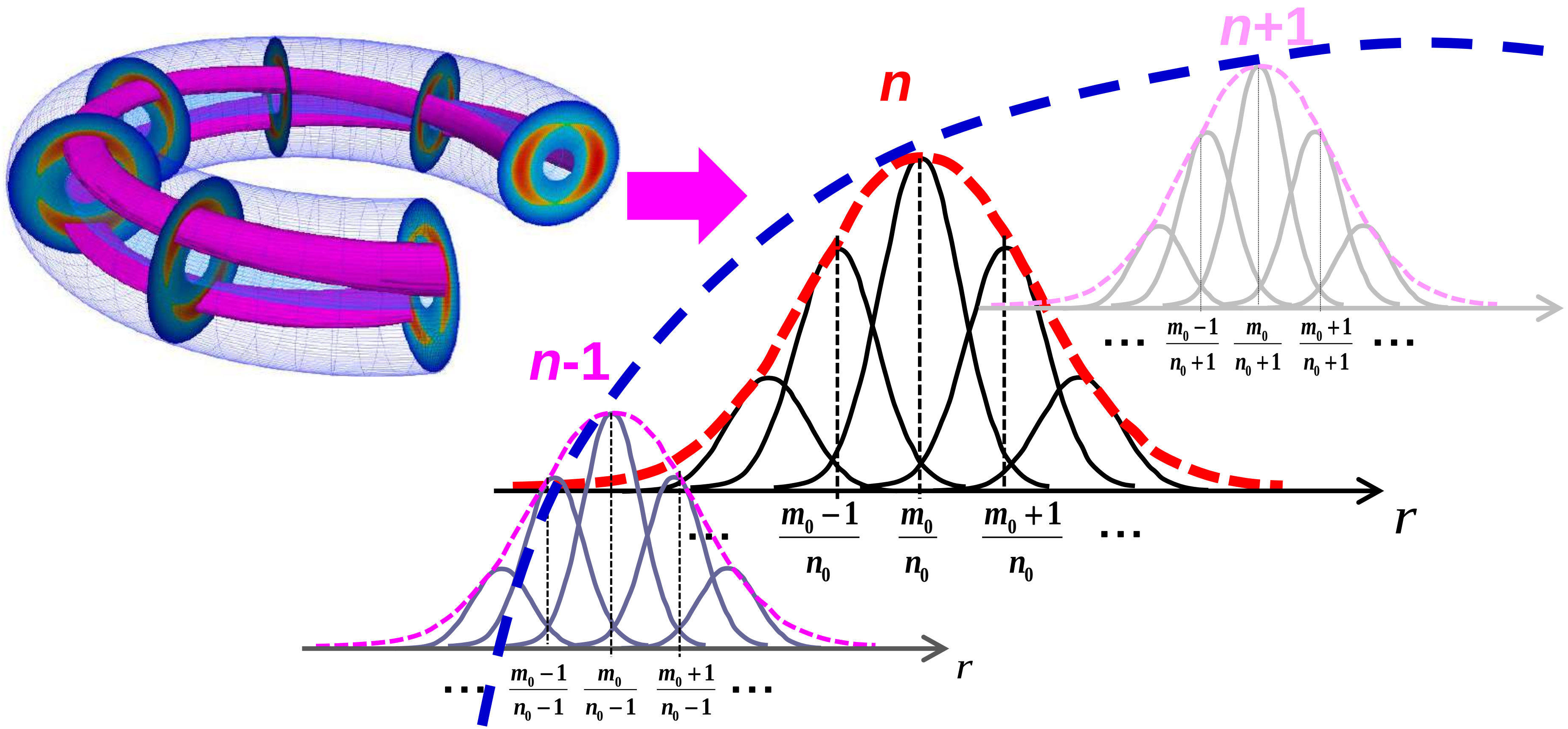

- ✓ **Island can enhance toroidal coupling (m-coupling);**
- ✓ **Island may link ballooning modes in “bad” and “good” curvature regions (i.e, n-coupling).**

…..

…, (m-1, n-1), (m, n-1), (m+1, n-1), …

…, (m-1, n), (m, n), (m+1, n), …

…, (m-1, n+1), (m, n+1), (m+1, n+1), …

……

Simulation with resonant island

➢ ITG **with** 3D (2, 1) resonant island (w=25)

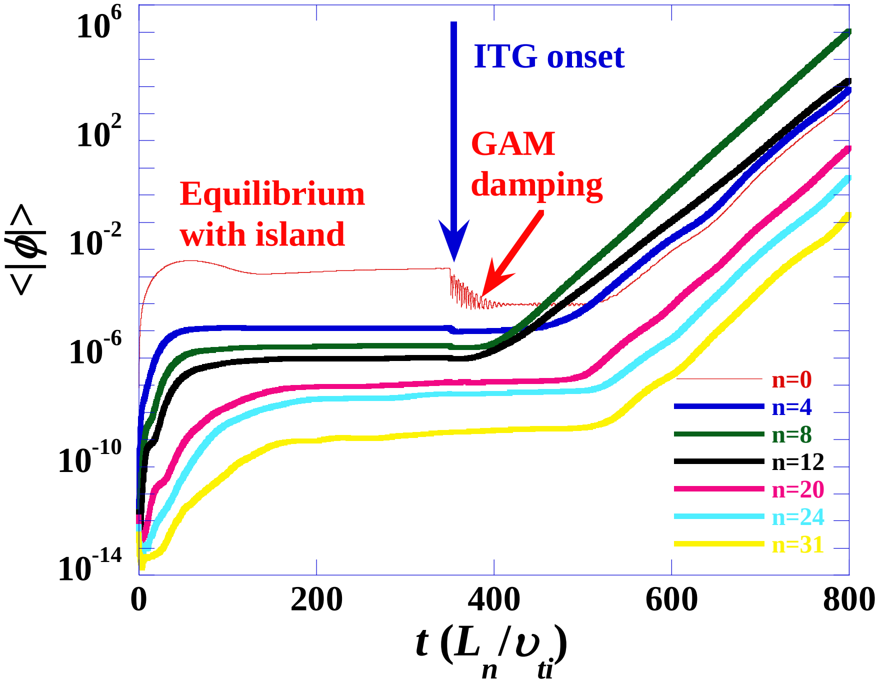

➢ ITG **without** island for comparison

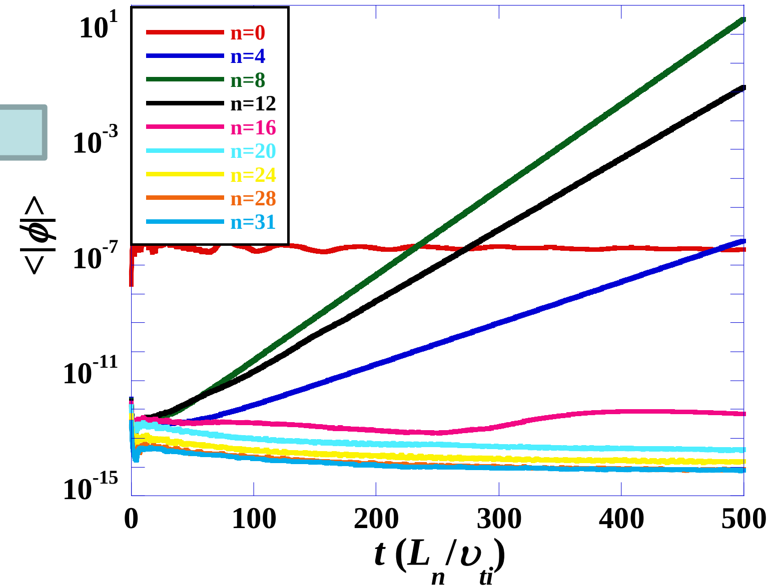

Simulation is performed with 2 stages

✓ t=0~350: equilibrium establishment (T_i & n_i flattening inside island)

✓ t=350~420: GAM damping;
t=350~ : ITG excitation with n-mode coupling

Equilibrium response to resonant island

- ➢ **Quasilinear flattening inside islands**
  - ✓ O-point region(low field side): flattening (NOT complete);
  - ✓ X-point region: steepening

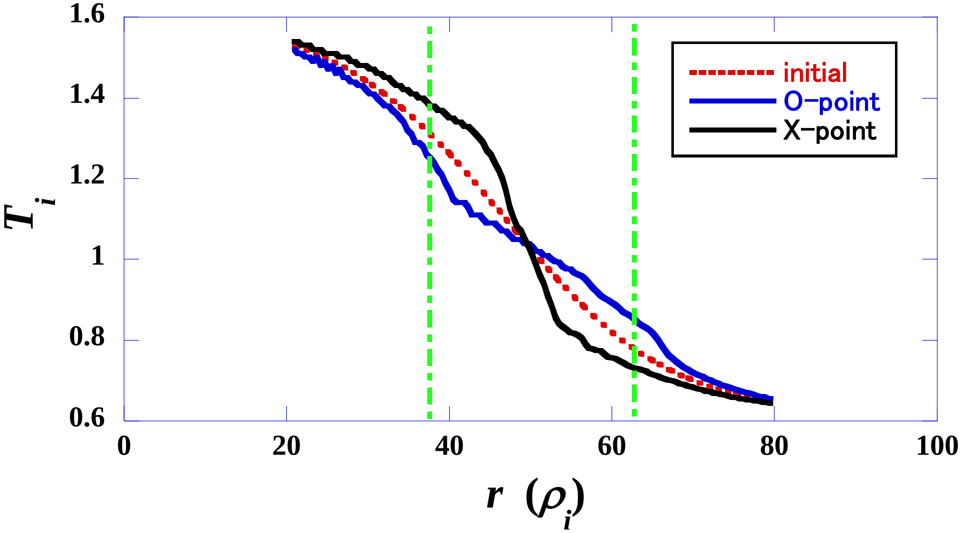

- ➢ **Equilibrium T_i response to (2,1) resonant island**

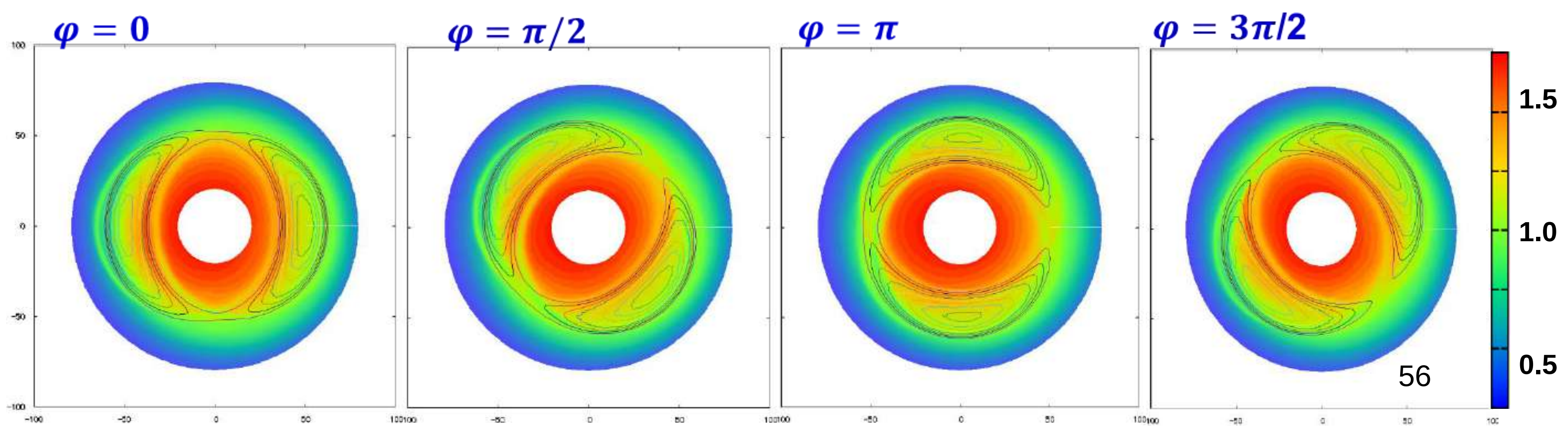

ITG growth rate vs island width

➢ Magnetic island with (1, 1)

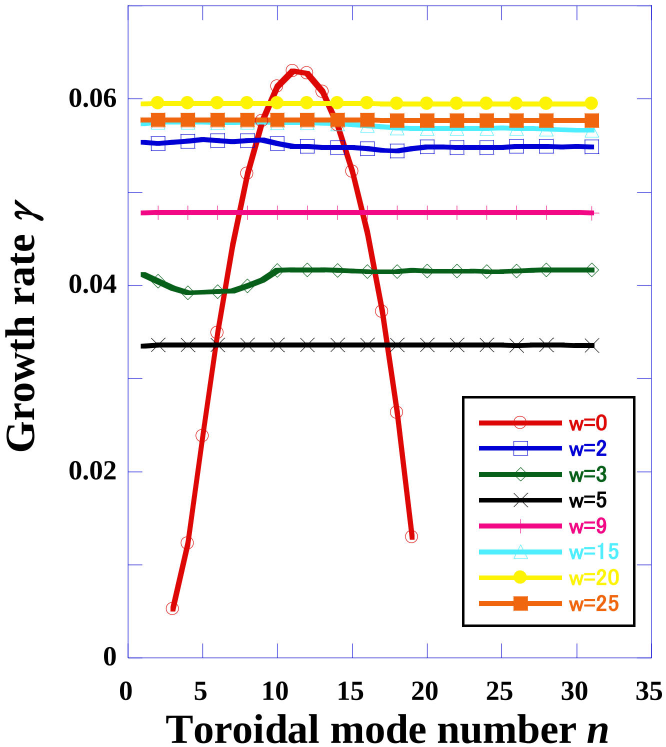

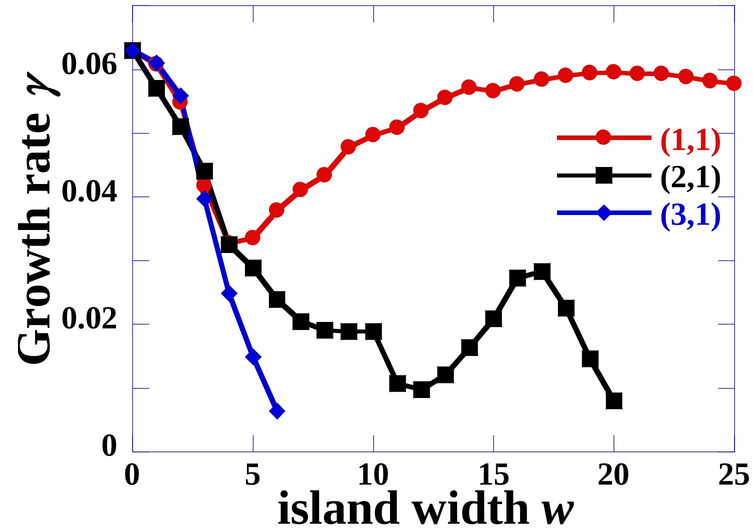

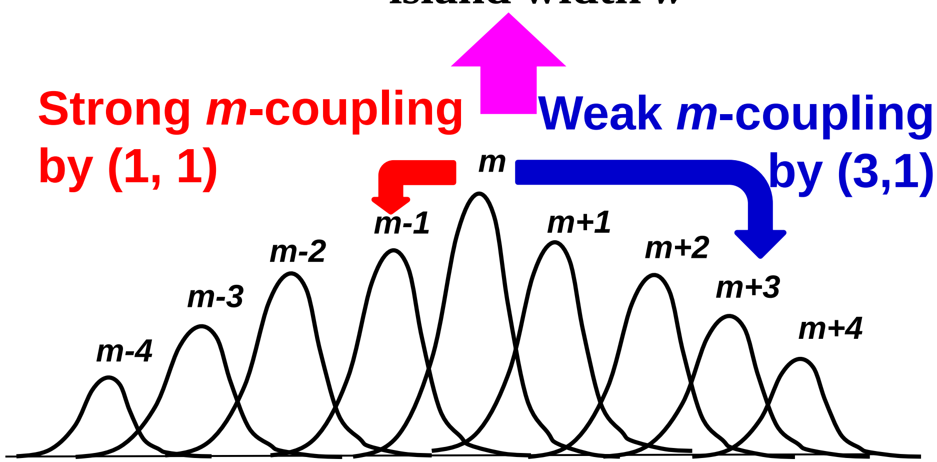

✓ Strong 3D magnetic perturbation with small island width stabilizes toroidal ITG mode; BUT larger island plays a destabilization role.

✓ Destabilization mechanism: island induced *m*-coupling enhances "toroidal coupling", destabilize ITG.

ITG stabilization mechanism

➢ **Magnetic island with (1,1) and *w*=11**

✓ **Geometric stabilization due to island in "bad" curvature region;**

✓ **ITG structure is distorted by island.**

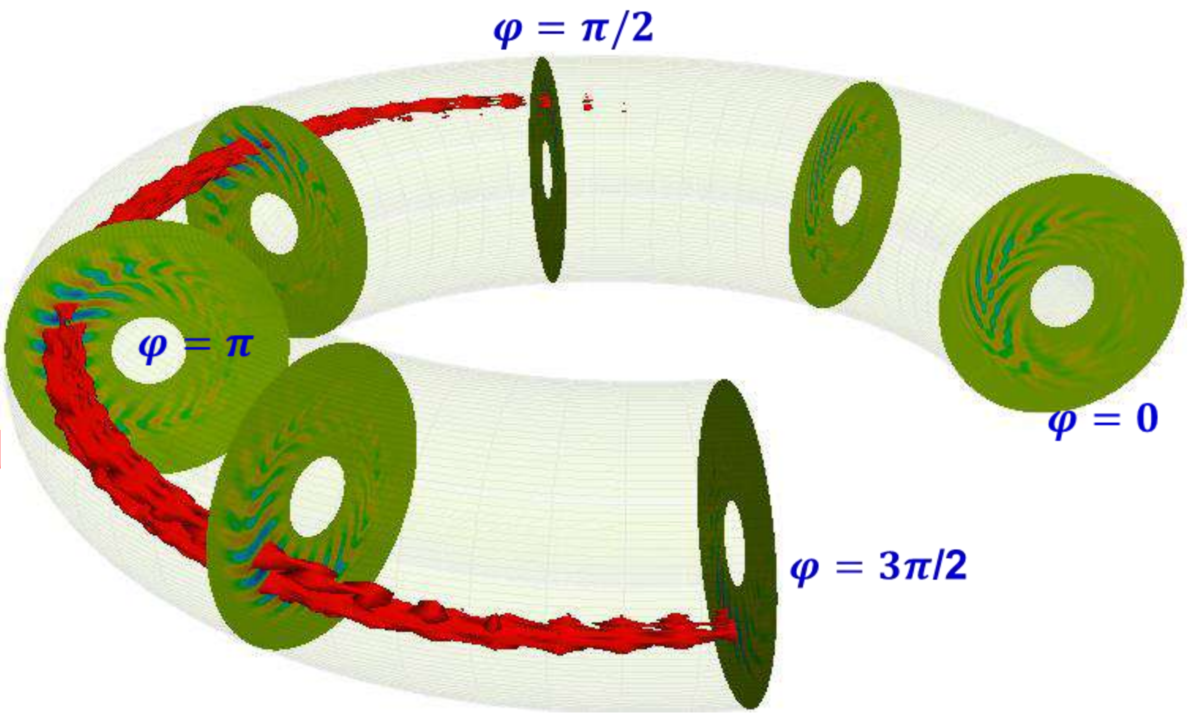

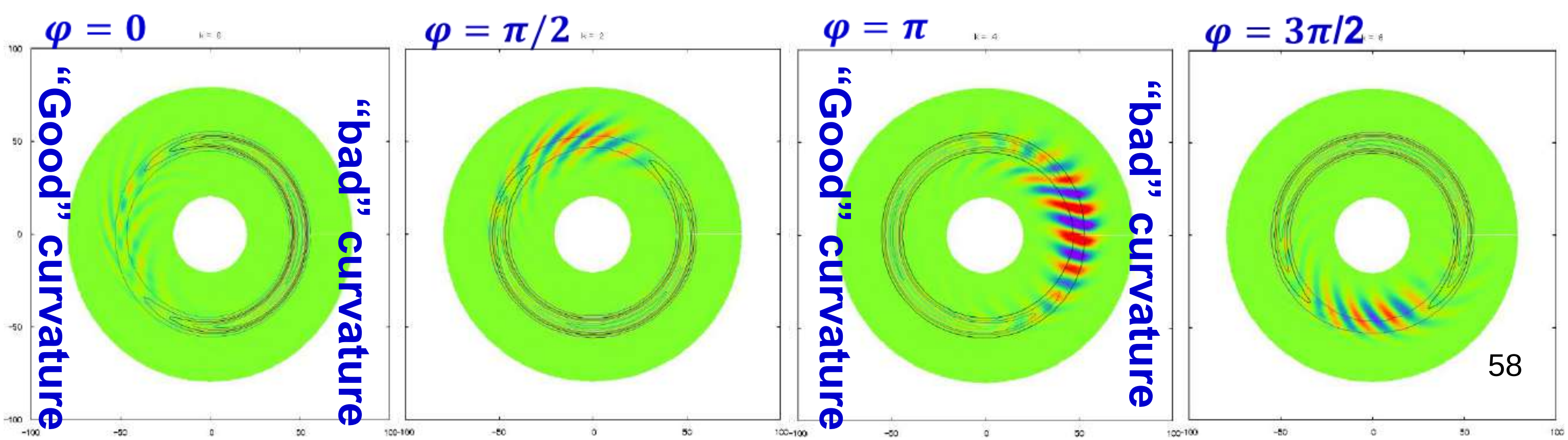

Applications of GKNET code

➢ Effect of 3D helical island on GK toroidal ITG instability;

➢ **Simulation of flux-driven GK turbulence on profile stiffness and ITB formation**

Profile Stiffness in Toroidal Plasmas

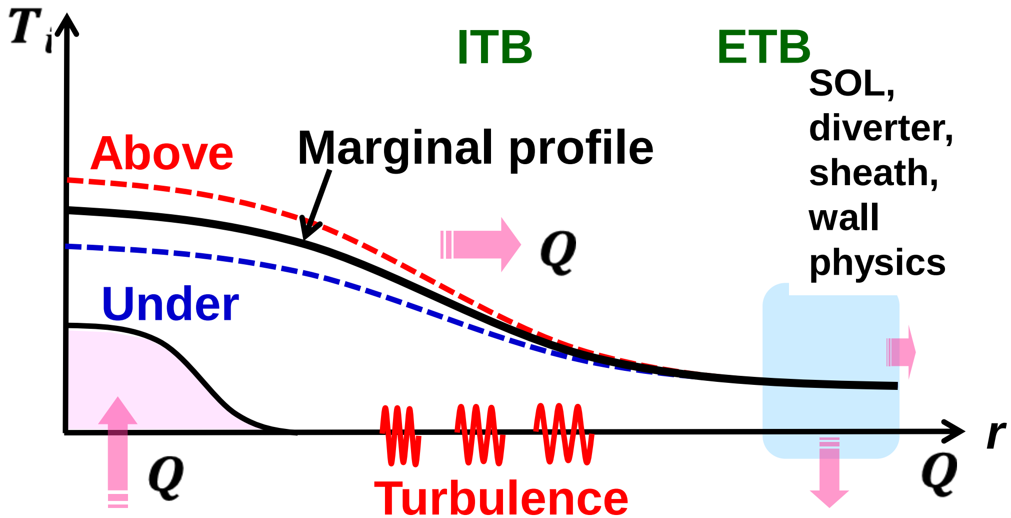

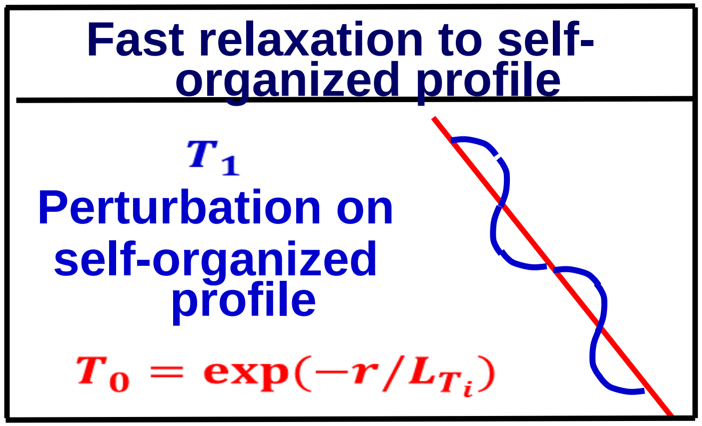

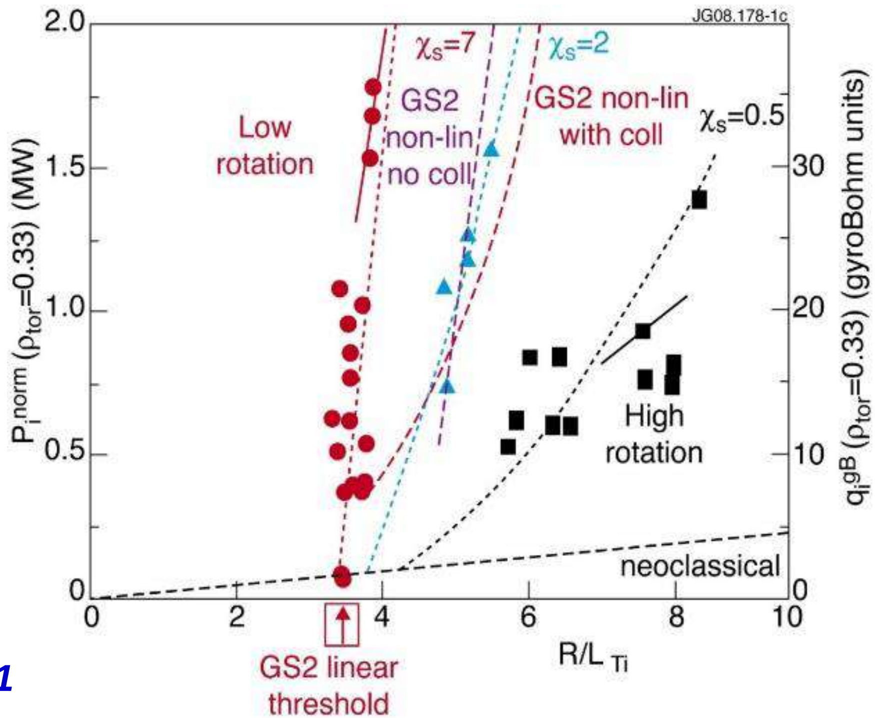

✓ **Ion temperature gradient tends to be a constant around the critical value to drive ITG instability.**
--> Profile stiffness

JET: Mantica, et.al., PRL 2011

Profile stiffness in profile & flux driven ITG

➢ **Full-kinetic global simulations with low zonal flows show a strong constraint on the functional form of temperature profile.**

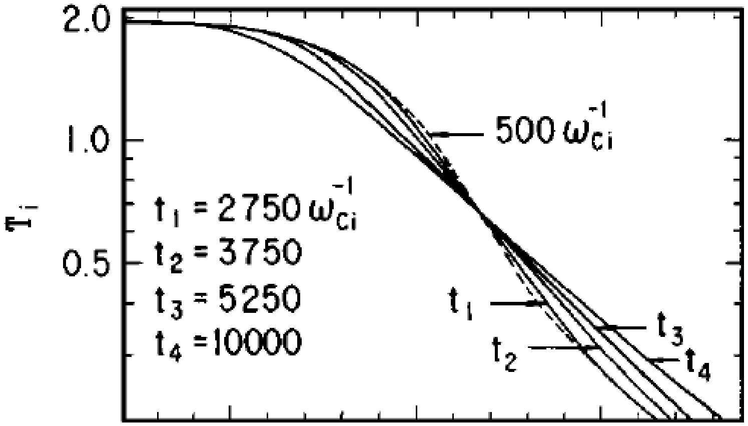

Kishimoto, et.al. PoP 1996

➢ **Flux-driven full-*f* GK simulations also reveal a strong stiffness of T_i profile even with strong mean and zonal flows.**

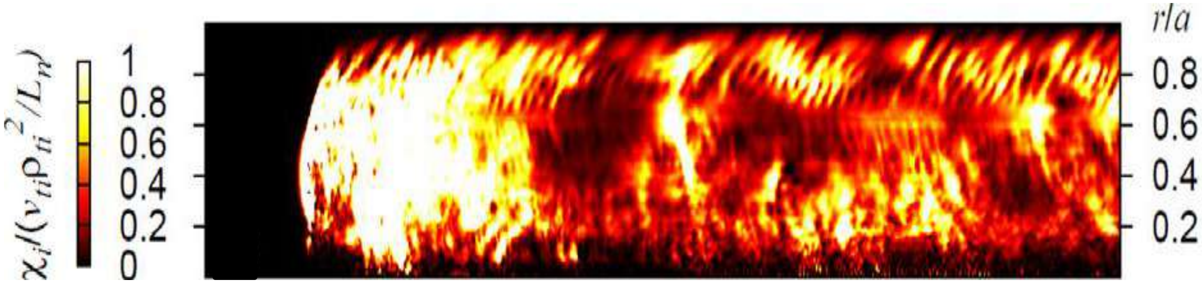

Idomura, et al. NF 2009

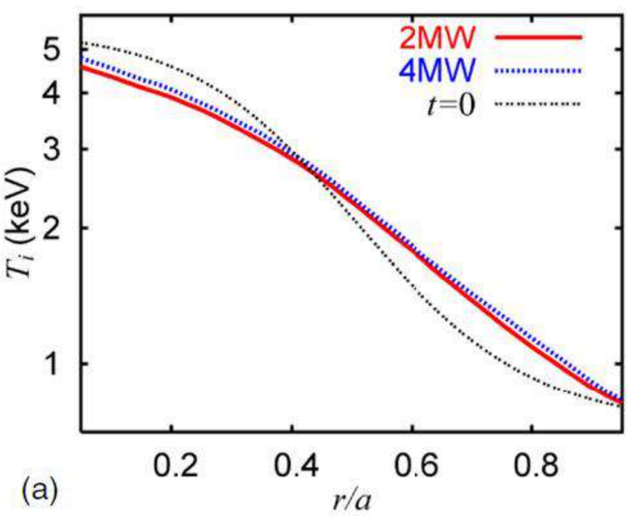

Why is profile stiffness dominant even in flux-driven turbulence with mean and zonal flows?

Flow effects on ballooning mode(Theory)

➢ Ballooning mode with flows

Kishimoto, et.al., PPCF 1998; NF 2000

$$\theta_b = \mp \left| \frac{\partial_r(\omega_r + \omega_f)}{2k_\theta \gamma_0 \hat{s}} \right|^{1/3}$$

$$\omega_r \sim \omega_D = -k_\theta \frac{2T_i}{eBR_0}, \quad \omega_f \sim -k_\theta \frac{E_r}{eB}$$

$$\Delta r = \left| \frac{sin\theta_b}{k_\theta^2 \hat{s}^2 \theta_b^3} \right|^{1/2}$$

$$\gamma = \gamma_0 cos\theta_b$$

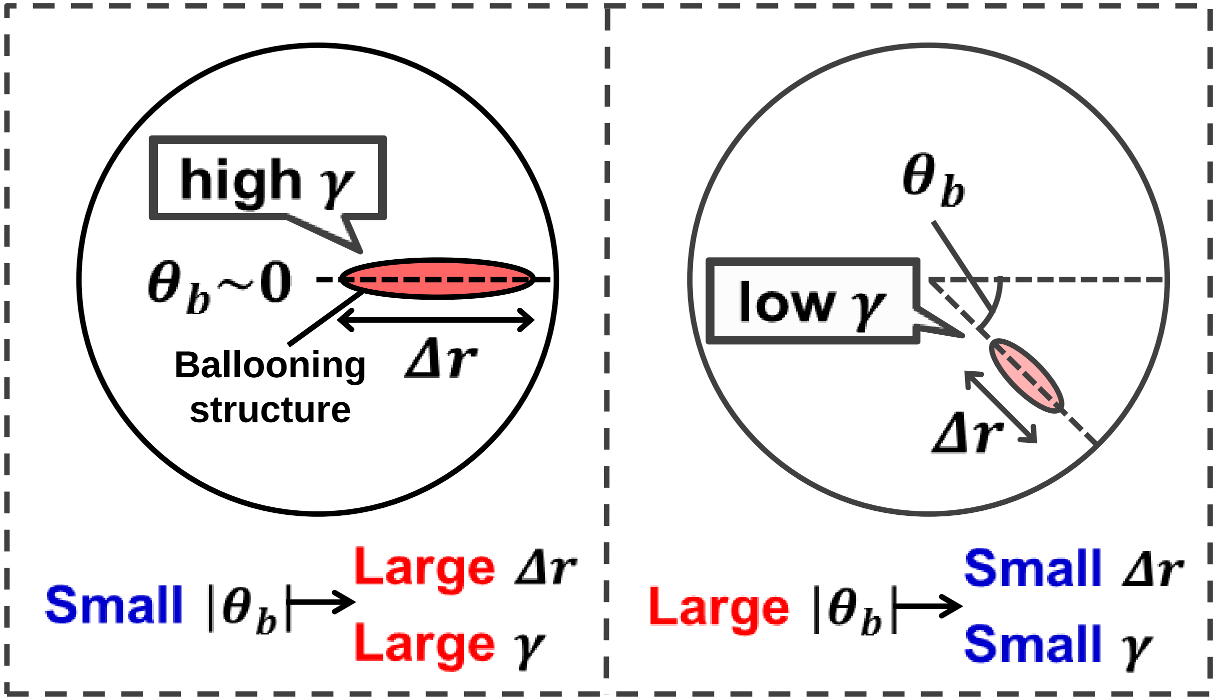

✓ Mean flow can recover ballooning symmetry

Origin of flow in ballooning mode(Theory)

➢ **Radial force balance**

$$E_r - v_\theta B_\varphi + v_\varphi B_\theta - \frac{1}{n_i e}\frac{\partial p_i}{\partial r} = 0 \longrightarrow E_r = \frac{rB}{qR}U_\parallel - \frac{T_i}{e}\left(\frac{1}{L_n} + \frac{1-k}{L_{T_i}}\right)$$

$$v_\theta = \frac{k}{eB}\frac{\partial T_i}{\partial r}, v_\varphi = U_\parallel, n_i = n_{i0}\exp\left(-\frac{r}{L_n}\right), T_i = T_{i0}\exp\left(-\frac{r}{L_{T_i}}\right)$$

Eigenfrequency + Doppler shift frequency

$$\omega_r + \omega_f \sim \frac{k_\theta}{eB}\left[\left(\underbrace{\frac{2}{R_0}}_{\text{Diamagnetic drift}} - \underbrace{\frac{1}{L_n} - \frac{1-k}{L_{T_i}}}_{\text{Mean flow}}\right)T_i - \underbrace{\frac{erB}{qR}U_\parallel}_{\text{Toroidal rotation}}\right]$$

Diamagnetic drift *Mean flow* *Toroidal rotation*

✓ **Cancellation by mean flow**

✓ **Impact of toroidal rotation**

Flow effect on ballooning mode(simulation)

A. Without E_r and $U_\parallel$ | **B. With E_r** | **C. With E_r and $U_\parallel$**

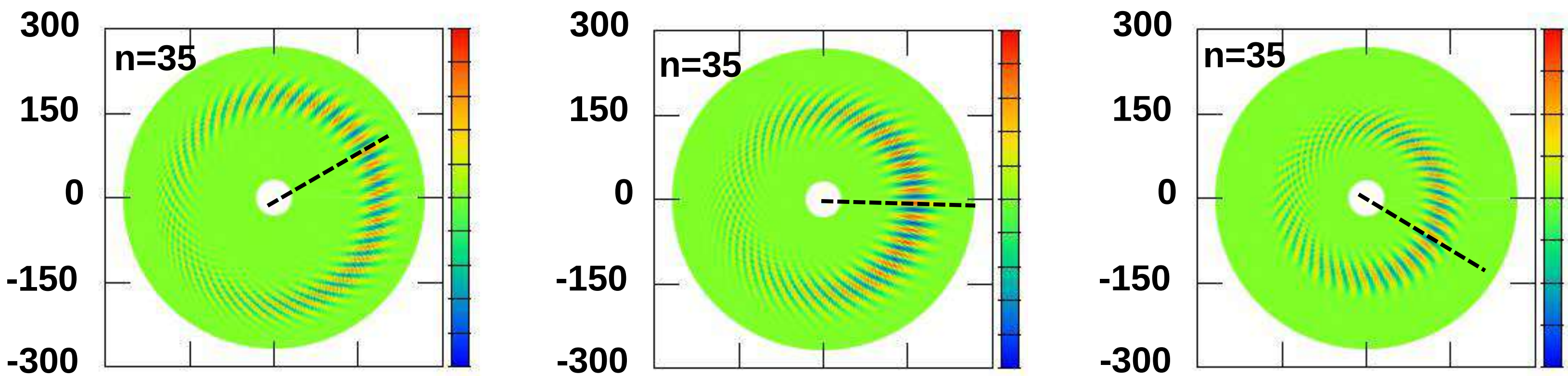

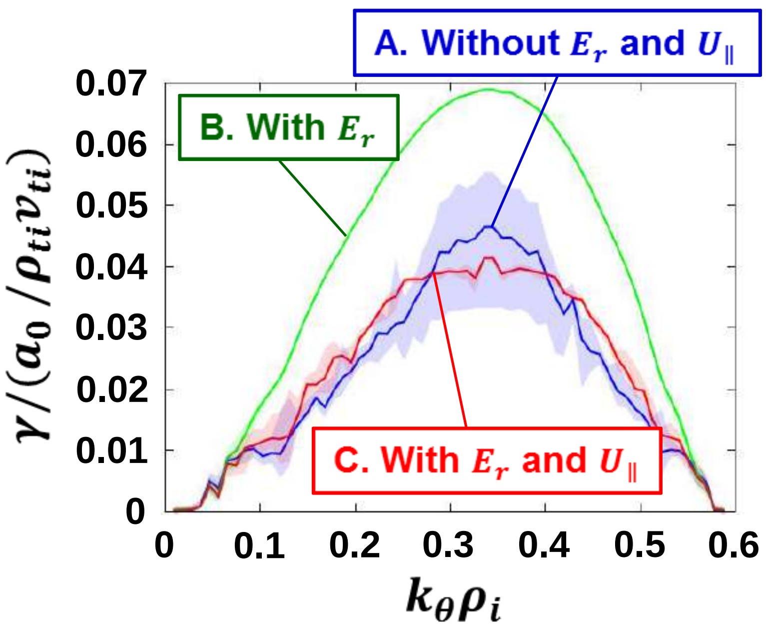

	γ	θ_b	Δr
A	0.07～0.12	0.5～0.6	28～42
B	0.15	0	49
C	0.09	-0.7～-0.6	25～27

- ✓ **E_r recovers ballooning symmetry, destabilizing ITG mode;**
- ✓ **E_r is modulated by moderate $U_\parallel$ to stabilizes ITG mode.**

Parameter setting for flux-driven simulations

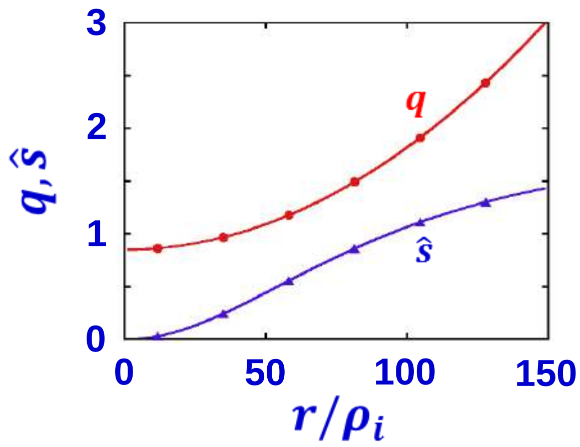

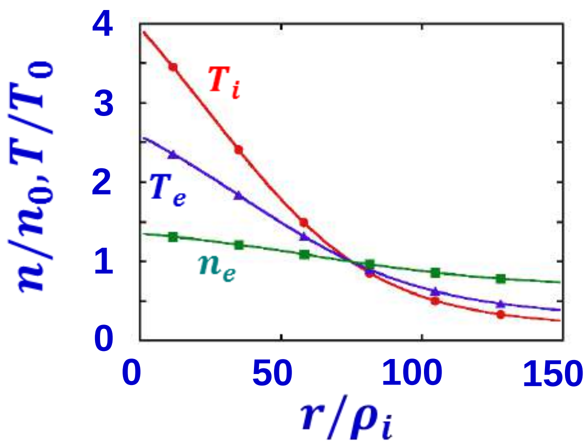

Parameter	Value
a_0/ρ_i	150
a_0/R_0	0.36
$(R_0/L_n)_{r=a_0/2}$	2.22
$(R_0/L_{T_i})_{r=a_0/2}$	10.0
$(R_0/L_{T_e})_{r=a_0/2}$	6.92
ν_*	0.28
P_{in}	16 [MW]
$\tau_{snk}^{-1}R_0/v_{ti}$	0.25

➢ Source/sink operators

$$S_{src} = A_{src}(r)\tau_{src}^{-1}[f_M(2\overline{T}) - f_M(\overline{T})]$$

✓ **Constant heat input near axis**

$$S_{snk} = A_{snk}(r)\tau_{snk}^{-1}[f(t) - f(t=0)]$$

✓ **Krook-type operator to *f* in boundary region**

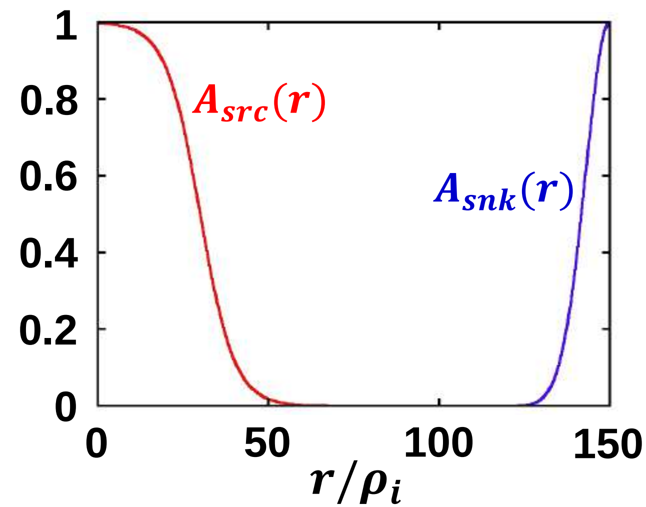

Idomura, et al. NF 2009

Time-Spatial features of Q_{turb}, L_T and E_r shear

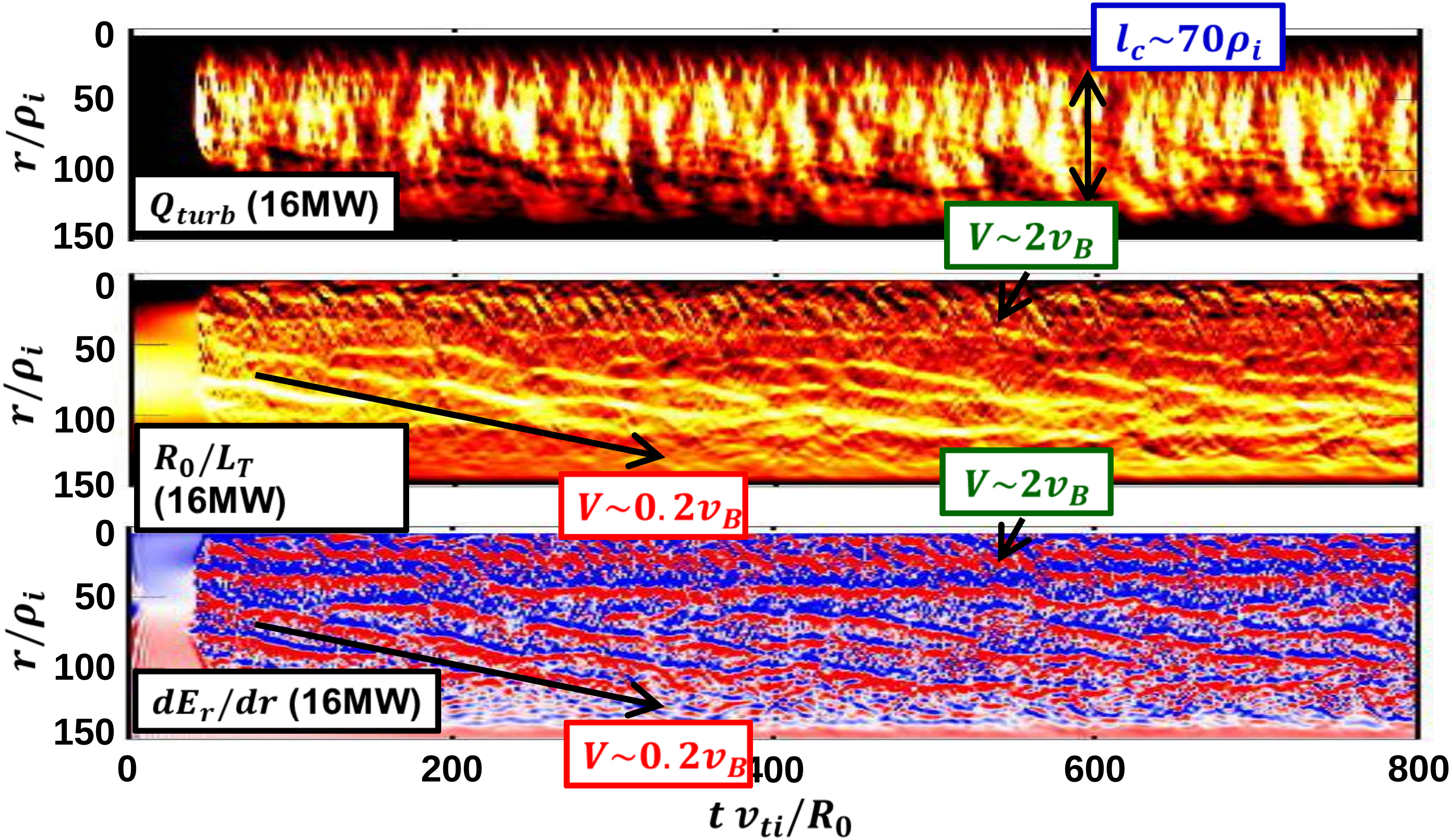

- ✓ **Flux-driven turbulent transport is mainly dominated by three process; (a)fast-scale avalanches; (b)slow-scale avalanches; (c)global transport.**

Details of time-Spatial features

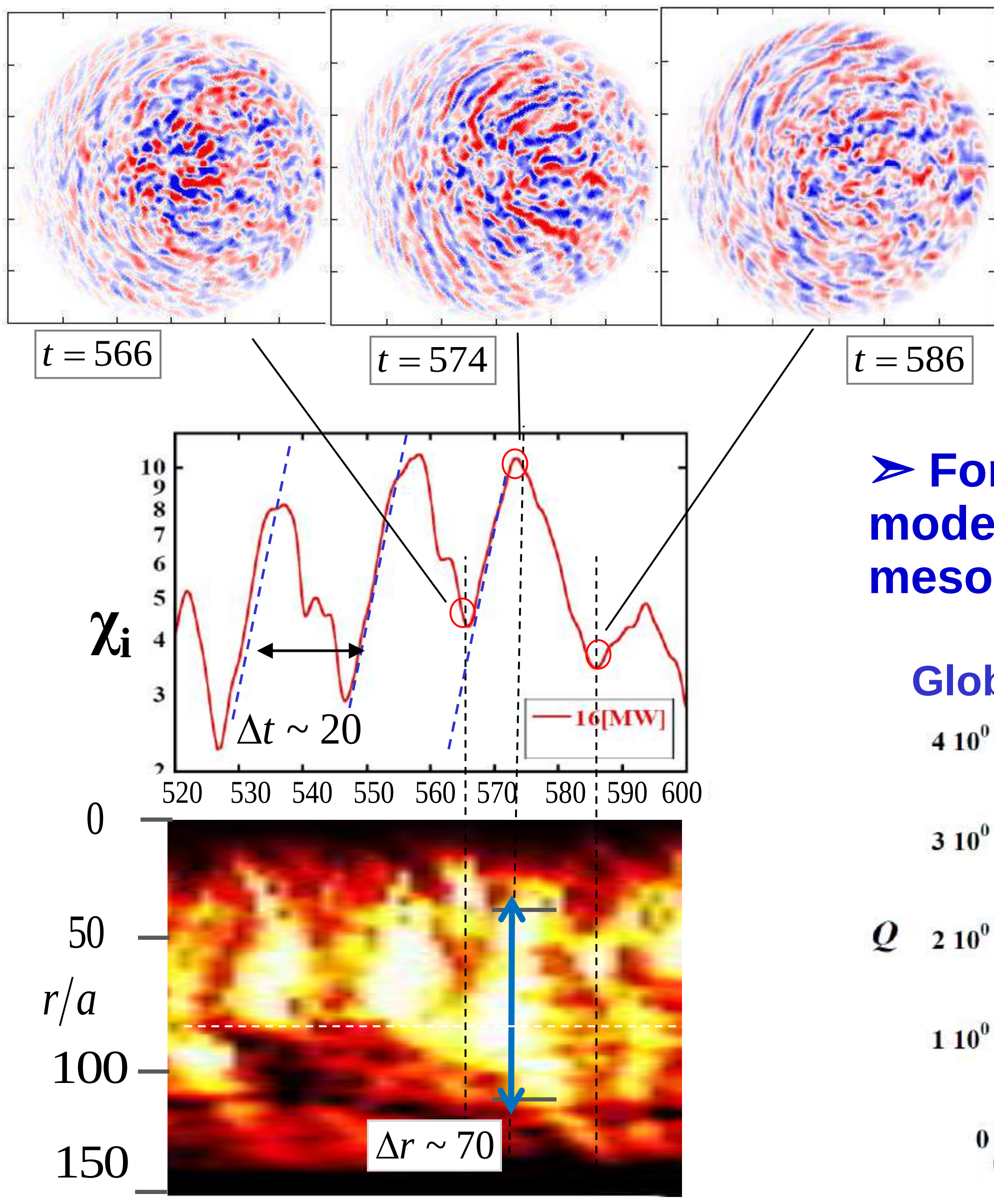

- Quasi-periodic burst exhibiting exponential growth and damping

$$\omega_{E\times B} \le \boxed{\gamma_{sp}} < \gamma_L$$

$$\sim 0.1 \qquad \sim 0.15 \qquad \sim 0.45$$

(linear growth rate)

- Formation of radially extended global mode, leading to burst which ranges from meso- to macro-scale

Global relaxation (an origin of profile stiffness)

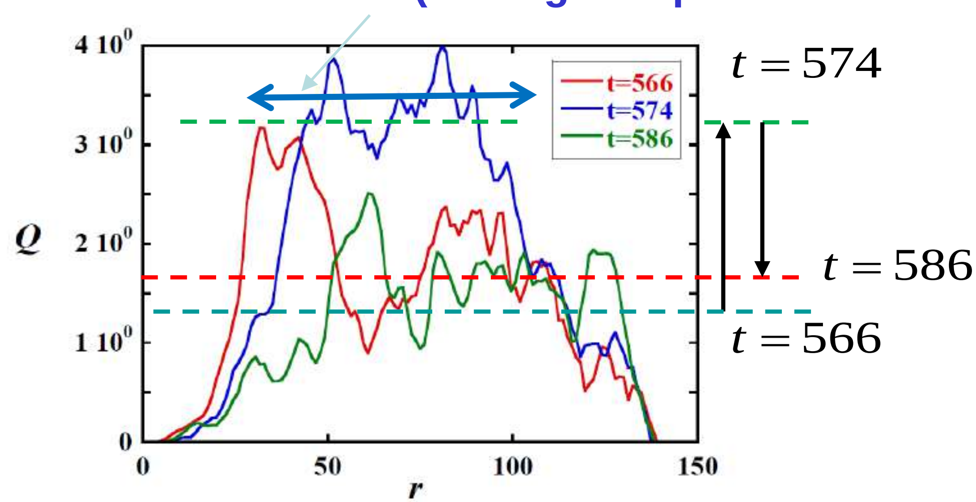

"Spontaneous phase alignment"

Phase alignment is established more easily when ballooning symmetry is recovered due to MF.

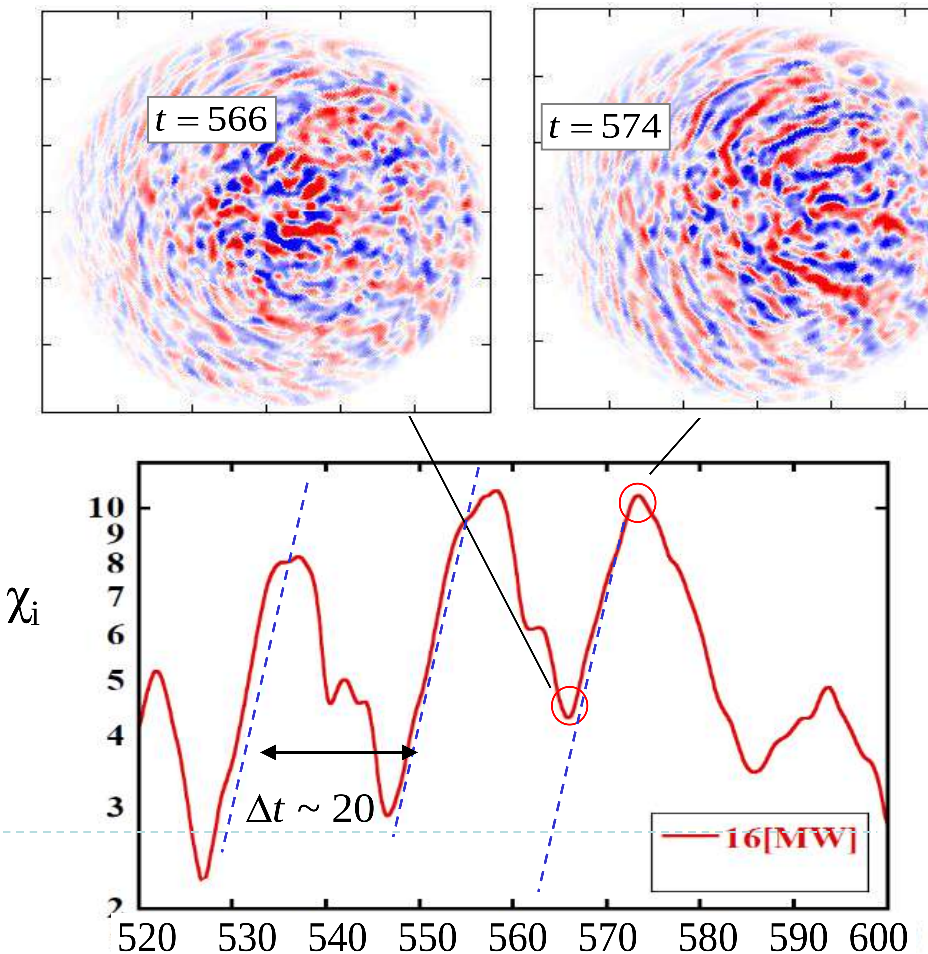

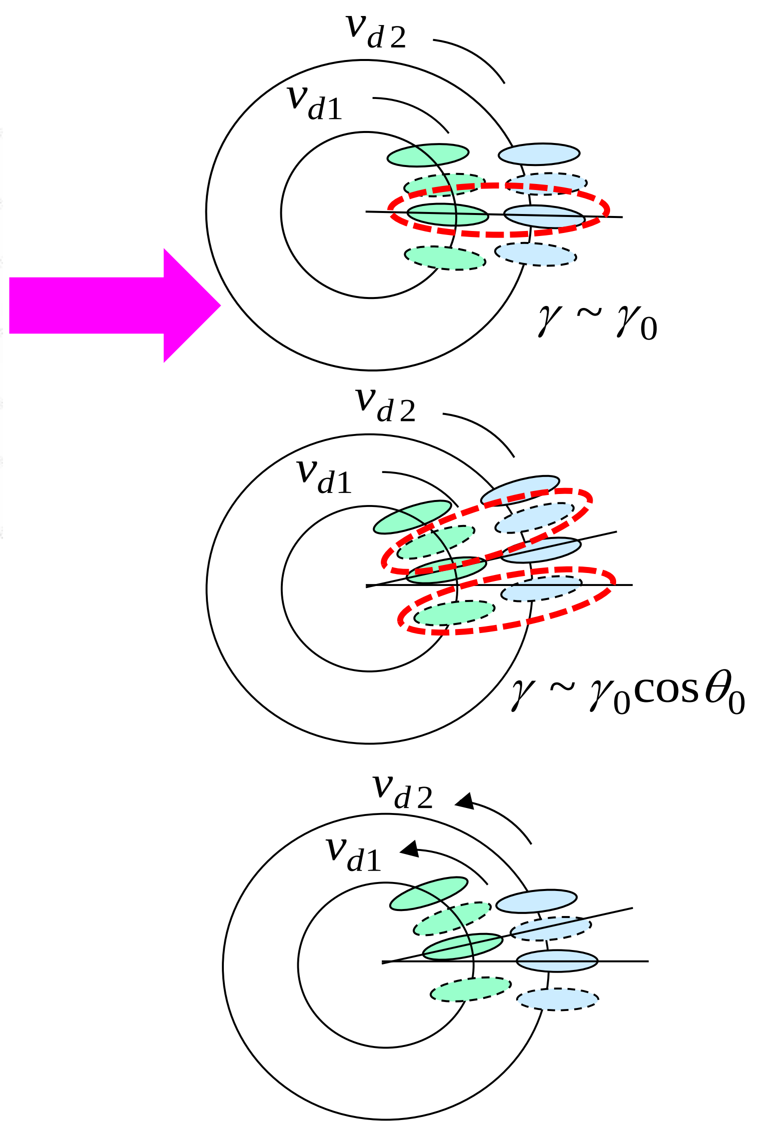

Effect of zonal shear flows

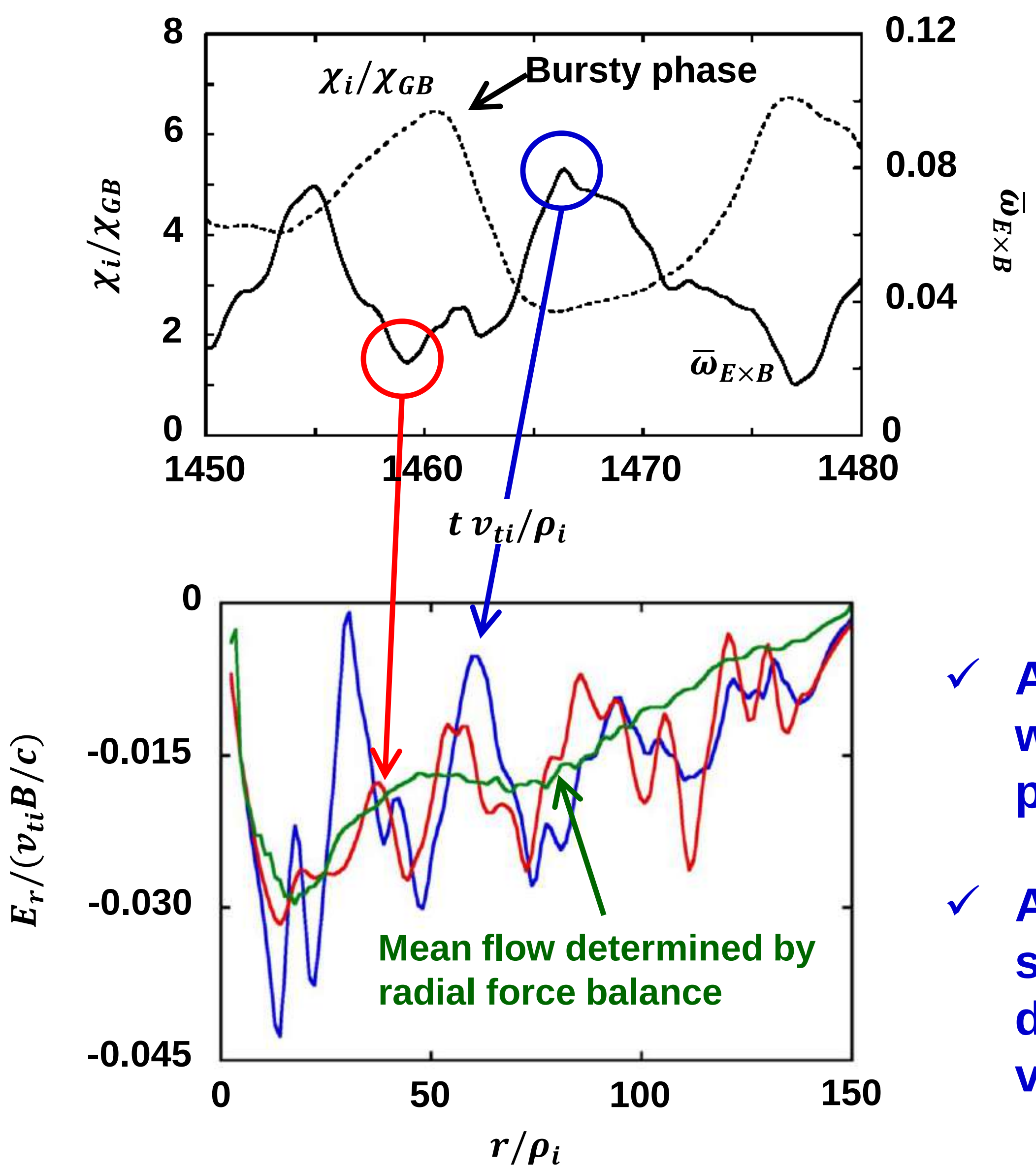

Linear ITG eigen-mode

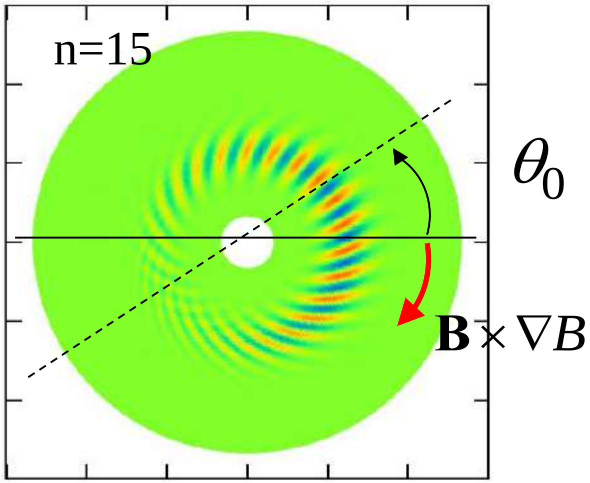

- ✓ **Among bursty phase, E_r does not work to stabilize the turbulence, as predicted in global linear theory;**
- ✓ **After explosive transport, meso-scale zonal flow grows to quickly disintegrates radially extended vortices.**

Ballooning symmetry and profile stiffness

➢ 2D spatial correlation analysis (16MW)

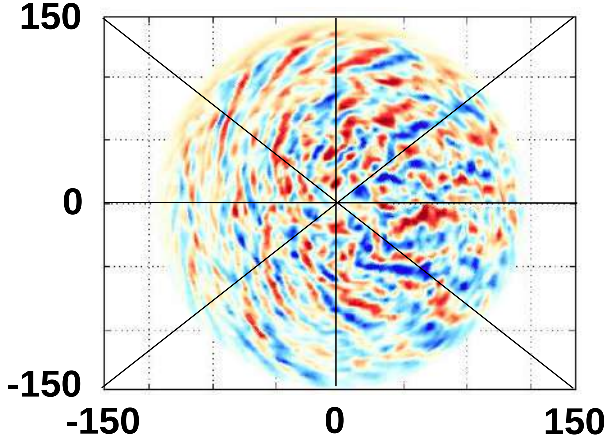

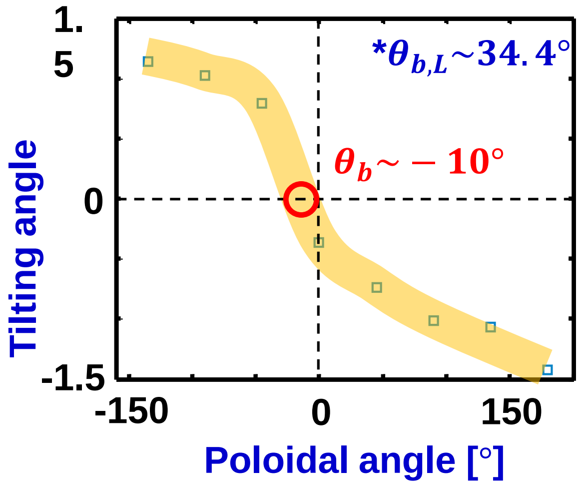

- ✓ Ballooning angle is smaller than that estimated from linear analysis without E_r.

➢ Profile stiffness mechanism

Time-averaged T_i profile

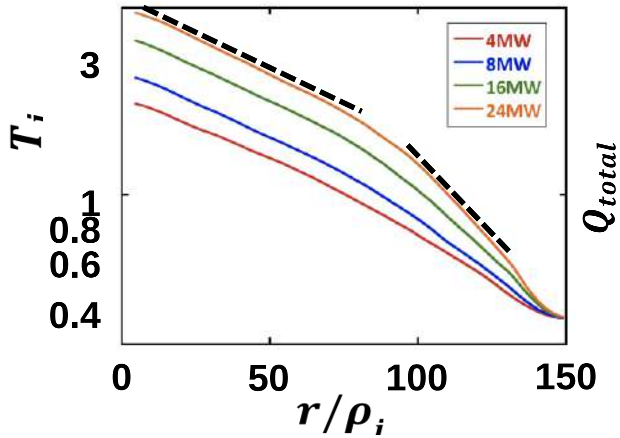

Gradient-Flux relation

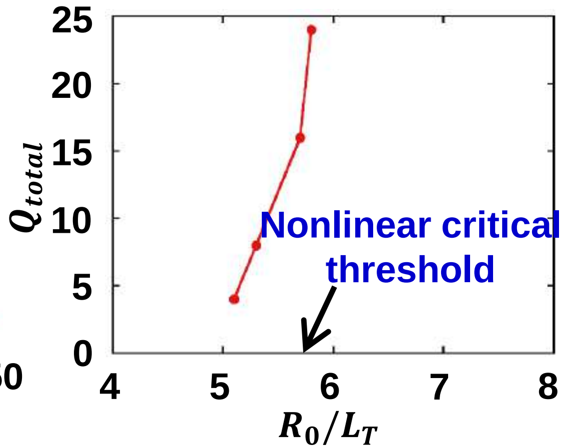

- ✓ T profile stiffness may result from explosive global transport triggered by instantaneous formation of radially extended vortices, in which ballooning symmetry is recovered.

How to break profile stiffness?

Radial force balance: $$E_r + \frac{k}{e}\frac{\partial T_i}{\partial r} - \frac{rB}{qR}U_{\parallel} - \frac{1}{n_i e}\frac{\partial p_i}{\partial r} = 0$$

- ✓ **Mean flow shear recovers the symmetry or weakly reverses the ballooning angle so that its stabilization effect is small.**

⬇

- ✓ **Toroidal rotation can change the mean flow shear through radial force balance, by which we may enhance its stabilization effect.**

⬇

- ✓ **Especially, toroidal rotation in outer region with small safety factor (weak/reversed magnetic shear) may be effective.**

Flux-Driven turbulence with Momentum input

➢ Momentum source operator

$$S_M = \tau_M^{-1} A\,(r)\left[f_{LM}(n_0, 0.5v_{ti}, T_0) - f_{LM}(n_0, 0, T_0)\right]$$

$$f_{LM}(n, U_{||}, T) = \frac{n}{\sqrt{2\pi T^3/m_i^3}}\, exp\left[-\frac{0.5(v_{\parallel} - U_{\parallel})^2 + \mu B}{T/m_i}\right]$$

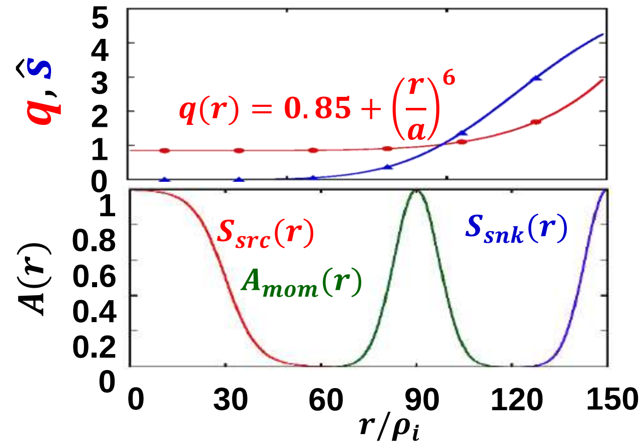

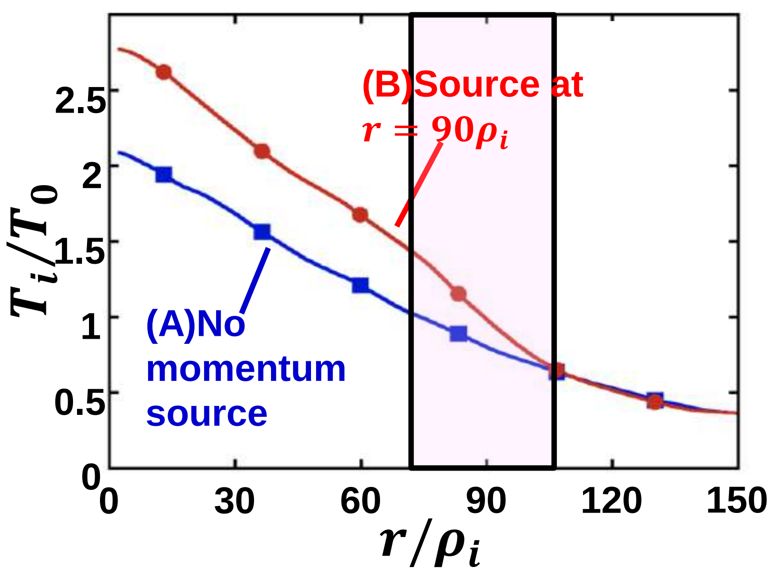

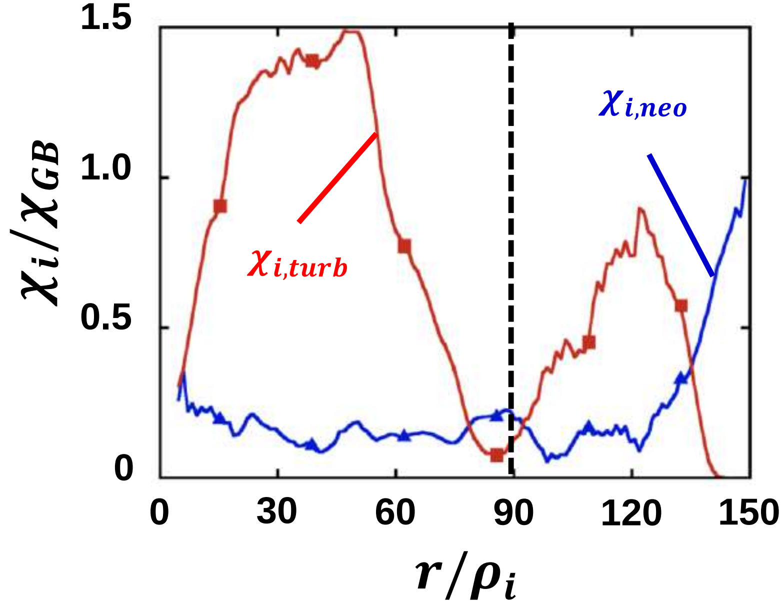

✓ **Strong E_r shear triggered by toroidal rotation suppresses turbulence, leading to an ITB formation.**

Impact of Momentum Source

Radial force balance: $\boxed{1}\ \boxed{2}\ \boxed{3}\ \boxed{4}$

$$\underbrace{E_r}_{1} + \underbrace{\frac{k}{e}\frac{\partial T_i}{\partial r}}_{2} - \underbrace{\frac{rB}{qR}U_\parallel}_{3} - \underbrace{\frac{1}{n_i e}\frac{\partial p_i}{\partial r}}_{4} = 0$$

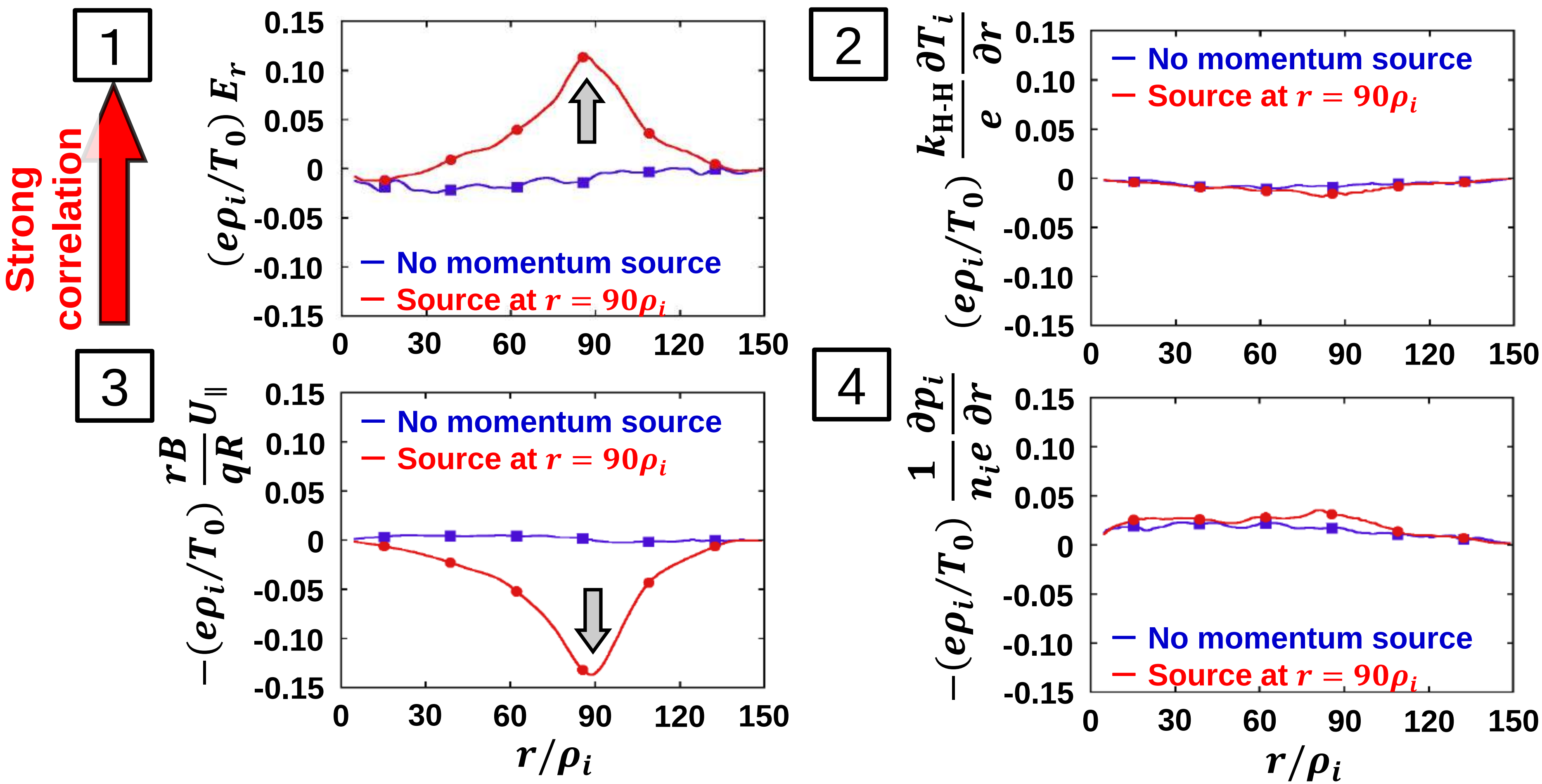

Effect of Rotation Direction on ITB formation

Camenen, et al. NF 2011

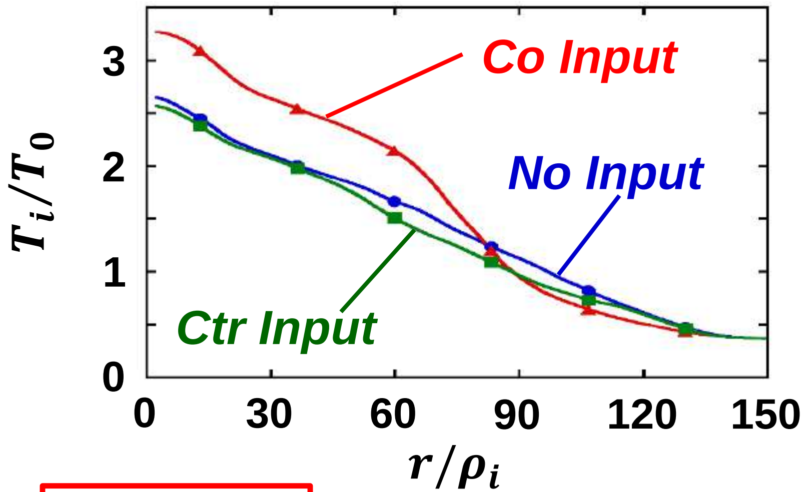

$$R_\varphi \equiv \frac{\Gamma_\varphi^r}{Q_i^r}\frac{v_{ti}}{R_0} = \frac{2}{R/L_T}\frac{\chi_\varphi}{\chi_i}\left[u' + \frac{R_0 V_{co}}{\chi_\varphi}u + \frac{C^*}{\chi_\varphi}\right]$$

$$\frac{C^*}{\chi_\varphi} \sim -\frac{\hat{s}}{2qk_\theta\rho_{ti}}\left[\frac{R_0}{L_n} + 4\right]\theta_b$$

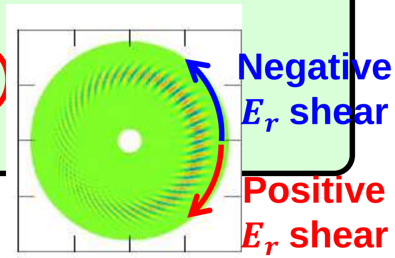

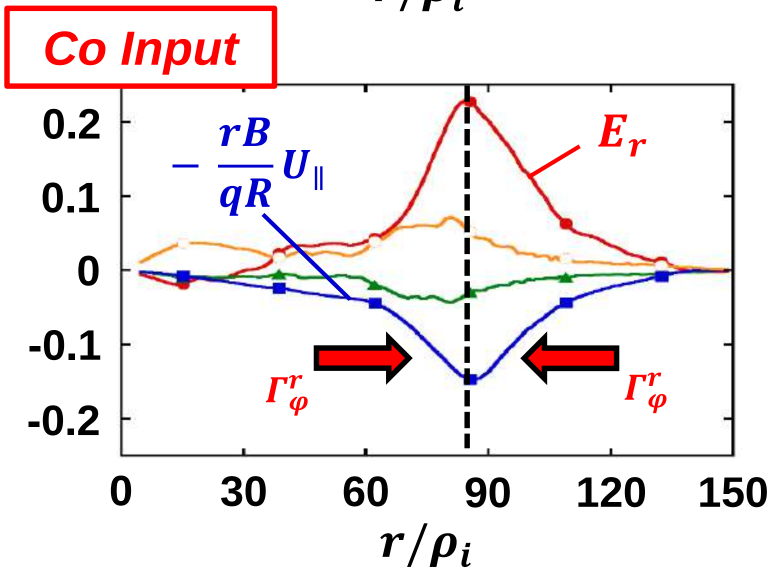

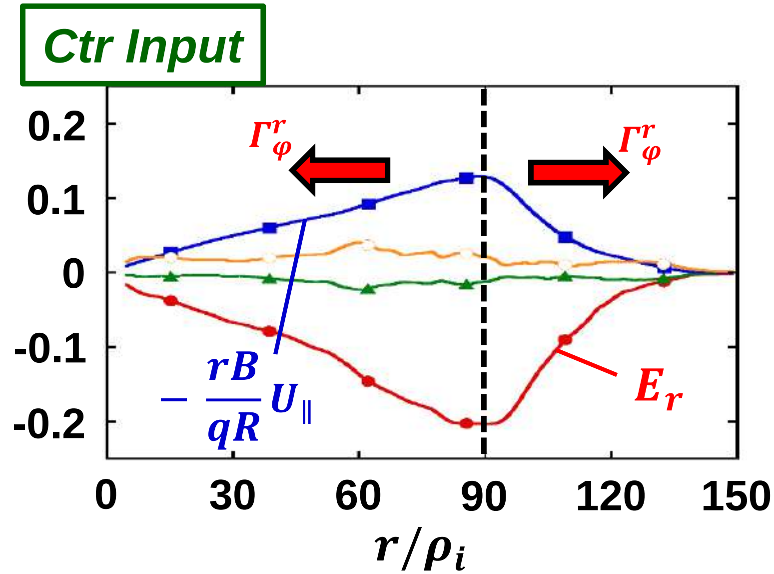

- ✓ Toroidal rotation enhances E_r shear through radial force balance;
- ✓ Co-rotation is more effective (this E_r reduces momentum diffusion).

ITB formation in reversed shear plasma

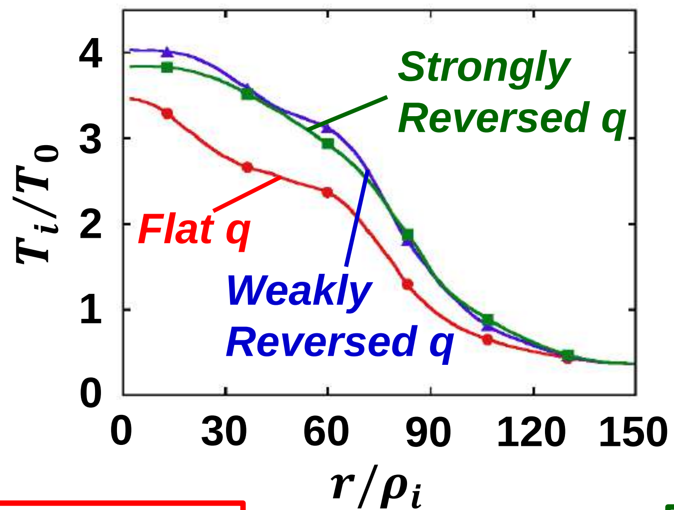

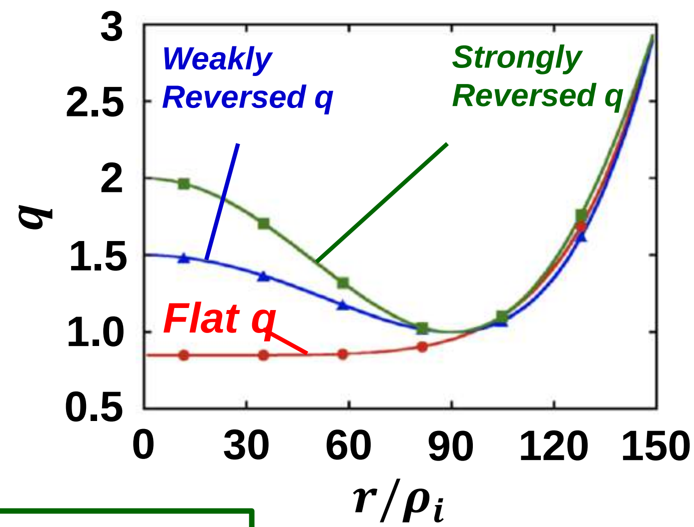

Flat q, Co

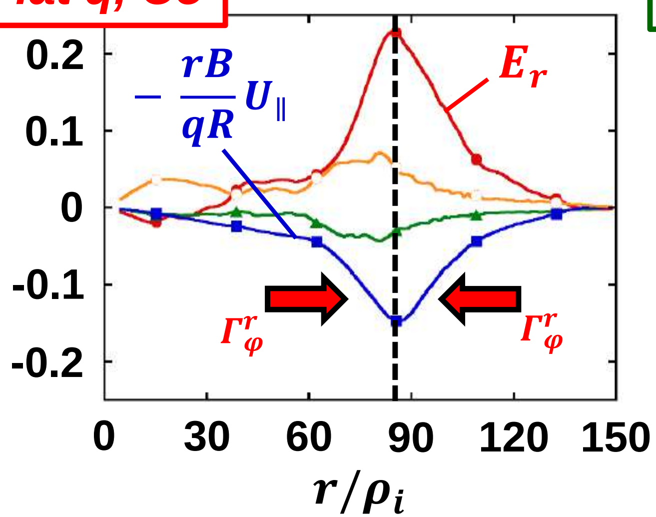

Strongly Reversed q, Co

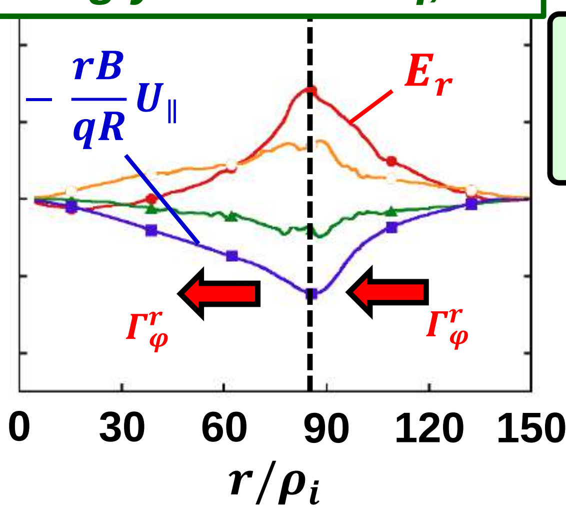

$$\frac{C^*}{\chi_\varphi} \sim -\frac{\hat{s}}{2qk_\theta\rho_{ti}}\left[\frac{R_0}{L_n}+4\right]\theta_0$$

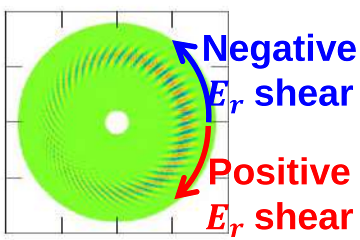

- ✓ **In the reversed magnetic shear case, peaking effect becomes weak since momentum flux in the left side becomes opposite.**

Summary

➢ **Multi-scale phenomenon in MCF plasma is common and multi-scale turbulence is of essential importance in confinement and transport;**

➢ **Both gyrofluid and gyrokinetic simulations are of advantages;**

➢ **Reduced model for multi-scale turbulence simulation is necessary;**

Partial near-scale modeling is the first-step job and first-principle full-scale simulation is pursued.

- ✓ **Mixed MHD-ITG scale simulation on nonlinear interaction between tearing mode (magnetic island) and micro-turbulence;**
- ✓ **Micro-scale flow (e.g., ITG) may drive a dynamo current action to influence island dynamics;**
- ✓ **Large magnetic island can also induce new micro-scale instability to enhance the transport**

- ✓ **Multi-scale transport processes and ITB formation are simulated in flux-driven global GK turbulence.**